



UNIVERSITÀ DELLA CALABRIA

Department of Computer Engineering, Modeling, Electronics and Systems

PhD in

INFORMATION AND COMMUNICATION TECHNOLOGY

CYCLE XXXVI

THESIS TITLE:

**A NOVEL BIOPLASTIC-BASED ACTIVE PACKAGING: FUNCTIONALIZATION,
CHARACTERIZATION AND PRODUCT OPTIMIZATION OPPORTUNITIES
THROUGH FINITE ELEMENTS MODELING AND ARTIFICIAL NEURAL
NETWORKS**

DISCIPLINARY SCIENTIFIC SECTOR: ING-IND/24

Coordinator: Prof. Giancarlo Fortino

Supervisors: Prof. Stefano Curcio

Prof. Sudip Chakraborty

PhD student: Gerardo Coppola



Firma oscurata in base alle linee
guida del Garante della privacy

*To my family,
since just like truth
it dwells whether if it is sought or not.*

Table of Contents

Introduction 8

Chapter 1: Bioplastic from Renewable Biomass: A Facile Solution for a Greener Environment.	14
<i>Premises to Chapter 1.</i>	14
1.0 - Abstract.....	15
1.1– Introduction.....	17
1.2 – Bioplastic Materials	21
1.2.1 – Biodegradable.....	23
1.2.2 – Bio-Based Certification Standards.....	25
1.3 – Bioplastics Applications	26
1.3.1 – Food Packaging.....	26
1.3.2 – Agricultural applications.....	30
1.3.3 – Medical applications	31
1-3-4 – Novel industrial applications.....	32
1.3.5 – Other applications	33
1.4 – Environmental aspects of Bioplastics.....	35

1.4.1 - Sustainability and environmental footprint	35
1.4.2 - Disposal Processes and Environmental Impact of Bioplastic Packaging	37
1.5 - Bioplastic Sources	40
1.5.1 - Agricultural Crops	40
1.5.2 - Organic Waste Sources	42
1.5.3 – Algae-based Sources	47
1.6 – Conclusions.....	50
1.7 – References (<i>Chap.1</i>)	52
Chapter 2: Plasticized PLA films for food applications by “green” solvent casting – method and characterization.	62
<i>Premises to Chapter 2.</i>	62
2.1. - Introduction	63
2.2 - Materials and Methods	66
2.2.1 - PLA/ ^P G solution preparation	66
2.2.2 - Film casting.....	67
2.2.3 - Film characterization	68
2.3 - Results	70

2.3.1 - FT-IR analysis.....	70
2.3.2 - Water contact angle.....	71
2.3.3 - Scanning electron microscopy	72
2.3.4 - X-Ray diffraction	73
2.3.5 - Thermal stability	73
2.3.6. - Mechanical properties	74
2.3.7. - Water vapor transmissison rate	76
2.4 - Discussion.....	78
2.4.1 FT-IR analysis	78
2.4.2 Water contact angle	79
2.4.3 - SEM imaging	79
2.4.4 - Thermal stability	80
2.4.5 - Mechanical properties	81
2.4.6 - WVTR tests.....	83
2.5 – Conclusions.....	85
2.5 – References (<i>Chap. 2</i>).....	86
Chapter 3: Modeling of specific migration from food contact materials.	88
<i>Premises to Chapter 3.</i>	88

3.0 - Abstract.....	89
3.1 - Introduction	90
3.2 - Specific migration models.....	95
3.2.1 - Specific migration in a food matrix	96
3.2.2 - Nickel, manganese and chromium release from AISI 316L stainless steel.	100
3.2.3 - Standalone application of stainless steel components release in acid solutions.....	103
3.3 - Experimental.....	104
3.4 - Results and discussions	105
3.4.1 - Concentration profiles of polymeric additives in a food matrix	106
3.4.2 - Concentration profiles of nickel, manganese and chromium from a stainless-steel piping part	108
3.4.3 - Standalone application uses.....	110
3.5 - Conclusions	112
3.6 - Appendix	115
A. Model data set.....	115
B. Diffusion coefficient.....	116

C. Boundary conditions.....	116
D. PDE solve	116
References (<i>Chap.3</i>)	117
Chapter 4: Modeling HVED functional compounds extraction.	121
<i>Premises to Chapter 4</i>	121
4.1 – Introduction.....	123
4.2 - Experimental data fitting	125
4.3 - Comsol 5.6 implementation	128
4.3.1 – Parameters	128
4.3.2 - Definitions.....	130
4.3.3 - Transport of Diluted Species in Porous Media.....	132
4.3.4 - Mesh.....	134
4.4 - Time Dependent Study - results.	135
4.5 – Conclusions.....	139
References (<i>Chap.4</i>)	140
Chapter 5: ANNs as a valid tool for active food bio packaging optimization.	141
<i>Premises to Chapter 5</i>	141
5.1 - Introduction	143

5.2 - Materials and methods – samples and testing	145
5.3 – ANN architecture.....	149
5.4 – ANN results and performances.....	154
5.5 - Conclusions	157
References (<i>Chap 5</i>)	158

Conclusions 159

List of Publications..... 164

List of Courses..... 167

Conferences 168

Other activities..... 170

Introduction

This thesis represents a summary of the research activities brought out during a three-year PhD course. All the activities fall under the means of producing a valid bio-based biodegradable active packaging to be addressed for food-industry scopes. The whole activity has been brought out by merging multiple research areas, these being Material Science, Chemical Engineering, and Information and Communication Technologies (ICT). As a main outcome, a new array of functionalized PLA-based food-grade packaging materials were produced at a laboratory scale, while a product development process has been hypothesized as follows - through the application of the above-mentioned research areas - to achieve a fast and reliable product optimization based on explicit needs and requests of the market. Each chapter of this work belongs to a specific phase of the theorized product development method in which the main core should follow an iterative study between the three main areas of research, as shown in Figure 1 below.

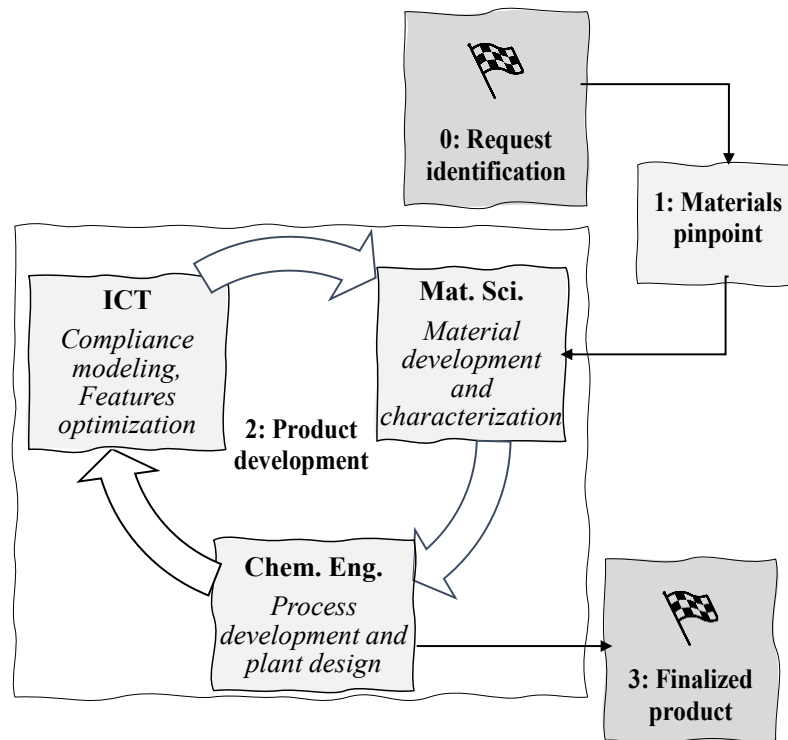


Figure 1: Scheme of the Product Development iterative method theorized.

While figure 1 reports a block-schematic of the theorized method; all the phases of the method are described below. It is important to state that, at this point, no economic feasibility study has been included because - while being easily integrable along the phases of the method itself – doesn't strictly fall in the interest of this study.

0: Request identification.

The state of the art and the ecological demands that need to be addressed by the food industry dictates the identification of a request. More specifically, the need for unexpensive bio-compatible materials with active features sums up well one of the main current tendencies of the market. More and more food companies chose to implement bio-packaging and active packaging in their end-of-line processes to respond to an increasing

consumers demand for bio-compatible solutions and to reduce food wastes by considerable interventions in the packaging field capable to improve the shelf-life of the products.

1: Materials pinpoints.

The main material chosen for the development of a new active packaging formulation fell on (poly)lactic acid (PLA). PLA has decent mechanical properties, mediocre thermal stability but good biocompatibility and biodegradability. The main less desirable PLA feature is its high brittleness in comparison to other widely used synthetic polymers; in Chapter 2 this study gives an answer to this issue by choosing a food-grade and affordable solution. The active features of the materials were brought in by the embedding of a plasticizer and nanoparticles (NPs) in the material; the chosen NPs were picked among the most economically accessible and unharmed (either for humans and the environment) while being able to tailor transpiration, interfacial and antimicrobial features of the packaging, as described in Chapter 5.

2: Product development

The bulk of the process resides in an iterative process among three different areas: The first area is the Material Science one, by which the chosen materials are characterized by both chemical and physical points of view, so that the main material features are tested (mechanical properties, thermal stability, vapor transmission, and interfacial properties). All the outputs of the Material Science study feed the Chemical Engineering field, by which

the material handling/pretreatments and the material casting procedures are defined to obtain the desired features during the production procedures at laboratory scales. Once the materials features and the production procedures are defined, an array of samples are generated to further investigate the capabilities of the generated material. At this stage the optimization process takes place: the effect of process variables, compounds fractions and other variables on the main features of the material can be investigated by generating a dedicated design of experiment (DOE) by which complex unexplicit relationships define the link between the chosen variables and the features to be optimized. All the recorded data can be fed to finite elements modeling (FEM) and to dedicated artificial neural networks (ANNs) to test and disclose the unexplicit relationships mentioned above.

3: Finalized product.

The optimized product should finally undergo final compliance tests and industry standard tests, while accurate production process scaleup should be provided at this point.

Each chapter of this work belongs to one of the process development phases described above; more precisely those are clarified in the following Table 1.

Table 1: A description of which product development phase each chapter belongs to.

	Developing phase	Description	Chapter
	State of the art	Scanning existent possibilities and industry needs	1
	Bench-level novel material casting	Novel bio-based food-grade packaging film casting	2
ICT field	Compliance testing	Modeling of packaging-food interaction behavior	3
	Active compounds (high added value) recovery	Modeling of active components HVED extraction	4
	Features optimization	Features optimization by ANN development	5

As described in Table 1, Chapter 1 is a review that collects the state-of-the-art of the vast possibility of development of food bio-packaging. The review gathers the most up-to-date data about biopolymers and the possible bio-compatible material sources, showing the intrinsic potential of waste sources exploitation. All the above were the factors which led to the choice of the main material (Material pinpoint).

Chapter 2 deals with the Material Science and the Chemical Engineering aspect of the laboratory-scale development of the material, giving a wide characterization of the obtained samples from a mechanical, thermal, and interfacial standpoint, pointing the interest on the influence of the use of a chosen plasticizer on the main physical features of the material, and defining a dedicated solvent-casting method which is currently under patenting procedures.

In Chapters 3 and 4, two critical aspects of the product development procedure are faced by the use of Finite Elements Modeling: the first one is a valid and economical way to check the product compliance with the most updated European food legislation; the second one is a first attempt to develop a convenient way to retrieve high added value active compounds to be used as functional compounds by the exploitation of vegetal wastes.

In Chapter 5, a dedicated Artificial Neural Network is built and then used as a rapid way of optimizing the amount of multiple functional compounds to achieve mechanical and morphological features as a direct answer to precise industrial needs. A minimal array of samples has been generated by a Design of Experiment procedure and cast, while tests on one of the most critical material features - Water Vapor Transmission Rates (WVTR) - were performed as described in Chapter 2. Tests data were fed to a dedicated Artificial Neural Network to retrieve the direct dependency between the functional compounds amounts and the WVTR values. The results show how the definition of a minimal sample array, and the integration of ICT computing methods, successfully lead to the disclosure of the complete array of feature possibilities of the material. In this chapter, functional compounds and their amounts are kept undisclosed for patenting reasons.

Chapter 1: Bioplastic from Renewable Biomass: A Facile Solution for a Greener Environment.

~

Premises to Chapter 1.

The following review, published on Earth Systems and Environment (Springer, 2021), collects all the up-to-date knowledge about bioplastics and their bio-compatible sourcing. The possibilities unlocked by the use of waste or biological sources open a very wide range of opportunities for the whole packaging industry. After a clear view of the state of the art on the whole topic, a series of functionalized PLA samples was theorized to be tested as a new alternative for food bio-packaging needs, as shown in the next chapters.

~

Bioplastic from Renewable Biomass: A Facile Solution for a Greener Environment.

Gerardo Coppola¹ · Maria Teresa Gaudio¹ · Catia Giovanna Lopresto¹ · Vincenza Calabro¹ · Stefano Curcio¹ · Sudip Chakraborty¹

¹University of Calabria, Department of DIMES, via Pietro Bucci, Cubo 42A, 87036 Rende, Cosenza, Italy

PUBLISHED ON: Earth Systems and Environment – Springer
Volume 5, pages 231–251, (2021)
© The Author(s) 2021

<https://doi.org/10.1007/s41748-021-00208-7>

1.0 - Abstract

Environmental pollution is increasing day by day due to more plastic applications. Plastic material is going in our food chain as well as the environment employing microplastic and other plastic-based contaminants. From this point, bio-based plastic research is taking attention for a sustainable and greener environment with a lower footprint on the environment.

This evaluation should be made considering the whole life cycle assessment of the proposed technologies to make a whole range of biomaterials. Bio-based and biodegradable bioplastics can have similar features as conventional plastics while providing extra returns

because of their low carbon footprint as long as additional features in waste management, like composting.

Interest in competitive biodegradable materials is growing to limit environmental pollution and waste management problems. Bioplastics are defined as plastics deriving from biological sources and formed from renewable feedstocks or by a variation of microbes, owing to the ability to reduce the environmental effect. The research and development in this field of bio-renewable resources can seriously lead to the adoption of a low-carbon economy in medical, packaging, structural and automotive engineering, just to mention a few. This review aims to give a clear insight into the research, application opportunities, sourcing and sustainability, and environmental footprint of bioplastics production and various applications.

Bioplastics are manufactured from polysaccharides, mainly starch-based, proteins, and other alternative carbon sources, such as algae or even wastewater treatment byproducts. The most known bioplastic today is thermoplastic starch, mainly as a result of enzymatic bioreactions. In this work, the main applications of bioplastics are accounted for. One of them being food applications, where bioplastics seem to meet the food industry concerns about many the packaging-related issues and appear to play an important part for the whole food industry sustainability, helping to maintain high-quality standards throughout the whole production and transport steps, translating into cleaner and smarter delivery chains and waste management. High perspectives reside in agricultural and

medical applications, while the number of fields of applications grows constantly, for example, structural engineering and electrical applications. As an example, biocomposites, even from vegetable oil sources, have been developed as fibers with biodegradable features and are constantly under research.

Keywords: *Bioplastic · Biomaterials · Environmental Pollution · Biopolymer · Biodegradable polymers.*

I.1– Introduction

Today, bioplastic materials represent a valid alternative to conventional plastics and their applications. The bioplastics market share is around 1% of the 370 million tons of total global plastic produced. But their annual growth rates hover around 30% until 2025. European Bioplastics (EUBP)—the association representing the bio-plastics industry’s defined “bioplastic” as the biodegradable plastic materials and plastics produced from renewable resources.

IUPAC defined bioplastic as a derivative of “biomass or monomers with plant origin, at some point of processing can be designed” (Vert et al. 2012; Plastics Europe 2021). Plastic materials comprise polymers with relatively high molecular weight. They are typically produced by chemical synthesis processes. The term bioplastics is used to distinguish polymers that originate from renewable sources as biomass. The synthetic

polymers are made from monomers by polycondensation, or polyaddition or polymerization, and most of them have a simpler structure than natural ones.

They can be classified into four different groups: elastomers, thermosets, thermoplastics and synthetic fibers. The most communal synthetic polymers are polypropylene (PP); polyethylene (PE), acrylonitrile–butadiene–styrene (ABS), polycarbonate (PC), polyamides (PAs), polystyrene (PS), polyethylene terephthalate; polyvinyl chloride (PVC), polytetrafluoroethylene (Teflon), poly(methyl methacrylate) (PMMA), acrylic polyurethane (PU, PUR). Some of their applications are shown in Fig. 1, where the size of bubbles shows the relative importance. These plastics are traditionally petrochemically derived, but the demand for their production from renewable feedstocks is growing.

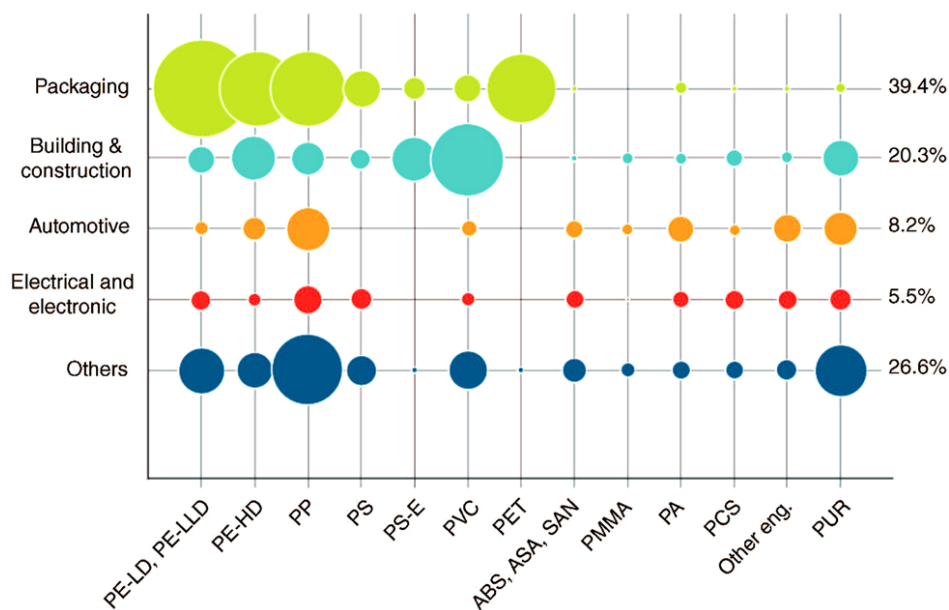


Figure 2: Typical applications of polymers (Plastics Europe 2021)

Theoretically, all usual plastics are generally degradable, but they have a slow breakdown, hence considered non-(bio) degradable.

Biodegradation of bioplastics depends on their physical and chemical structures in terms of polymer chains, functional groups and crystallinity, but also on the natural environment in which they are placed (i.e., moisture, oxygen, temperature and pH). Biodegradation is an enzymatic reaction catalysed in different ecosystems by microorganisms, such as actinobacteria (*Actinomyces*, *Streptomyces*), bacteria (*Paenibacillus*, *Pseudomonas*, *Bacillus*, *Burkholderia*) and fungi (*Aspergillus*, *Fusarium*, *Penicillium*) (Emadian et al. 2017). There are different concepts of biodegradation.

One very common degradation process is called hydrolysis. The hydrolysis mechanisms are exaggerated by diffusion of water through polymer matrix. Time duration for the degradation may vary for different material, such as polylactic acid, has very slow degradation which is about 11 months (Thakur et al. 2018). Moreover, the biodegradation rate be contingent on the end-of-life decisions and the physicochemical conditions, such as moisture, oxygen, temperature, presence of a specific microorganism, presence of light. The main end-of-life choices for biodegradable plastics include recycling and reprocessing, incineration and other recovery options, biological waste treatments, such as composting, anaerobic digestion and landfill (Mugdal et al 2012; Song et al. 2009). The composting process represents the final disposition most favorable from an environmental point of

view. The presence of ester, amide, or hydrolyzable carbonate increases biodegradation's susceptibility.

Bioplastics also do produce less greenhouse gases than that of usual plastics over their period. Therefore, bioplastics contribute to a more sustainable society. Therefore, there are bioplastic alternatives to conventional plastic materials. It already plays a vital part in different fields of application. Bioplastics that are bio-based, have the same properties as general plastics and offer added advantages because they have a lesser carbon footprint on environment. Nevertheless, their low mechanical strength limits their application. Glass and carbon fibers are synthetic fibers commonly used to reinforce bioplastics, but they are not biodegradable. For this reason, they can be replaced by more environmentally friendly, abundant, and low-cost materials, such as lignocellulosic fibers and lignin (Yang et al. 2019). Other physical strengthening methods are the mold temperature increase, dehydrothermal treatment, and ultrasounds application. When applied to soy protein-based bioplastics, the thermal treatment enhanced the mechanical properties, the dehydrothermal treatment increased the superabsorbent capacity and ultrasounds lead to a structure with smaller pores. As a consequence, the treated bioplastics could be used in different applications (Jiménez-Rosado et al. 2020).

A new green one-step water-based process was proposed to convert vegetable wastes into biodegradable bioplastic films having similar mechanical properties with other bioplastics (Perotto 2018).

Recent trends indicate the biocompatible and biodegradable polyhydroxyalkanoates (PHAs) as alternatives to conventional plastics which has wide variety of thermal and mechanical characteristics (Khatami et al. 2021). PHAs are linear polyesters, produced by microbiological, enzymatic, or chemical processes, but their industrial production is still not cost-competitive (Medeiros Garcia Alcântara et al. 2020). Renewable and inexpensive carbon sources—such as macroalgae, peanut oil, crude glycerol, and whey—have been studied to reduce production costs (El-malek et al. 2020). Innovative research proposed the production of PHAs by a three-step process consisting of CO₂ reduction to acetate and butyrate by microbial electrosynthesis, extraction/concentration of acetate and butyrate, and PHAs production from volatile fatty acids. This process meets the demand to decrease CO₂ emissions and convert a greenhouse gas to bioplastics (Pepè Sciarria et al. 2018).

Currently, researchers pay great attention to the production of biomass-derived next-generation advanced polymer, such as poly(ethylene 2,5-furandicarboxylate) (PEF) (Hwang et al. 2020; Algieri et al. 2013, 2012; Iben Nasser et al. 2016). Moreover, another very new trend investigates green microalgae cells as raw materials for the production of cell plastics (Nakanishi et al. 2020).

1.2 – Bioplastic Materials

Plastics are polymeric chains composed of repetitive units or monomers linked together. These macromolecules are conventionally synthesized by polymerization,

polycondensation or polyaddition reactions from fossil sources. Interest in competitive biodegradable materials is growing to limit environmental pollution and waste management problems.

Bioplastics are a new plastic generation, defined as plastics originating from a biological system and produced from renewable feedstocks or by a range of microorganisms. Since they significantly reduce the environmental impact in terms of greenhouse effect and energy consumption, they are a challenge for a greener future.

Having different properties, bioplastic materials are classified in three main groups, as shown in Fig. 2:

- Bio-based or partially bio-based plastics.
- Bio-based and biodegradable plastics.
- Fossil resources and biodegradable plastics.

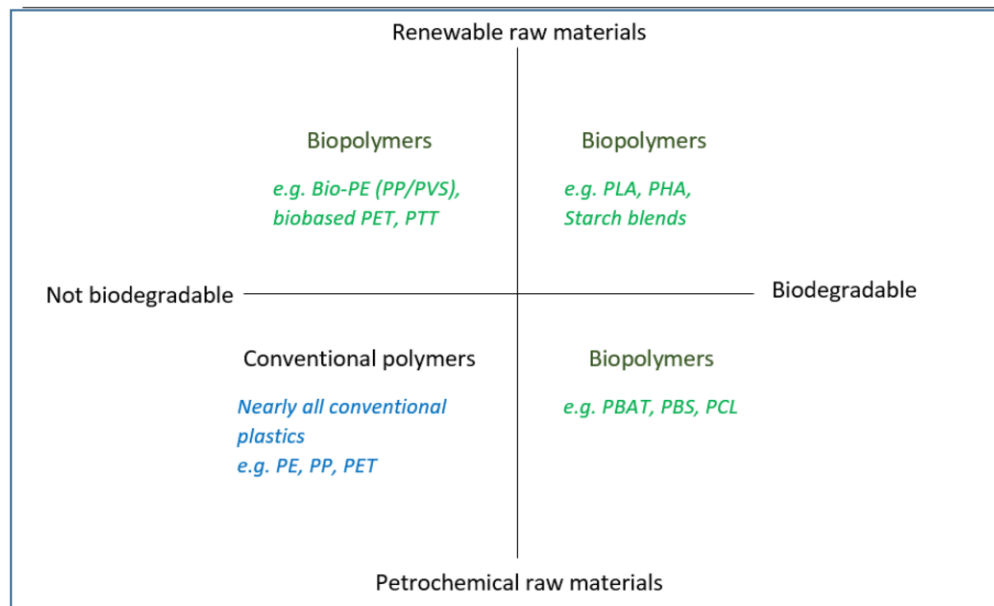


Figure 3: Types of bioplastics (Philp et al. 2013).

1.2.1 – Biodegradable

Plastics that are both biodegradable and bio-based, come from renewable natural resources, show the biodegradation property at some stage. This group includes the thermoplastically modified starch as well as other bio-degradable polymers like polyhydroxyalkanoates (PHA), polylactide (PLA), and polybutylene succinate (PBS).

Besides petrochemicals, PLA can be found from planned *Escherichia coli* (Jung and Lee 2011) or with woven bamboo fabric (Porras and Maranon 2012). Instead, PHAs in Fig. 3 shown a general structure are a varied cluster of biopolymers, but typically denote to poly(3-hydroxybutyrate) and poly(3-hydroxybutyrate-co-3-hydroxyvalerate) (PHBV). They are mostly produced from sugar or lipids by bacteria because PHAs represent an intracellular product of bacteria. Around 250 types of bacteria help to yield PHA. So, these

bioplastics are collected with the demolition of bacteria and then disconnected from the microbial cell matter. Moreover, PHAs have good barrier characteristic and attractive in different biomedical applications. They also have the standard specification from marine degradability, which is ASTM D7081.

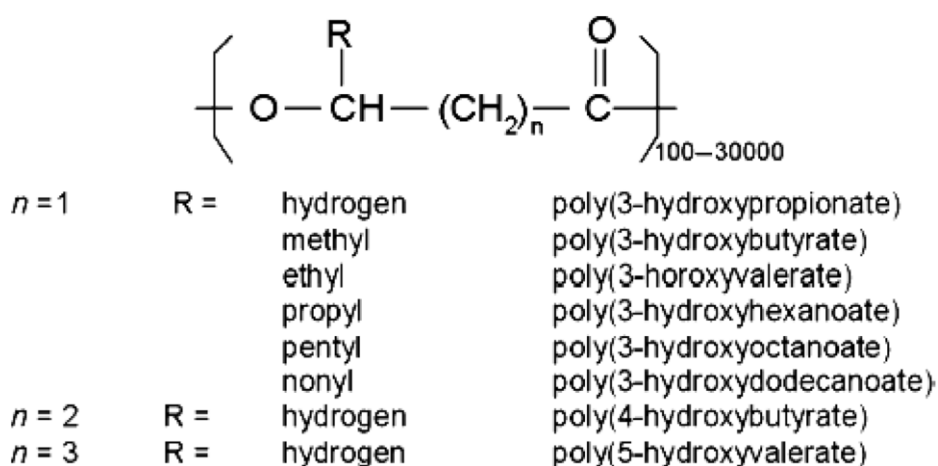


Figure 4: The general structure of polyhydroxyalkanoates (Ojumu et al. 2004).

PHAs have different attributes: fully bio-degradable either in water or even in soil (Meereboer et al. 2020); good resistance as well as printability to oil and grease; until a temperature of 120 °C (Philp et al. 2013).

Moreover, PHAs came from agro- and food wastes, such as wheat bran, rice husk, potato peel, mango peel, straw and bagasse and (Gowda and Shivakumar 2014). They degrade in different rate in different media. Thus, as seen as in the case of PHAs, in general, the property of biodegradability can be directly related to the structure of the polymer and can thus be benefited with specific applications, particularly in case of packaging. PCL is

a bio-degradable polyester which has a very low melting point (~ 60 °C). It has general application in biomedical, which includes the surgical structure.

1.2.2 – Bio-Based Certification Standards

The term “bio-based” refers to material derived from biomass. The most common biomass for bioplastic uses is, for example, corn, sugarcane, and cellulose. Bio-based plastics have the exceptional advantage over general plastics materials which can reduce the dependency on fossil resources, resulting in a lesser amount of emission of greenhouse gas. Consequently, help the EU achieve the goals of CO₂ emission in 2020 (Bioplastics-Facts and Figures 2021).

Usually, companies indicate their bio-based products with the wording “bio-based carbon content” or with “biobased mass content”, but some other standard certifications exist to individuate them. A methodology to measure the bio-based carbon content in materials exists which is called the 14C-method. Thanks to this method, the European standard, and the corresponding USA standards exist. They are CEN7TS 16,137 and ASTM 6866, respectively, for EU standard and US standard. Moreover, a method to individuate a bio-based mass content was introduced by the French Association Chimie du Vegetal (ACDV) with a corresponding certification scheme. It consists in taking chemical elements—such as oxygen, nitrogen, and hydrogen— into account, besides the bio-based carbon.

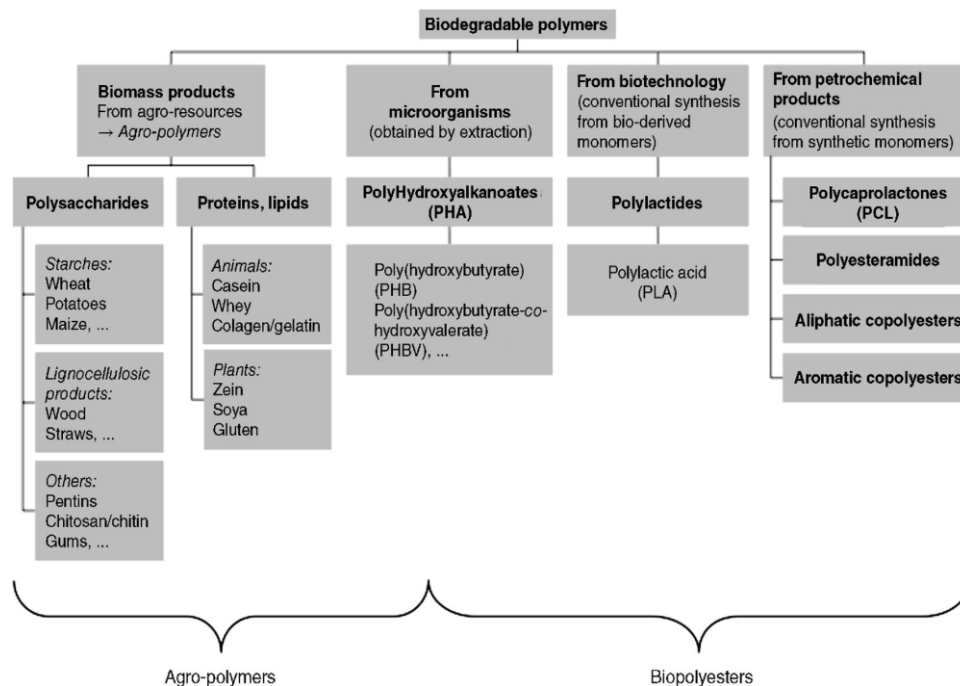


Figure 5: Different biodegradable polymers and corresponding their raw materials used (Vilpoux and Averous 2014).

1.3 – Bioplastics Applications

1.3.1 – Food Packaging

One of the main recent focuses of the food industry concerns packaging-related issues, which defines a whole industry by itself. This kind of industry is constantly following the needs and criteria of the food production world, and its focus on the development of new biopolymer-based packaging is crucial for the whole food industry sustainability as well as its quality standards, leading to more clean and sustainable delivery chains from the production facilities and their internal storage systems, to transport facilities, to marketplaces to consumer houses.

The need for high-standard storage features and the urge for packaging with high economic, low ecological impact, ease of customization, and low encumbrance can be answered by compostable or degradable bioplastics (Jabeen et al. 2015).

Still, the effective applications of packaging in the food industry are few in respect to other fields and need to be enlarged; but nowadays, the biggest food distribution organizations are sensitive to the problem and seem willing to convert to bioplastics as much as possible.

One important aspect to consider when developing this kind of material is that diverse food products need different packaging features, resulting in the need for the development of many technologies, such as multi-layer films, modified atmosphere packaging, and smart and active packaging.

One of the main requested features for food packaging is the shielding from water and oxygen. While it is not difficult to develop bio-based multicomponent synthetic coatings to act as a barrier, this arises as a downside, the difficulty for a recycling option, as long as the recycling itself is practicable for single-component materials.

To have a quick view as shown in Table 1 below (Pilla 2011), the main features required in food packaging are moisture and oxygen permeability and mechanical properties. The Table 1 below compares the main materials, both bio-based and synthetic, used in the field (see Table 2).

Table 2: Comparison between main polymers used in the food industry.

Polymers	Moisture permeability	Oxygen permeability	Mechanical properties
Bio-based			
Cellulose (CA) acetate	Moderate	High	Moderate
Starch/polyvinyl alcohol	High	Low	Satisfactory
Proteins	High-medium	Low	Satisfactory
Cellulose/cellophane	High-medium	Very High	Satisfactory
Polyhydroxyalkanoates (PHA)	Low	Low	Satisfactory
Polyhydroxybutyrate /valerate (PHBA)			
Poly lactate	Moderate	High-moderate	Satisfactory
Synthetic			
Low density polyethylene	Low	Very High	Moderate-good
Polystyrene	High	Very High	Poor-moderate

The main issues of bio-based polymers in the food industry field are their relative high price than conventional plastic and the less-than-ideal water barrier features, but to mention the most widely applied materials in this field, starch-based films are mostly used for fruit and vegetable packaging and transportation. Here, this materials' main positive feature is the high breathability, a key element for preserving the shelf life of the fresh products (Bastioli 2001).

Wolf et al. (2005), in 2005, mentioned a price range for modified starch polymers from €1.50 to €4.50 per kg, the cheaper mostly being injection molding foams, so that an average price would sit around €2.50–3.00 per kg.

As different types of food require diverse features, a distinction by food typology is hereby adopted to give a comprehensive view.

Fruits and vegetables have a high respiration rate, which can lead to a fast decaying of optimal conditions, besides, they are highly susceptible to water, carbon dioxide, and ethylene concentration. So as the main features, a package should provide a good carbon

oxide/oxygen ratio in the atmosphere around the product, a good barrier against light, good mechanical properties, and a barrier to odors. Raw meat is highly susceptible to spoilage bacteria and pathogens growth. High oxygen concentration in the packaging is requested to preserve the fresh meat's color, so high oxygen permeability is required. So vacuum packaging is often considered a good choice, while adding oxygen adsorbing layers, resulting in active packaging, can better preserve cured meat (Andersen and Rasmussen 1992).

Dairy products need low oxygen permeability materials to avoid oxidation and microbial growth. In addition to that, a good barrier to light can preserve fats' oxidation. Other main features are the water evaporation factor and the avoiding of odor absorption from the exteriors. These features can reside in some forms of polysaccharides as pectins, which are mainly produced by extraction from fruit and vegetable sources and could act as a safety barrier for food products (Baldino et al. 2018). For example, the study of Cerqueira et al. (The bioplastics global market to grow by 36% within the next five years 2021) on polysaccharide edible coatings to preserve cheese showed good results in terms of the lower ratio of superficial mold growth compared to uncoated cheese.

The following Table 2 (Kumar and Thakur 2017) is a collection of the main current applications of bioplastics in the food industry.

Table 3: Main bioplastics applications in the food industry.

Application	Biopolymer	Company or users	References
PLA			
Coffe and other bevarages	Cardboard and cups with PLA coating	KLM	Jager (2010)
Beverages	Cups made with PLA	Mosburger (JP)	Sudesh and Iwata (2008)
Fresh salads	bowls made with PLA	MCDonald's	Haugaard et al. (2001)
Carbonted water, juices and dairy drinks	bottles Cups made with PLA	Biota, noble	Auras et al. (2004)
Fresh cut fruits, vegetables, bakery goods	trays and packs made with PLA	Asda (retailer)	Jager (2010), Koide and Shi (2007)
Organic pretzels, potato chips	bags made with PLA	Snyder's of Hanover, PepsiCo's Frito-lay	Weston (2012)
Bread	Paper bags with PLA window	Delhaize (retailer)	Delhaize (2007)
Organic poultry	bowls made with PLA, absorb pads	Delhaize (retailer)	
Starch based			
Milk chocolate	Corn starch trays	Cadbury food group, Marks and Spencer	Highlights in Bioplastics, Website European bioplastics (2021)
Organic tomatoes	Packaging based on Corn	Iper supermarkets (Italy), Coop in Italy	
Cellulose-based			
Kiwi	Bio-based trays wrapped whit cellulose film	Wal-Mart	Blakistone and Sand 2008)
Potato chips	Metalized cellulose film	Boulder Canyon	Highlights in Bioplastics, Website European bioplastics (2021)
Organic pasta	Cellulose based packaging	BirkeL	
Sweets	Metalized cellulose film	Quality street, Thorn ton	

1.3.2 – Agricultural applications.

Agricultural applications of PHAs-based bioplastics are limited to nets, grow bags, and mulch films. Bioplastics-based nets are alternatives to high-density polyethylene, traditionally used to increase the crop's quality and yield and protect it from birds, insects, and winds. Grow bags, known also as planter bags or seedling bags, are commonly made of low-density polyethylene. Instead, PHAs-based grow bags would be biodegradable, root-friendly, and non-toxic to the surrounding water bodies. Finally, bioplastics in mulch films are essential to uphold exceptional soil structure, moisture retention, control weeds, and prevent contamination, in substitution of fossil-based plastics (El-malek et al. 2020).

1.3.3 – Medical applications

Advancements in biomedical applications of biodegradable plastics lead to the development of drug delivery systems and therapeutic devices for tissue engineering, such as implants and scaffolds (Narancic et al. 2020).

Polymers play a crucial role in many medical and biomedical applications (Parisi 2015, 2018). These fields can take advantage of cellulose as the main green bioplastic. Thanks to its nontoxicity, non-mutagenicity, and biocompatibility, cellulose has been deeply studied for implants, tissue, and neural engineering, and pharmaceutical fields, as shown in Fig. 5 (Picheth 2017). Cellulose is organized in a fibrillar structure, with fibrils being the elementary structural unit with a cell diameter of 10 nm organized to macroscopically form fibers. Bacterial cellulose is used in the development of cellulosic membranes to be applied for tissue repair scopes. These membranes exhibit pores in a range of 60–300 μm . Also, modified cellulose matrix and bacterial nano-networks have been studied (Verma et al. 2008; Li et al. 2009; Liu et al. 2013).

Nanocelluloses and their composites are the main sources for any green plastic studies about the fabrication of medical implants, either in dental, orthopedic, and biomedical fields. More recent studies are developing 3D printing and magnetically responsive nanocellulose-based materials (Gumrah Dumanli 2016).

Another application worth mentioning is wound dressing nano-cellulosic membranes, with features as wound pain reduction, extruding retention reepithelialization acceleration and of infection reduction. Patented products of this kind are already available on the market, such as Bioprocess®, XCell®, and Biofill® (Magnocavallo et al. 1993; Fontana 1990).

Also, the biocompatibility of PHAs makes them ideal for medical applications, such as cancer detection, wound healing dressings, post-surgical ulcer treatment, bone tissue engineering, heart valves, artificial blood vessels, artificial nerve conduits and drug delivery matrices (El-malek et al. 2020).

I-3-4 – Novel industrial applications

PHAs-based wood-plastic composites are novel industrial applications of bioplastics. They are very interesting for their low cost, biodegradability, mechanical and physical properties that can be enhanced by suitable pre-treatments. PHAs-based lignin composites are recently applied as films in 3D printing, thanks to their shear-thinning profile that helped in the layer adhesion and reduced the warpage (El-malek et al. 2020).

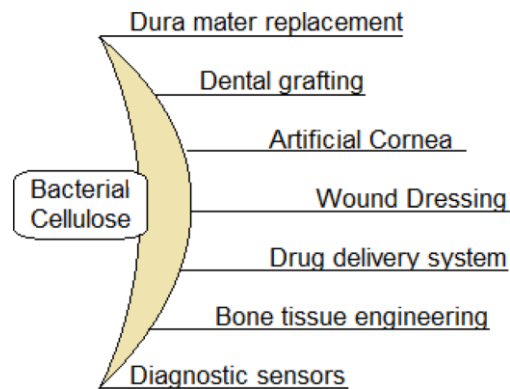


Figure 6: Biomedical applications of bacterial cellulose (Picheth 2017).

1.3.5 – Other applications

Bioplastics applications are constantly researched in many other fields, such as structural and electrical engineering. Although relying on biopolymers can result in less-than-ideal features, in respect to conventional plastics, bio-composite materials are crucial for research developments and for widening the application fields (Luca et al. 2017). Polymer composites are produced combining natural textile (basalt, carbon), natural fibers (jute, kenaf, hemp and sisal),-fillers (clays, zeolite, graphene) commonly used in many traditional application (Candamano et al. 2021, 2020), with polymers (Mohammed et al. 2015; Candamano et al. 2017), which can be chosen to be biodegradable (Rouf and Kokini 2016; Díez- Pascual 2019). Re-inforced biocomposites include recycled wood fibers or by-products from food crops harvesting. Even regenerated cellulose fibers from renewable sources like vegetal by-products or bacterial (Reddy et al. 2015) are included in this field, as sourcing nanofibrils of cellulose and chitin (Roy et al. 2014).

As an example, starches, which are considered one of the main resources in this field, can be used in a multitude of applications, which are collected in Fig. 6 below. Civil engineering applications include the utilization of foam composite made from vegetable oil sources. Their main features are generally low weight, acceptable physical properties, and good thermal insulation features. They are mostly used in composite-layers panels, in addition to metal or polymeric panels for construction. Some developments were brought to re-inforce rigid foam composites using fillers, short fibers, and long fibers. Bio foams obtained from vegetable oils are mainly produced from soybean, palm, and rapeseed oils (Lu and Larock 2009), and they derive from a chemical modification of the oils: -OH groups are added to an unsaturated triglyceride through hydroxylation of doublebonded carbons or triglyceride alcoholysis or by the esterification of the fatty acids and glycerol molecules contained in the oils, thus producing a monoglyceride utilizing a catalytic reaction (Pilla 2011). The mechanical and thermo-acoustical properties of bio foams are dependent on the cell structure and size. As an example, closed-cell foams are best suited for high compressive strength and impact robustness, while open-cell structures are a good choice for acoustic insulation means.

Rigid foam composites can be re-inforced with a wide range of fillers and fibers. Inorganic fillers, such as layered silicates, have considered the realization of synthetic polymer structures, while lignocellulosic fillers and fibers of vegetal sources, like soy or

wood flours, fillers from paper and hemp fibers. Those kinds of re-inforcing materials can help the sustainability of the vegetable oil-derived rigid foams production and utilization.

1.4 – Environmental aspects of Bioplastics

1.4.1 - Sustainability and environmental footprint

The sustainability of the whole family of bioplastics can be properly seen if all the stages of the materials, like sourcing, production, utilization, and disposal, are considered. In a more precise manner, the economic and environmental features of each of these stages are weighted. For example, the manufacture of biocomposites for construction applications gives direct benefits to the whole construction engineering industry's ecological impact.

Bio-based sustainable packaging aims to use renewable material sources and food and agricultural processing byproducts, which are sources that are not in competition with the food production chains (Reichert 2020). To classify the sources of materials used, we can utilize a biofuel classification, segregating first-, second-, and third-generation feedstocks. First-generation feedstock involves edible biomass like sugarcane, whey, and maize. The second generation comprises non-edible biomasses from lignocellulosic sources, ranging from agriculture, forest, and animal processing by-products to municipal wastes. The most unconventional sources listed as third-generation feedstock comprise biomass from algae (Naik et al. 2010).

The main biopolymer that seems to have good features and high versatility to compete with conventional plastics is polylactic acid (PLA) (Andreas Detzel 2006), made entirely from renewable sources. It exhibits mechanical properties similar to PET and PP. As a drawback, Andreas Detzel and Kauertz (2015) state how bioplastic bags are usually made with thicker films than conventional plastic bags, resulting in higher mass utilization. In addition to that, considering an average range, bioplastic films are made by 40% to 70% of fossil source components. These two features can lead to the conclusion that bioplastic bags can easily be the cause of a consistent environmental load in respect to conventional plastic bags. To have a better idea on how much the weight difference can be a problem for sustainability, we can consider that the weight per unit area of bioplastic-based bags exceeds by 30% circa the weight of PE films, this due to a higher density of the source materials (Andreas Detzel and Kauertz 2015).

Biodegradable plastics sources need high areas of farmland and vast volumes of water for their production, with the consistent downside of using these resources otherwise allocated to food production. In addition to that, bioplastic production contributes to pollution because of the pesticides used for the crops and the chemicals used in the transformation processes, but here, the use of eco-friendly alternative methods can overcome the issue (Colwill et al. 2012).

As the last main drawback, bioplastic not composted after use may be trashed in landfills and consequently produce methane because of oxygen deprivation, resulting in a

cause for greenhouse production. Even recycling brings up some issues: the recycling process of these materials cannot be processed with conventional plastics and therefore need separate process streams.

Adhesive <ul style="list-style-type: none"> - Hot-melt glues - Stamps, bookbinding, envelopes - Labels (regular and waterproof) - Wood adhesive, laminations - Automotive, engineering - Pressure sensitive adhesives corrugation paper 	Construction Industry <ul style="list-style-type: none"> - Concrete block binder - Asbestos, clay/limestone binder - Fire-resistant wallboard - Plywood/chipboard adhesive -Gypsum board binder -Paint filler 	
Paper Industry <ul style="list-style-type: none"> - Internal sizing - Filler retention -Surface sizing -Paper coating (regular and color) - Carbonless paper stilt material - Disposable diaspers - Feminine products sacks 	Cosmetic and Pharmaceutical Industry <ul style="list-style-type: none"> - Dusting powder - Make-up - Soap filler/extender - Face creams - Pill coating, dusting agent tablet binder/dispersing agent 	
Explosives Industry <ul style="list-style-type: none"> - Wide range binding agent - Match-head binder 	Mining Industry <ul style="list-style-type: none"> - Ore flotation - Ore sedimentation - Oil well drilling mud 	Miscellaneous <ul style="list-style-type: none"> - Biodegradable plastic film - Dry cell batteries - Printed circuit boards - Leather finishing

Figure 7: Non-food uses of starch.

1.4.2 - Disposal Processes and Environmental Impact of Bioplastic Packaging

When considering packaging applications, market prices of bioplastics still result higher than the conventional plastic ones, so they access the market mainly for private consumption. This consideration leads us to the fact that bioplastic disposal routes mainly involve household consumption.

Figure 7 below reports the actual discarding processes followed for some bioplastic packaging types (Andreas Detzel and Kauertz 2015). As a result, composting is the main route end for disposal, but still a consistent fraction of the total mass reaches the residual

waste and eventually be sent to incinerators, this because of mistakes in the disposal process or even separation by screening in the disposal plants (Ahamed et al. 2021).

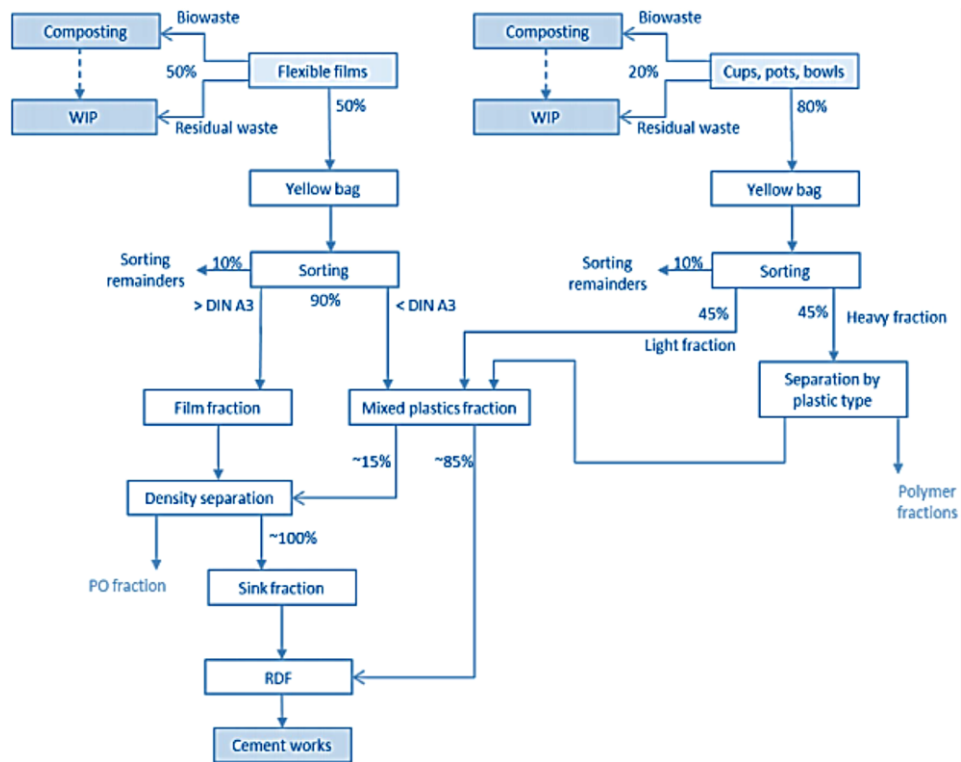


Figure 8: Disposal flowchart of bioplastic packaging (Andreas Detzel and Kauertz 2015).

Grundmann and Wonschik published a study on how bioplastic bags could interact in some fermentation disposal plants in Germany (Grundmann and Wonschik 2011). Anaerobic fermentation, as well as hydrolysis analysis, has been done to test this behaviour. Results show how thermophilic features are needed actually to act fermentation processes, while the higher degradation degrees fall around 20% values.

An extended life cycle assessment analyses have been addressed in the study of bio-PE systems by considering the steps below (Andreas Detzel and Kauertz 2015):

- Manufacture of the primary materials (bio-PE and PE-LD).
- Transport of the new product to processing.
- Manufacture of the film products.
- Transport of the film products.
- Disposal of the films (WIP).
- Utilization of the films (recycling).
- Allocation of the use of secondary materials and secondary energy from recycling and disposal processes in the form of credits .
- Accounting (credit) for the CO₂ bound in the bio-PE.

The following graphs present some of the results of the above-mentioned LCA analysis (see Table 3). As a conclusion, it emerges that, compared to fossil-based plastics, bio-PE has better responses in Climate Change and Consumption of Fossil Resources impact, but lacks in other features like Acidification, Eutrophication, and Human Toxicity impact factors.

Table 4: Climate Change and Consumption of Fossil Resources indicators, comparative LCA of film packaging made of fossil PE and bio-PE (Algieri et al. 2013).

	Climate change [PE_film_30g/ m ²]		Fossil resources [PE_film_30g/m ²]	
	kg CO ₂ equivalents per m ² of film		kg crude oil equivalents per m ² of film	
	bio-PE	fossil PE	bio-PE	fossil PE
Disposal in the 2nd LC	0.02	0.02	–	–
Recycling	0.005	0.005	0.001	–
Disposal in the 1st LC	0.05	0.05	–	–
Transport of finished product	0.02	0.02	–	–
Processing	0.01	0.01	0.001	0.001
Transport of new goods	0.005	0.005	0.001	–
Manufacture of primary materials	0.04	0.06	0.01	0.039
CO ₂ uptake	–0.07	–	–	–
Secondary energy allocation LC1	–0.02	–0.02	–0.005	–0.005
Secondary energy allocation LC2	–0.01	–0.01	–0.001	–0.001
Secondary material allocation	–0.01	–0.01	–0.005	–0.005

1.5 - Bioplastic Sources

1.5.1 - Agricultural Crops

Bioplastics can be produced from polysaccharides (e.g., starch, cellulose, chitosan/chitin), proteins (e.g. casein, gluten), and other carbon sources (Nachwachsende and Agency 2020).

Currently, the most used bioplastic is thermoplastic starch, obtained by enzymatic saccharification and microbial fermentation (Fig. 8) or by modifying starch with plasticizers with hydrophilic properties (Mojibayo et al. 2020).

Nevertheless, starch-based bioplastics treated with plasticizers and stored for long time face recrystallization and consequent deterioration of mechanical properties. To overcome this problem, starch-based bioplastics' performance may be improved by the addition of nanoparticles to obtain nanocomposite bioplastics used in automotive components, packaging materials, and drug delivery (Mose and Maranga 2011).

Starch is usually obtained from different terrestrial crops. Distilled water, glycerol, and vinegar were used to modify cassava starch for the production of bioplastic sheets (Mojibayo et al. 2020). Bioplastics from cassava starch were re-inforced also by coconut husk fibers (Babalola and Olorunnisola 2019). Condensation polymerization was performed to produce bioplastic from corn starch and glycerin to obtain nanocomposites for packaging applications (Ateş and Kuz 2020). Other starch sources are potatoes, wheat, and tapioca. The finest, smoothest, flexible and strong bioplastic was produced from tapioca starch (Gokce 2018), but the potato-derived starch showed the best properties in terms of extraction, ease of working, texture, and potential drying (Hamidon 2018). Composite bioplastics from tapioca starch and sugarcane bagasse fiber were recently investigated and ultrasounds treatment improved properties by enhancing the tensile strength and decreasing the moisture absorption rate (Asrofi et al. 2020).

Among proteins, wheat gluten can be processed to produce bioplastics (Rasheed 2011; Jimenez-Rosado et al. 2019). Sugarcane is exploitable for bioplastic production by bacterial sugar assimilation (Pohare et al. 2017).

Finally, oil is a good carbon source for the production of bioplastic. Cottonseed oil (Magar et al. 2015), soybean oil (Park and Kim 2011), crude palm kernel oil, jatropha oil, crude palm oil, palm olein, corn oil, and coconut oil were typically investigated (Wong et al. 2012). Lignocellulosic biomass is another promising resource for bioplastic production avoiding the consumption of food crops. Nevertheless, it requires suitable cost-effective pretreatments for decomposition into sugar monomers (Brodin et al. 2017; Govil 2020).

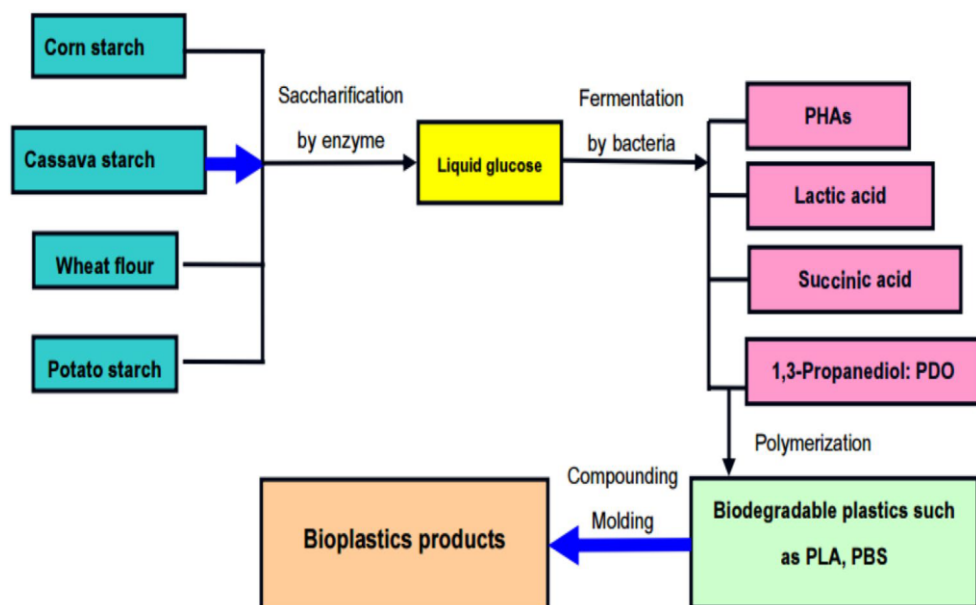


Figure 9: Bioplastic production from starch (Chaisu 2016).

1.5.2 - Organic Waste Sources

Cassava and other crops require large land areas, water, and nutrients. Moreover, they compete with the food supply, and their use to produce bioplastics is not sustainable. Instead, it is interesting to consider the organic waste source to valorize a residue and turn a problem into an opportunity in a circular economy approach (Yadav et al. 2019).

Wastes from the food-processing industry are an important potential source of bioplastics (Tsang 2019; Jogi and Bhat 2020). Vegetable wastes used to produce novel bioplastic films were carrots, radicchio, parsley, and cauliflowers (Perotto 2018). Novel starch- and/or cellulose-based bioplastics were produced from rice straw (Fig. 9), an agricultural waste usually used for bioethanol production (Agustin et al. 2014; Bilo 2018), and other agricultural wastes (Chaisu 2016).

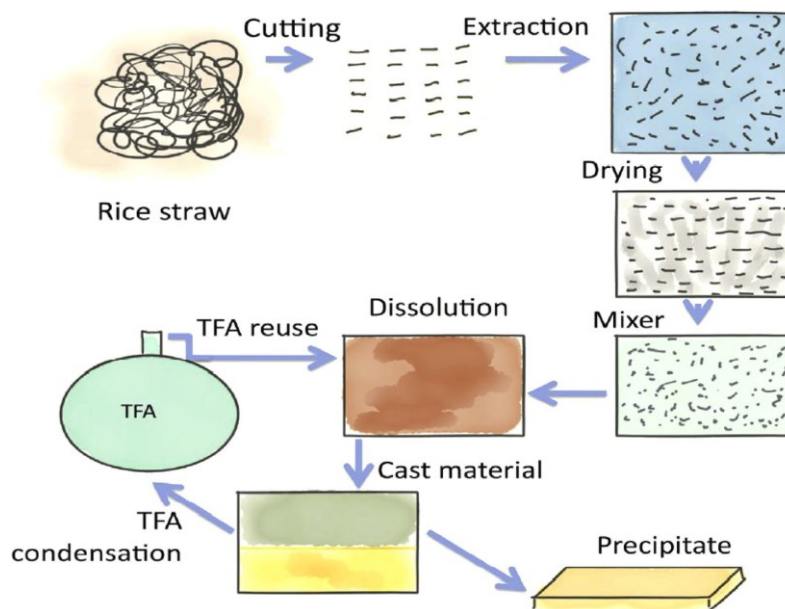


Figure 10: Synthesis of bioplastics from rice straw (TFA: trifluoroacetic acid) (Bilo 2018)

Extrusion of rice bran and kraft lignin—that are industrial by-products of brown rice production and wood pulping process, respectively—produced a bioplastic with good extrudability and mechanical properties (Klanwan et al. 2016).

A residual product of crude oil palm production is an empty fruit bunch, composed of cellulose, hemicellulose, and lignin. Having high cellulose content (36.67%), this

abundant waste could be used to produce bioplastics (Isroi and Panji 2016; Isroi et al. 2017). Microcrystalline cellulose and glycerol were added to keratin from waste chicken feathers to produce biopolymeric films (Ramakrishnan et al. 2018; Sharma et al. 2018). Microcrystalline cellulose was a re-inforcing additive in bioplastic production also from avocado seeds (Sartika et al. 2018), jackfruit seeds (Lubis et al. 2018), and cassava peels (Maulida and Tarigan 2016). Waste cassava peels were investigated in combination with kaffir lime essential oil for future applications in industry and medicine (Masruri et al. 2019). Cocoa pod husk and sugarcane bagasse, which are wastes from the chocolate industry and the sugar industry, respectively, are promising for the production of biodegradable plastic films (Azmin et al. 2020).

Bioplastics could be produced by injection molding from rapeseed oil production by-products, such as press cake or meal (Delgado et al. 2018). New bioplastics were prepared from potato peels and waste potato starch with eggshells and/or chitosan (from exoskeleton seafood wastes) as additives (Kasmuri and Zait 2018; Bezirhan Arikan and Bilgen 2019). Also, banana peels were used to produce a bioplastic with the addition of corn starch, potato starch, sage, and glycerol (Sultan and Johari 2017; Azieyanti et al. 2020). Bloodmeal is a low-value protein-rich by-product from meat processing, that is convertible into a bioplastic material (Low et al. 2014). Bioplastic fibers were fabricated also from gum arabic by electrospinning method (Padil et al. 2019). Polyhydroxyalkanoates (PHA) is a

group of biodegradable plastics produced by microorganisms from renewable sources (Shraddha et al. 2011) by the three pathways in Fig. 10.

Among PHAs sources, researchers investigated chicken feather hydrolysate (Benesova et al. 2017), animal fat waste (Riedel 2015), lignocellulosic biomass hydrolysate (Bhatia 2019), grass biomass (Davis 2013), fruit pomace, waste frying oils (Follonier 2014), olive oil mill pomace (Waller et al. 2012), saponified waste palm oil (Mozejko and Ciesielski 2013), low-quality sludge palm oil (Kang 2017), waste oil palm biomass (Hassan 2013), spent coffee grounds (Nielsen et al. 2017) and other carbon sources (rice straw, maltose, glucose, sugarcane liquor, corn steep liquor, corn stover liquor, cheese whey, waste potato starch, sugar beet molasses, etc.) (Khatami et al. 2021; Marjadi and Dharaiya 2010; Tripathi et al. 2012). Another interesting resource is the organic fraction of municipal solid wastes convertible into PHAs by acidogenic fermentation of pre-treated and hydrolyzed biomass (Ivanov et al. 2015; Ebrahimian et al. 2020).

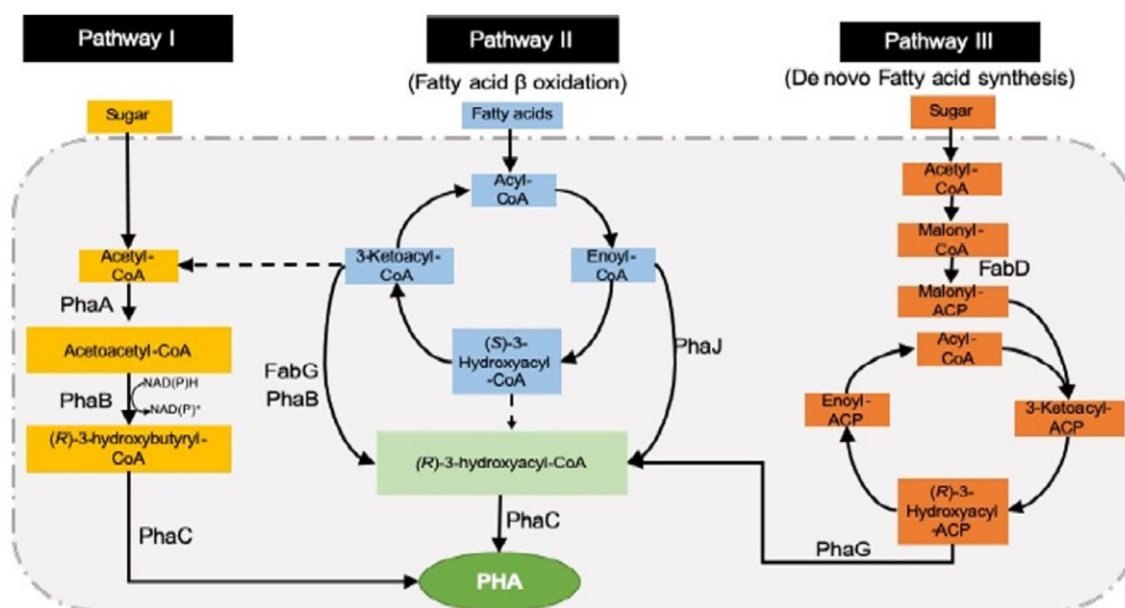


Figure 11: The three metabolic pathways for PHA production (PhaA: β -ketothiolase; PhaB: acetoacetyl coenzyme A (CoA) reductase; PhaC: PHA synthase; FabG: 3- ketoacyl acyl carrier protein (ACP) reductase; PhaG: acyl-ACP-CoA transacylase; PhaJ: enoyl-C ketoacyl acyl carrier protein (ACP) reductase; PhaG: acyl-ACP-CoA transacylase; PhaJ: enoyl-C) (Khatami et al. 2021)

Recent works investigated PHA production from volatile fatty acids, obtained by the anaerobic digestion of waste paper (Al-Battashi 2019; Al Battashi et al. 2020). The most common PHA is polyhydroxybutyrate (PHB), produced from low-cost sugarcane molasses by *Bacillus cereus* (Suryawanshi et al. 2020) or *Staphylococcus epidermidis* (Sarkar et al. 2014), cheap agro-residues by *Bacillus* sp. (Getachew and Woldesenbet 2016), date syrup by *Pseudomonas xiamenensis* (Mostafa et al. 2020), non-food sugars from oil palm frond (Zahari et al. 2015) or biodiesel industry by-products (García 2013) or used cooking oil (Martino 2014) by *Cupriavidus necator*, wheat straw lignocellulosic hydrolysates by *Burkholderia sacchari* (Cesário et al. 2014), wheat bran hydrolysate by *Ralstonia eutropha* (Annamalai and Sivakumar 2016), bakery waste hydrolysate by *Halomonas boliviensis*

(Pleissner 2014). An innovative approach consists of PHB production from landfill methane by methanotrophs (Chidambarampadmavathy et al. 2017).

1.5.3 – Algae-based Sources

Microalgae are a promising alternative source for bioplastics production because of their fast growth and no competition with food (Rahman and Miller 2017). Recently, several works investigated the synthesis of bioplastics from microalgae (Beckstrom et al. 2020; Simonic and Zemljic 2020).

Microalgae could be used directly as biomass to produce bioplastics or indirectly by the extraction of PHBs and starch within microalgae cells. Other approaches include the production of microalgae-polymer blends through compression/hot molding, melt mixing, solvent casting, injection molding, or twin-screw extrusion (Cinar et al. 2020).

The most investigated microalgae were *Chlorella* and *Spirulina*. *Chlorella* seems to have better bioplastic behavior, whereas *Spirulina* showed better blend performance (Zeller et al. 2013). Different species of *Chlorella* were used in biomass-polymer blends containing polymers and additives (Cinar et al. 2020). Moreover, bioplastic may be produced from *Chlorella pyrenoidosa* (Das et al. 2018) and *Chlorella sorokiniana*-derived starch granules (Gifuni et al.

2017). Similar to *Chlorella*, *Spirulina* was investigated for bioplastic production (Cinar et al. 2020). For example, a bioplastic-based film was produced from salt-rich

Spirulina sp. residues with the addition of polyvinyl alcohol (Zhang et al. 2020). Another bioplastic was prepared from *Spirulina platensis*, showing good biodegradability (Maheshwari and Ahilandeswari 2011). Other microalgae or cyanobacteria used to produce bioplastics were *Chlorogloea fritschii* (Monshupanee et al. 2016), *Calothrix scytonemicola* (Johnsson and Steuer 2018), *Neochloris oleoabundans* (Johnsson and Steuer 2018), residual *Nannochloropsis* after oil extraction (Yan 2016), *Nannochloropsis gaditana* (Torres et al. 2015; Fabra et al. 2017), *Phaeodactylum tricornutum* (Hempel 2011), and *Scenedesmus almeriensis* (Johnsson and Steuer 2018). Ten green microalgae were screened for starch production and starch-based bioplastic development.

C. reinhardtii 11-32A resulted in the most promising starchproducing strain with interesting plasticization properties with glycerol at 120 °C (Mathiot et al. 2019).

A microalgae consortium cultivated and harvested in a wastewater treatment plant was used as biomass to be mixed with glycerol as a plasticizer to obtain bioplastics (López Rocha et al. 2019).

New composites were formed by combination of microalgal biomass and petroleum. (Cinar et al. 2020; Chia et al. 2020). The PHB production is feasible in microalgae used as bioreactors by the introduction of bacterial pathways into microalgal cells (Hempel 2011) (Fig. 11).

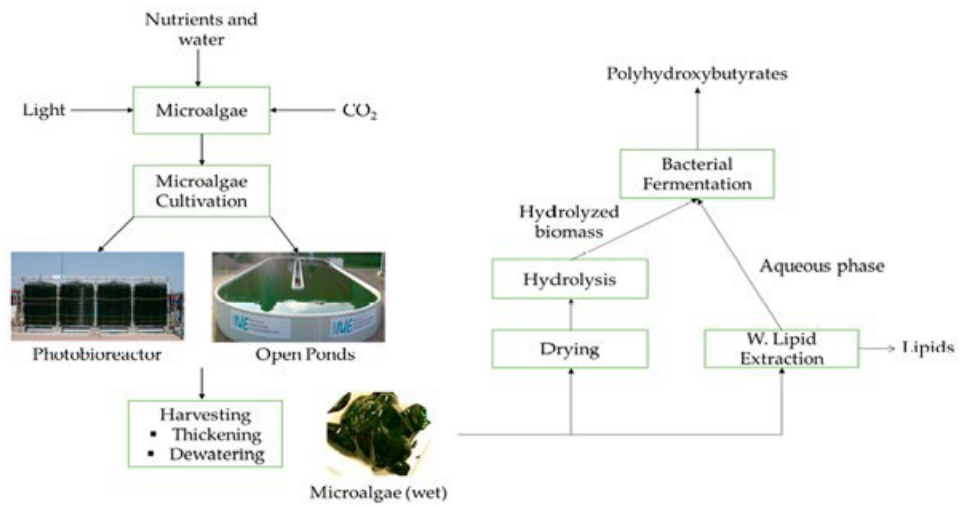


Figure 12: PHB production from microalgae (Cinar et al. 2020).

Besides microalgae, macroalgae or seaweeds are aquatic plants rich in polysaccharides and potentially promising sources of bioplastics (Rajendran et al. 2012; Thiruchelvi et al. 2020). The whole red macroalga *Kappaphycus alvarezii* was recently investigated to produce a bioplastic film with the addition of polyethylene glycol as a plasticizer for food packaging applications (Sudhakar et al. 2020).

Table 5: Advantages and disadvantages of different bioplastic source categories.

Bioplastic source category	Advantages	Disadvantages
Agricultural crops	<ul style="list-style-type: none"> Renewability Abundance Closed carbon cycle Mature processing technology in large scale 	<ul style="list-style-type: none"> Threat to food security and eco-systems Use of large fertile land, water, and nutrients Negative contribute to the eco-balance Conflict food vs bioenergy/ biofuels/ biomaterials Long-term unsustainability Necessary pre-treatment of lignocellulosic biomass Long time for production
Organic wastes	<ul style="list-style-type: none"> Abundant low-cost/free sources Management of environmentally problematic wastes Conversion of wastes to valuable resources No competition with food and feed 	<ul style="list-style-type: none"> Possible localization and/or seasonability of wastes Cost and complexity of logistic operations Necessary pre-treatment of lignocellulosic biomass
Microalgae	<ul style="list-style-type: none"> Fast growth rates High productivity. Cultivation on non-arable land Utilization of degraded and saline water sources Integration with waste streams Wastewater remediation Broad environmental tolerance Reduced competition with food 	<ul style="list-style-type: none"> Large volumes of water are required for industrial scale Expensive technology of cultivation, harvesting, extraction and fractionation of components in a large scale High energy costs of cultivation and processing
Macroalgae	<ul style="list-style-type: none"> High biomass Cost-effective Easily cultivated in natural environment Able to grow in wide range of environments Harvested throughout the year 	<ul style="list-style-type: none"> Biotechnological and genetic engineering techniques required Premature large-scale processing technology
Wastewaters	<ul style="list-style-type: none"> High availability Abundant and cheap No competition with food and feed A waste becomes a resource 	<ul style="list-style-type: none"> Complex new technologies, generating further wastes Low production yield

1.6 – Conclusions

The research, application opportunities, sourcing and sustainability of bioplastics production have been discussed to clarify the field. To further advance the application of bioplastic, it is very necessary to manage carefully the waste disposal. Recycling appears the best solution from that point, for disposal of the bio-based product to maximize the environmental footprint as well as reduce the renewable resources consumption.

Recycling of bioplastics leads to an overall decrease of environmental impact which may be associated with the production and disposal of the bioplastic itself. It is worth noting that due to the improper management and applications of bioplastics, the information reported in this paper can be useful for environmental reliability. PHA materials are the

main resource to substitute conventional plastic use in most of the engineering applications fields. Nowadays, the PHA costs of production are too high, but further research on technology and sourcing can reduce manufacturing costs for versatility and heterogeneity and strengthen the applications of bioplastics.

Funding: *Open access funding provided by UniversitA della Calabria within the CRUI-CARE Agreement.*

Open Access: *This article is licensed under a Creative Commons Attribution 4.0 International License, which permits use, sharing, adaptation, distribution and reproduction in any medium or format, as long as you give appropriate credit to the original author(s) and the source, provide a link to the Creative Commons licence, and indicate if changes were made. The images or other third party material in this article are included in the article's Creative Commons licence, unless indicated otherwise in a credit line to the material. If material is not included in the article's Creative Commons licence and your intended use is not permitted by statutory regulation or exceeds the permitted use, you will need to obtain permission directly from the copyright holder. To view a copy of this licence, visit <http://creativecommons.org/licenses/by/4.0/>.*

1.7 – References (Chap.1)

- Ahamed A et al (2021) Life cycle assessment of plastic grocery bags and their alternatives in cities with confined waste management structure: a Singapore case study. *J Clean Prod* 278:123956
- Agustin MB, Ahmmad B, Alonzo SMM, Patriana FM (2014) Bioplastic based on starch and cellulose nanocrystals from rice straw. *J Reinf Plast Compos* 33(24):2205–2213. <https://doi.org/10.1177/0731684414558325>
- Al Battashi H, Al-Kindi S, Gupta VK, Sivakumar N (2020) Polyhydroxyalkanoate (PHA) production using volatile fatty acids derived from the anaerobic digestion of waste paper. *J Polym Environ* 1:10. <https://doi.org/10.1007/s10924-020-01870-0>
- Al-Battashi H et al (2019) Production of bioplastic (poly-3-hydroxybutyrate) using waste paper as a feedstock: optimization of enzymatic hydrolysis and fermentation employing *Burkholderia sacchari*. *J Clean Prod* 214:236–247. <https://doi.org/10.1016/j.jclepro.2018.12.239>
- Algieri C, Drioli E, Donato L (2013) Development of mixed matrix membranes for controlled release of ibuprofen. *J Appl Polym Sci* 128(1):754–760. <https://doi.org/10.1002/app.38102>
- Algieri C, Donato L, Giorno L (2017) Tyrosinase immobilized on a hydrophobic membrane. *Biotechnol Appl Biochem* 64(1):92–99. <https://doi.org/10.1002/bab.1462>
- Algieri C, Donato L, Bonacci P, Giorno L (Jul. 2012) Tyrosinase immobilised on polyamide tubular membrane for the L-DOPA production: Total recycle and continuous reactor study. *Biochem Eng J* 66:14–19. <https://doi.org/10.1016/j.bej.2012.03.013>
- Andersen HJ, Rasmussen MA (1992) Interactive packaging as protection against photodegradation of the colour of pasteurized, sliced ham. *Int J Food Sci Technol* 15:14. <https://doi.org/10.1111/j.1365-2621.1992.tb01172.x>
- Andreas Detzel CDG, Kauertz K (2015) Study of the environmental impacts of packagings made of biodegradable plastics. <http://www.uba.de/uba-info-medien/4446.html>
- Andreas Detzel MKAO (2006) Assessment of bio-based packaging materials. In: *Renewables-based technology: sustainability assessment*, pp. 281–297, 2006.
- Annamalai N, Sivakumar N (2016) Production of polyhydroxybutyrate from wheat bran hydrolysate using *Ralstonia eutropha* through microbial fermentation. *J Biotechnol* 237:13–17. <https://doi.org/10.1016/j.jbiotec.2016.09.001>
- Arikan EB, Ozsoy D (2011) Waste to bioplastic: bioplastic production from potato processing industry wastewater
- Asrofi M, Sapuan SM, Ilyas RA, Ramesh M (2020) Characteristic of composite bioplastics from tapioca starch and sugarcane bagasse fiber: Effect of time duration of ultrasonication (Bath-Type). *Mater Today Proc*. <https://doi.org/10.1016/j.matpr.2020.07.254>
- Ateş M, Kuz P (2020) Starch-based bioplastic materials for packaging industry. *J Sustain Constr Mater Technol* 5(1):399–406. <https://doi.org/10.29187/jscmt.2020.44>
- Auras R, Harte B, Selke S (2004) An overview of polylactides as packaging materials. *Macromol Biosci*. <https://doi.org/10.1002/mabi.200400043>
- Azieyanti NA, Amirul A, Othman SZ, Misran H (2020) Mechanical and morphology studies of bioplastic-based banana peels. *J Phys Conf Ser* 1529:032091. <https://doi.org/10.1088/1742-6596/1529/3/032091>
- Azmin SNHM, Binti NA, Hayat M, Nor MSM (2020) Development and characterization of food packaging bioplastic film from cocoa pod husk cellulose incorporated with sugarcane bagasse fibre. *J*

- Bioresour Bioprod 5:248–255. <https://doi.org/10.1016/j.jobab.2020.10.003>
- Babalola OA, Olorunnisola AO (2019) Evaluation of coconut (*Cocos nucifera*) husk fibre as a potential reinforcing material for bioplastic production. *Mater Res Proc* 11:195–200. <https://doi.org/10.21741/9781644900178-14>
- Baldino N, Mileti O, Lupi FR, Gabriele D (2018) Rheological surface properties of commercial citrus pectins at different pH and concentration. *LWT*. <https://doi.org/10.1016/j.lwt.2018.03.037>
- Bastioli C (2001) Global status of the production of biobased packaging materials. *Starch/Staerke*. [https://doi.org/10.1002/1521-379X\(200108\)53:8%3c351::AID-STAR351%3e3.0.CO;2-R](https://doi.org/10.1002/1521-379X(200108)53:8%3c351::AID-STAR351%3e3.0.CO;2-R)
- Beckstrom BD, Wilson MH, Crocker M, Quinn JC (2020) Bioplastic feedstock production from microalgae with fuel co-products: a techno-economic and life cycle impact assessment. *Algal Res* 46:101769. <https://doi.org/10.1016/j.algal.2019.101769>
- Ben M, Mato T, Lopez A, Vila M, Kennes C, Veiga MC (2011) Bioplastic production using wood mill effluents as feedstock. *Water Sci Technol* 63(6):1196–1202. <https://doi.org/10.2166/wst.2011.358>
- Benesova P, Kucera D, Marova I, Obruca S (2017) Chicken feather hydrolysate as an inexpensive complex nitrogen source for PHA production by *Cupriavidus necator* on waste frying oils. *Lett Appl Microbiol* 65(2):182–188. <https://doi.org/10.1111/lam.12762>
- Bezirhan Arian E, Bilgen HD (2019) Production of bioplastic from potato peel waste and investigation of its biodegradability. *Int Adv Res Eng J* 03(02):93–97. <https://doi.org/10.35860/iarej.420633>
- Bhatia SK et al (2019) Bioconversion of plant biomass hydrolysate into bioplastic (polyhydroxyalkanoates) using *Ralstonia eutropha* 5119. *Bioresour Technol* 271:306–315. <https://doi.org/10.1016/j.biortech.2018.09.122>
- Bilo F et al (2018) A sustainable bioplastic obtained from rice straw. *J Clean Prod* 200:357–368. <https://doi.org/10.1016/j.jclepro.2018.07.252>
- Bioplastics - Facts and Figures (2021)
- Blakistone B, Sand CK (2008) Using sustainable packaging technologies to respond to consumer, retailer, and seafood industry needs. <https://doi.org/10.4027/isscp.2008.16>
- Bluemink ED, Van Nieuwenhuijzen AF, Wypkema E, Uijterlinde CA (2016) Bio-plastic (poly-hydroxy-alkanoate) production from municipal sewage sludge in the Netherlands: A technology push or a demand driven process? *Water Sci Technol* 74(2):353–358. <https://doi.org/10.2166/wst.2016.191>
- Brodin M, Vallejos M, Opedal MT, Area MC, Chinga-Carrasco G (2017) Lignocellulosics as sustainable resources for production of bioplastics—a review. *J Clean Prod* 162:646–664. <https://doi.org/10.1016/j.jclepro.2017.05.209>
- Candamano S, Frontera P, Macario A, Crea F (2017) Effect of commercial LTA type zeolite inclusion in properties of structural epoxy adhesive. *Adv Sci Lett*. <https://doi.org/10.1166/asl.2017.9071>
- Candamano S, Crea F, Iorfida A (2020) Mechanical characterization of basalt fabric-reinforced alkali-activated matrix composite: a preliminary investigation. *Appl Sci*. <https://doi.org/10.3390/AP10082865>
- Candamano S, Crea F, Coppola L, De Luca P, Coffetti D (2021) Influence of acrylic latex and pre-treated hemp fibers on cement based mortar properties. *Constr Build Mater*. <https://doi.org/10.1016/j.conbuilmat.2020.121720>
- Carlozzi P, Giovannelli A, Traversi ML, Touloupakis E (2020) Poly(3-hydroxybutyrate) bioproduction in a two-step sequential process using wastewater. *J Water Process Eng*. <https://doi.org/10.1016/j.jwpe.2020.101700>
- Cesario MT, Raposo RS, de Almeida MCMD, van Keulen F, Ferreira BS, da Fonseca MMR (2014) Enhanced bioproduction of poly-3-hydroxybutyrate from wheat straw lignocellulosic

- hydrolysates. *N Biotechnol* 31(1):104–113. <https://doi.org/10.1016/j.nbt.2013.10.004>
- Chaisu K (2016) Bioplastic Industry from Agricultural Waste in Thailand. *J Adv Agric Technol* 3(4):310–313. <https://doi.org/10.18178/joaat.3.4.310-313>
- Chia WY, Ying Tang DY, Khoo KS, Kay Lup AN, Chew KW (2020) Nature's fight against plastic pollution: algae for plastic biodegradation and bioplastics production. *Environ Sci Ecotechnol* 4:100065. <https://doi.org/10.1016/j.esec.2020.100065>
- Chidambarampadmavathy K, Karthikeyan OP, Heimann K (2017) Sustainable bio-plastic production through landfill methane recycling. *Renew Sustain Energy Rev* 71:555–562. <https://doi.org/10.1016/j.rser.2016.12.083>
- Cinar SO, Chong ZK, Kucuker MA, Wiecek N, Cengiz U, Kuchta K (2020) Bioplastic production from microalgae: A review. *Int J Environ Res Public Health* 17:3842. <https://doi.org/10.3390/ijerph17113842>
- Colwill JA, Wright EI, Rahimifard S, Clegg AJ (2012) Bioplastics in the context of competing demands on agricultural land in 2050. *Int J Sustain Eng.* <https://doi.org/10.1080/19397038.2011.602439>
- Das SK, Sathish A, Stanley J (2018) Production of biofuel and bioplastic from *Chlorella pyrenoidosa*. *Mater Today Proc* 5(8):16774–16781. <https://doi.org/10.1016/j.matpr.2018.06.020>
- Dasgupta J, Singh A, Kumar S, Sikder J, Chakraborty S, Curcio S, Arafat HA (2016) Poly (sodium-4-styrenesulfonate) assisted ultrafiltration for methylene blue dye removal from simulated wastewater: optimization using response surface methodology. *J Environ Chem Eng* 4(2):2008–2022. <https://doi.org/10.1016/j.jece.2016.03.033>
- Davis R et al (2013) Conversion of grass biomass into fermentable sugars and its utilization for medium chain length polyhydroxyalkanoate (mcl-PHA) production by *Pseudomonas* strains. *Bioresour Technol* 150:202–209. <https://doi.org/10.1016/j.biortech.2013.10.001>
- De Luca P, Pane L, Vuono D, Siciliano C, Candamano S, Nagy JB (2017) Preparation and characterization of natural glues with carbon nanotubes. *Environ Eng Manag J.* <https://doi.org/10.30638/eemj.2017.181>
- Delgado M, Felix M, Bengoechea C (2018) Development of bioplastic materials: from rapeseed oil industry by products to added-value biodegradable biocomposite materials. *Ind Crop Prod* 125:401–407. <https://doi.org/10.1016/j.indcrop.2018.09.013>
- Delhaize (2007) “No Title http://www.delhaize.be/_webdata/pressreleases/_NL/Pr070829-hoevekip%20bourgognel-nl-sdl%204.pdf,” 2007, [Online]. Available: http://www.delhaize.be/_webdata/pressreleases/_NL/Pr070829-hoevekip%2520bourgognel-nl-sdl%25204.pdf.
- Diez-Pascual AM (2019) Synthesis and applications of biopolymer composites. *Int J Mol Sci.* <https://doi.org/10.3390/ijms20092321>
- Ebrahimian F, Karimi K, Kumar R (2020) Sustainable biofuels and bioplastic production from the organic fraction of municipal solid waste. *Waste Manag* 116:40–48. <https://doi.org/10.1016/j.wasman.2020.07.049>
- El-malek FA, Khairy H, Farag A, Omar S (2020) The sustainability of microbial bioplastics, production and applications. *Int J Biol Macromol* 157:319–328. <https://doi.org/10.1016/j.ijbmac.2020.04.076>
- Emadian SM, Onay TT, Demirel B (2017) Biodegradation of bioplastics in natural environments. *Waste Manag* 59:526–536. <https://doi.org/10.1016/j.wasman.2016.10.006>
- Fabra MJ, Martinez-Sanz M, Gomez-Mascaraque LG, Coll-Marques JM, Martinez JC, Lopez-Rubio A (2017) Development and characterization of hybrid corn starch-microalgae films: Effect of ultrasound pre-treatment on structural, barrier and mechanical performance. *Algal Res* 28:80–87. <https://doi.org/10.1016/j.algal.2017.10.010>

- Follonier S et al (2014) Fruit pomace and waste frying oil as sustainable resources for the bioproduction of medium-chain-length polyhydroxyalkanoates. *Int J Biol Macromol* 71:42–52. <https://doi.org/10.1016/j.ijbio.mac.2014.05.061>
- Fontana JD et al (1990) *Acetobacter cellulose pellicle* as a temporary skin substitute. *Appl Biochem Biotechnol*. <https://doi.org/10.1007/BF02920250>
- Fricke A, Murphy JD, O’Leary ND (2019) Dairy processing wastewater as a feedstock for microbial bioplastic production. *Access Microbiol* 1(1A):892. <https://doi.org/10.1099/acmi.ac2019.po0580>
- Garcia IL et al (2013) Evaluation of by-products from the biodiesel industry as fermentation feedstock for poly(3-hydroxybutyrate-co-3-hydroxyvalerate) production by *Cupriavidus necator*. *Bioresour Technol* 130:16–22. <https://doi.org/10.1016/j.biortech.2012.11.088>
- Getachew A, Woldesenbet F (2016) Production of biodegradable plastic by polyhydroxybutyrate (PHB) accumulating bacteria using low cost agricultural waste material. *BMC Res Notes* 9:509. <https://doi.org/10.1186/s13104-016-2321-y>
- Gifuni I, Olivieri G, Krauss IR, D’Errico G, Pollio A, Marzocchella A (2017) Microalgae as new sources of starch: Isolation and characterization of microalgal starch granules. *Chem Eng Trans* 57:1423–1428. <https://doi.org/10.3303/CET1757238>
- Gokce E (2018) Rethinking sustainability: A research on starch based bioplastic. *J Sustain Constr Mater Technol* 3(3):249–260. <https://doi.org/10.29187/jscmt.2018.28>
- Govil T et al (2020) Lignocellulosic feedstock: a review of a sustainable platform for cleaner production of nature’s plastics. *J Clean Prod* 270:122521. <https://doi.org/10.1016/j.jclepro.2020.122521>
- Gowda V, Shivakumar S (2014) Agrowaste-based polyhydroxyalkanoate (PHA) production using hydrolytic potential of *Bacillus thuringiensis* IAM 12077. *Brazil Arch Biol Technol* 57(1):55–61. <https://doi.org/10.1590/S1516-89132014000100009>
- Grundmann V, Wonschik C-R (2011) Hydrolyse und anaerobe Co-Vergärung verschiedener biologisch abbaubarer Kunststoffe. MULL und ABFALL. <https://doi.org/10.37307/j.1863-9763.2011.07.05>
- Gumrah Dumanli A (2016) Nanocellulose and its composites for biomedical applications. *Curr Med Chem*. <https://doi.org/10.2174/0929867323666161014124008>
- Hamidon N et al (2018) Potential of production bioplastic from potato starch. *Sustain Environ Technol* 1:115–123 Hassan MA et al (2013) Sustainable production of polyhydroxyalkanoates from renewable oil-palm biomass. *Biomass Bioenerg* 50:1–9. <https://doi.org/10.1016/j.biombioe.2012.10.014>
- Haugaard VK, Udsen AM, Mortensen G, Hoegh L, Petersen K, Monahan F (2001) Potential food applications of biobased materials. An EU-concerted action project. *Starch/Staerke*. [https://doi.org/10.1002/1521-379X\(200105\)53:5%3c189::AID-STAR189%3e3.0.CO;2-3](https://doi.org/10.1002/1521-379X(200105)53:5%3c189::AID-STAR189%3e3.0.CO;2-3)
- Hempel F et al (2011) Microalgae as bioreactors for bioplastic production. *Microb Cell Fact* 10:2–7. <https://doi.org/10.1186/1475-2859-10-81>
- Highlights in Bioplastics, Website European bioplastics (2021)
- Plastics Europe (2021) Home :: PlasticsEurope
- Hwang KR, Jeon W, Lee SY, Kim MS, Park YK (2020) Sustainable bioplastics: Recent progress in the production of bio-building blocks for the bio-based next-generation polymer PEF. *Chem Eng J* 390:124636. <https://doi.org/10.1016/j.cej.2020.124636>
- Iben Nasser I, Algieri C, Garofalo A, Drioli E, Ahmed C, Donato L (2016) Hybrid imprinted membranes for selective recognition of quercetin. *Sep Purif Technol* 163:331–340. <https://doi.org/10.1016/j.seppur.2016.03.015>

- Isroi AC, Panji T (2016) Bioplastic production from oil palm empty fruit bunch. In: International Conference on Biomass, 2016.
- Isroi AC, Panji T, Wibowo NA, Syamsu K (2017) "Bioplastic production from cellulose of oil palm empty fruit bunch. IOP Conf Ser Earth Environ Sci. 65:11. <https://doi.org/10.1088/1755-1315/65/1/012011>
- Ivanov V, Stabnikov V, Ahmed Z, Dobrenko S, Saliuk A (2015) Production and applications of crude polyhydroxyalkanoate containing bioplastic from the organic fraction of municipal solid waste. *Int J Environ Sci Technol* 12:725–738. <https://doi.org/10.1007/s13762-014-0505-3>
- Jabeen N, Majid I, Nayik GA (2015) Bioplastics and food packaging: A review. *Cogent Food Agric*. <https://doi.org/10.1080/23311932.2015.1117749>
- Jager A (2010) Ingeo™ polylactide een natuurlijke keus. In: Presentation given at VMT conference: green packaging." 2010
- Jiang Y, Marang L, Tamis J, van Loosdrecht MCM, Dijkman H, Kleerebezem R (2012) Waste to resource: Converting paper mill wastewater to bioplastic. *Water Res* 46:5517–5530. <https://doi.org/10.1016/j.watres.2012.07.028>
- Jimenez-Rosado M, Zarate-Ramirez LS, Romero A, Bengoechea C, Partal P, Guerrero A (2019) Bioplastics based on wheat gluten processed by extrusion. *J Clean Prod* 239:117994. <https://doi.org/10.1016/j.jclepro.2019.117994>
- Jimenez-Rosado M, Bouroudian E, Perez-Puyana V, Guerrero A, Romero A (2020) Evaluation of different strengthening methods in the mechanical and functional properties of soy protein based bioplastics. *J Clean Prod*. <https://doi.org/10.1016/j.jclepro.2020.121517>
- Jogi K, Bhat R (2020) Valorization of food processing wastes and by-products for bioplastic production. *Sustain Chem Pharm* 18:100326. <https://doi.org/10.1016/j.scp.2020.100326>
- Johnsson N, Steuer F (2018) Bioplastic material from microalgae: extraction of starch and PHA from microalgae to create a bioplastic material. Stockholm
- Jung YK, Lee SY (2011) Efficient production of polylactic acid and its copolymers by metabolically engineered *Escherichia coli*. *J Biotechnol* 151(1):94–101. <https://doi.org/10.1016/j.jbiotec.2010.11.009>
- Kang DK et al (2017) Production of polyhydroxyalkanoates from sludge palm oil using *Pseudomonas putida* S12. *J Microbiol Biotechnol* 27(5):990–994. <https://doi.org/10.4014/jmb.1612.12031>
- Kasmuri N, Zait MSA (2018) Enhancement of bioplastic using eggshells and chitosan on potato starch based. *Int J Eng Technol* 7(3):110–115
- Khatami K, Perez-Zabaleta M, Owusu-Agyeman I, Cetecioglu Z (2021) Waste to bioplastics: How close are we to sustainable polyhydroxyalkanoates production? *Waste Manag* 119:374–388. <https://doi.org/10.1016/j.wasman.2020.10.008>
- Klanwan Y, Kunanopparat T, Menut P, Siriwanayotin S (2016) Valorization of industrial by-products through bioplastic production: defatted rice bran and kraft lignin utilization. *J Polym Eng* 36(5):529–536. <https://doi.org/10.1515/polymeng-2015-0301>
- Koide S, Shi J (2007) Microbial and quality evaluation of green peppers stored in biodegradable film packaging. *Food Control*. <https://doi.org/10.1016/j.foodcont.2006.07.013>
- Kumar S, Thakur K (2017) Bioplastics - classification, production and their potential food applications. *J Hill Agric*. <https://doi.org/10.5958/2230-7338.2017.00024.6>
- Mugdhal et al (2012) Options to improve the biodegradability requirements in the Packaging Directive FINAL REPORT," 2012
- Li J, Wan Y, Li L, Liang H, Wang J (2009) Preparation and characterization of 2,3-dialdehyde bacterial cellulose for potential biodegradable tissue engineering scaffolds. *Mater Sci Eng C*. <https://doi.org/10.1016/j.msec.2009.01.006>

- Liu L, Son M, Chakraborty S, Bhattacharjee C, Choi H (2013) Fabrication of ultra-thin polyelectrolyte/carbon nanotube membrane by spray-assisted layer-by-layer technique: characterization and its anti-protein fouling properties for water treatment. *Desalin Water Treat* 51(31–33):6194–6200. <https://doi.org/10.1080/19443994.2013.780767>
- Liu F, Li J, Zhang XL (2019) Bioplastic production from wastewater sludge and application. *IOP Conf Ser Earth Environ Sci* 344:012071. <https://doi.org/10.1088/1755-1315/344/1/012071>
- Lopez Rocha CJ, Alvarez-Castillo E, Estrada Yanez MR, Bengoechea C, Guerrero A, Orta Ledesma MT (2020) Development of bioplastics from a microalgae consortium from wastewater. *J Environ Manag* 263:19. <https://doi.org/10.1016/j.jenvman.2020.110353>
- Low A, Verbeek CJR, Lay MC (2014) Treating bloodmeal with peracetic acid to produce a bioplastic feedstock. *Macromol Mater Eng* 299:75–84. <https://doi.org/10.1002/mame.201200447>
- Lu Y, Larock RC (2009) Novel polymeric materials from vegetable oils and vinyl monomers: Preparation, properties, and applications. *Chemoschem*. <https://doi.org/10.1002/cssc.200800241>
- Lubis M, Gana A, Maysarah S, Ginting MHS, Harahap MB (2018) Production of bioplastic from jackfruit seed starch (*Artocarpus heterophyllus*) reinforced with microcrystalline cellulose from cocoa pod husk (*Theobroma cacao* L.) using glycerol as plasticizer. *IOP Conf Ser Mater Sci Eng* 309:012100. <https://doi.org/10.1088/1757-899X/309/1/012100>
- Magar SP, Ingle AB, Ganorkar RN (2015) Production of bioplastic (PHA) from emulsified cotton seed oil medium by *Ralstonia* Spp. *Int J Eng Res Gen Sci* 3(1):436–441
- Magnocavallo C, Baratti C, Lavezzari M, Pamparana F, Pellegrini C (1993) The use of a synthetic film (Bioprocess) in abrasions and second degree burns. Preliminary study in the emergency room.
- Minerva Chir Maheshwari V, Ahilandeswari NU (2011) Production of bioplastic using *Spirulina platensis* and comparison with commercial plastic. *Res Environ Life Sci* 4(3):133–136
- Mannina G, Presti D, Montiel-Jarillo G, Suarez-Ojeda ME (2019) Bioplastic recovery from wastewater: a new protocol for polyhydroxyalkanoates (PHA) extraction from mixed microbial cultures. *Bioresour Technol* 282:361–369. <https://doi.org/10.1016/j.biortech.2019.03.037>
- Marjadi D, Dharaiya N (2010) Bioplastic: a better alternative for sustainable future. *Everyman's Sci XLV*(2):90–92
- Martino L et al (2014) Recovery of amorphous polyhydroxybutyrate granules from *Cupriavidus necator* cells grown on used cooking oil. *Int J Biol Macromol* 71:117–123. <https://doi.org/10.1016/j.ijbio mac.2014.04.016>
- Masruri M, Azhar AZ, Rosyada I, Febrianto A (2019) The effect of kaffir lime (*Citrus hystrix* DC) essential oil on bioplastic derived from cassava peel waste. *J Phys Conf Ser* 1374:012015. <https://doi.org/10.1088/1742-6596/1374/1/012015>
- Mathiot C, Ponge P, Gallard B, Sassi JF, Delrue F, Le Moigne N (2019) Microalgae starch-based bioplastics: Screening of ten strains and plasticization of unfractionated microalgae by extrusion. *Carbohydr Polym* 208:142–151. <https://doi.org/10.1016/j.carbpol.2018.12.057>
- Maulida MS, Tarigan P (2016) Production of starch based bioplastic from cassava peel reinforced with microcrystalline cellulose avicel PH101 using sorbitol as plasticizer. *J Phys Conf Ser* 710:012012. <https://doi.org/10.1088/1742-6596/710/1/012012>
- Medeirosgarciaalcantara J, Distante F, Storti G, Moscatelli D, Morbidelli M, Sponchioni M (2020) Current trends in the production of biodegradable bioplastics: the case of polyhydroxyalkanoates. *Biotechnol Adv* 42:107582. <https://doi.org/10.1016/j.biotechadv.2020.107582>
- Meereboer KW, Misra M, Mohanty AK (2020) Review of recent advances in the biodegradability of polyhydroxyalkanoate (PHA) bioplastics and their composites. *Green Chem*

22(17):5519-5558. <https://doi.org/10.1039/d0gc01647k>

Mohammed L, Ansari MNM, Pua G, Jawaid M, Islam MS (2015) A review on natural fiber reinforced polymer composite and its applications. *Int J Polym Sci*. <https://doi.org/10.1155/2015/243947>

Mojibayo I, Samson AO, Johnson OY, Joshua IOASA (2020) A preliminary investigation of cassava starch potentials as natural polymer in bioplastic production". *Am J Interdiscip Innov Res* 02(09):31–39. <https://doi.org/10.37547/tajir/volum e02issue09- 05>

Monshupanee T, Nimdach P, Incharoensakdi A (2016) Two-stage (photoautotrophy and heterotrophy) cultivation enables efficient production of bioplastic poly-3-hydroxybutyrate in auto-sedimenting cyanobacterium. *Sci Rep* 6(1):1–9. <https://doi.org/10.1038/srep37121>

Mose BR, Maranga SM (2011) A Review on Starch Based Nanocomposites for Bioplastic Materials. *J Mater Sci Eng B* 1:239–245

Mostafa YS, Alrumman SA, Alamri SA, Otaif KA, Mostafa MS, Alfaify AM (2020) Bioplastic (poly-3-hydroxybutyrate) production by the marine bacterium *Pseudomonas xiamenensis* through date syrup valorization and structural assessment of the biopolymer. *Sci Rep* 10:8815. <https://doi.org/10.1038/s41598-020-65858-5>

Mozejko J, Ciesielski S (2013) Saponified waste palm oil as an attractive renewable resource for methyl-polyhydroxyalkanoate synthesis. *J Biosci Bioeng* 116(4):485–492. <https://doi.org/10.1016/j.jbiosc.2013.04.014>

Nachwachsende F, Agency VFNR (2020) *Bioplastics - Plants, Raw Materials, Products.* Fachagentur Nachwachsende Rohstoffe e.V. (FNR) - Agency for Renewable Resources, Gulzow-Pruzen, 2020

Naik SN, Goud VV, Rout PK, Dalai AK (2010) Production of first and second generation biofuels: a comprehensive review. *Renew Sustain Energy Rev*. <https://doi.org/10.1016/j.rser.2009.10.003>

Nakanishi A, Iritani K, Sakihama Y (2020) Developing Neo-bioplastics for the Realization of Carbon Sustainable Society. *J Nanotechnol Nanomater* 1(2):72–85. <https://doi.org/10.33696/nanot echnol.1.010>

Narancic T, Cerrone F, Beagan N, Oconnor KE (2020) Recent advances in bioplastics: application and biodegradation. *Polymers (Basel)*. <https://doi.org/10.3390/POLYM12040920>

Nielsen C, Rahman A, Rehman AU, Walsh MK, Miller CD (2017) Food waste conversion to microbial polyhydroxyalkanoates. *Microb Biotechnol* 10(6):1338–1352. <https://doi.org/10.1111/1751-7915.12776>

Ojumu TV, Yu J, Solomon BO (2004) Production of polyhydroxyalkanoates, a bacterial biodegradable polymer. *Afr J Biotechnol* 3(1):18–24

Padil VVT, Senan C, Waclawek S, Černik M, Agarwal S, Varma RS (2019) Bioplastic fibers from gum arabic for greener food wrapping applications. *ACS Sustain Chem Eng* 7:5900–5911. <https://doi.org/10.1021/acssu.schem.eng.8b05896>

Parisi OI et al (2015) Controlled release of sunitinib in targeted cancer therapy: smart magnetically responsive hydrogels as restricted access materials. *RSC Adv*. <https://doi.org/10.1039/c5ra12229e>

Parisi OI et al (2018) Molecularly imprinted microrods via mesophase polymerization. *Molecules*. <https://doi.org/10.3390/molecules23010063>

Park DH, Kim BS (2011) Production of poly(3-hydroxybutyrate) and poly(3-hydroxybutyrate-co-4-hydroxybutyrate) by *Ralstonia eutropha* from soybean oil. *N Biotechnol* 28(6):719–724. <https://doi.org/10.1016/j.nbt.2011.01.007>

Pepe Sciarria T et al (2018) Bio-electrorecycling of carbon dioxide into bioplastics. *Green Chem*. 20(17):4058–4066. <https://doi.org/10.1039/c8gc01771a>

Perotto G et al (2018) Bioplastics from vegetable waste: Via an ecofriendly water-based process. *Green Chem* 20(4):894–902. <https://doi.org/10.1039/c7gc03368k>

- Philp JC, Bartsev A, Ritchie RJ, Baucher M-A, Guy K (2013) Bioplastics science from a policy vantage point. *N Biotechnol*. <https://doi.org/10.1016/j.nbt.2012.11.021>
- Picheth GF et al (2017) Bacterial cellulose in biomedical applications: a review. *Int J Biol Macromol*. <https://doi.org/10.1016/j.ijbio.2017.05.171>
- Pilla S (2011) *Handbook of bioplastics and biocomposites engineering applications*. 2011
- Pittmann T, Menzel U, Steinmetz H (2013) Development of a process to produce bioplastic at municipal wastewater treatment plants. In: *Conf. Pap.*, 2013
- Pleissner D et al (2014) Fermentative polyhydroxybutyrate production from a novel feedstock derived from bakery waste. *Biomed Res Int*. <https://doi.org/10.1155/2014/819474>
- Pohare MB, Bhor SA, Patil PK (2017) Sugarcane for economical bioplastic production. *Pop Kheti* 5(1):20–23
- Porras A, Maranon A (Oct. 2012) Development and characterization of a laminate composite material from polylactic acid (PLA) and woven bamboo fabric. *Compos Part B Eng* 43(7):2782–2788. <https://doi.org/10.1016/j.compositesb.2012.04.039>
- Rahman MH, Bhoi PR (2021) An overview of non-biodegradable bioplastics. *J Clean Prod* 294:126218. <https://doi.org/10.1016/j.jclepro.2021.126218>
- Rahman A, Miller CD (2017) Microalgae as a source of bioplastics. In: Rastogi RP, Madamwar D, Pandey A (eds) *Algal green chemistry*. Elsevier, pp 121–138
- Rajendran N, Puppala S, Sneha RM, Ruth AB, Rajam C (2012) Seaweeds can be a new source for bioplastics. *J Pharm Res* 5(3):1476–1479
- Ramakrishnan N, Sharma S, Gupta A, Alashwal BY (2018) Keratin based bioplastic film from chicken feathers and its characterization. *Int J Biol Macromol* 111:352–358. <https://doi.org/10.1016/j.ijbio.2018.01.037>
- Rasheed F (2011) Production of Sustainable Bioplastic Materials from Wheat Gluten Proteins”, no. 4. The Swedish University of Agricultural Sciences
- Reddy N, Yang Y, Reddy N, Yang Y (2015) regenerated cellulose fibers using unconventional cellulosic sources. In: *Innovative biofibers from renewable resources*, 2015
- Reichert CL et al (2020) Bio-based packaging: Materials, modifications, industrial applications and sustainability. *Polymers*. <https://doi.org/10.3390/polym12071558>
- Riedel SL et al (2015) Polyhydroxyalkanoates production with *Ralstonia eutropha* from low quality waste animal fats. *J Biotechnol* 214:119–127. <https://doi.org/10.1016/j.jbiotec.2015.09.002>
- Rouf TB, Kokini JL (2016) Biodegradable biopolymer–graphene nanocomposites. *J Mater Sci*. <https://doi.org/10.1007/s10853-016-0238-4>
- Roy DPRSSB, Shit SC, Sengupta RA (2014) A review on bio-composites: fabrication, properties and applications. *Int J Innov Res Sci Eng Technol* 3(10):16814–16824
- Rujnić-Sokele M, Pilipović A (Feb. 2017) Challenges and opportunities of biodegradable plastics: a mini review. *Waste Manag Res* 35(2):132–140. <https://doi.org/10.1177/0734242X16683272>
- Ryder K, Ali MA, Billakanti J, Carne A (2020) Evaluation of dairy co-product containing composite solutions for the formation of bioplastic films. *J Polym Environ* 28:725–736. <https://doi.org/10.1007/s10924-019-01635-4>
- Sarkar K, Ray B, Banerjee R, Saha S, Roy S, Chatterjee S (2014) “Poly-β-hydroxybutyrate (Bioplastic) production utilizing Waste Effluent of a Sugar Industry. *IOSR J Environ Sci Toxicol Food Technol* 8(4):26–31. <https://doi.org/10.9790/2402-08422631>
- Sartika M, Lubis M, Harahap MB, Afrida E, Ginting MHS (2018) Production of bioplastic from avocado seed starch as matrix and microcrystalline cellulose from sugar palm fibers with Schweizer’s reagent as solvent. *Asian J Chem* 30(5):1051–1056

- Sharma S, Gupta A, Kumar A, Kee CG, Kamyab H, Saufi SM (2018) An efficient conversion of waste feather keratin into ecofriendly bioplastic film. *Clean Technol Environ Policy* 20:2157–2167. <https://doi.org/10.1007/s10098-018-1498-2>
- Shraddha G, Yogita R, Simanta S, Aparna S, Kamlesh S (2011) Screening and production of bioplastic (PHAs) from sugarcane rhizospheric bacteria. *Int Multidiscip Res J* 1(9):30–33
- Simonic M, Zemljic F (2020) Production of bioplastic material from algal biomass. *Chem Ind Chem Eng Q*. <https://doi.org/10.2298/ciceq191024026s>
- Song JH, Murph RJ, Narayan R, Davies GB (2009) Biodegradable and compostable alternatives to conventional plastics. <https://doi.org/10.1098/rstb.2008.0289>.
- Sudesh K, Iwata T (2008) Sustainability of biobased and biodegradable plastics. *Clean: Soil, Air, Water*. <https://doi.org/10.1002/clen.20070183>
- Sudhakar MP, Magesh Peter D, Dharani G (2020) Studies on the development and characterization of bioplastic film from the red seaweed (*Kappaphycus alvarezii*). *Environ Sci Pollut Res*. <https://doi.org/10.1007/s11356-020-10010-z>
- Sultan NFK, Johari WLW (2017) The development of banana peel /corn starch bioplastic film: a preliminary study. *Bioremediation Sci Technol* 5(1):12–17
- Suryawanshi SS, Sarje SS, Loni PC, Bhujbal S, Kamble PP (2020) Bioconversion of sugarcane molasses into bioplastic (Polyhydroxybutyrate) using *Bacillus cereus* 2156 under statistically optimized culture conditions. *Anal Chem Lett* 10(1):80–92. <https://doi.org/10.1080/22297928.2020.1746197>
- Thakur S, Chaudhary J, Sharma B, Verma A, Tamulevicius S, Thakur VK (2018) Sustainability of bioplastics: Opportunities and challenges. *Curr Opin Green Sustain Chem* 13:68–75. <https://doi.org/10.1016/j.cogsc.2018.04.013>
- The bioplastics global market to grow by 36% within the next five years (2021)
- Thiruchelvi R, Das A, Sikdar E (2020) Bioplastics as better alternative to petro plastic. *Mater Today Proc*. <https://doi.org/10.1016/j.matpr.2020.07.176>
- Torres S, Navia R, Campbel Murdy R, Cooke P, Misra M, Mohanty AK (2015) Green composites from residual microalgae biomass and poly(butylene adipate-co-terephthalate): Processing and plasticization. *ACS Sustain Chem Eng* 3(4):614–624. <https://doi.org/10.1021/sc500753h>
- Tripathi AD, Yadav A, Jha A, Srivastava SK (2012) Utilizing of sugar refinery waste (Cane Molasses) for production of bio-plastic under submerged fermentation process. *J Polym Environ* 20:446–453. <https://doi.org/10.1007/s10924-011-0394-1>
- Tsang YF et al (2019) Production of bioplastic through food waste valorization. *Environ Int* 127:625–644. <https://doi.org/10.1016/j.envint.2019.03.076>
- Van Der Hoek JP, De Fooij H, Struiker A (2016) Wastewater as a resource: strategies to recover resources from Amsterdam’s wastewater. *Resour Conserv Recycl* 113:53–64. <https://doi.org/10.1016/j.resconrec.2016.05.012>
- Verma V, Verma P, Ray P, Ray AR (2008) 2, 3-Dihydrazone cellulose: prospective material for tissue engineering scaffolds. *Mater Sci Eng C*. <https://doi.org/10.1016/j.msec.2008.03.014>
- Vert M et al (2012) Terminology for biorelated polymers and applications (IUPAC Recommendations 2012). *Pure Appl Chem* 84(2):377–410. <https://doi.org/10.1351/PAC-REC-10-12-04>
- Vilpoux O, Averous L (2004) Chapter 18 Starch-based plastics. Waller JL, Green PG, Loge FJ (2012) Mixed-culture polyhydroxyalkanoate production from olive oil mill pomace. *Bioresour Technol* 120:285–289. <https://doi.org/10.1016/j.biortech.2012.06.024>
- Weston S (2012) Packaging- assessing its environmental credentials Wolf O, Crank M, Patel M (2005) Techno-economic feasibility of large-scale production of bio-based polymers in Europe. 2005

Wong Y-M, Brigham CJ, Rha CK, Sinskey AJ, Sudesh K (2012) Biosynthesis and characterization of polyhydroxyalkanoate containing high 3-hydroxyhexanoate monomer fraction from crude palm kernel oil by recombinant *Cupriavidus necator*. *Bioresour Technol* 121:320–327. <https://doi.org/10.1016/j.biortech.2012.07.015>

Yadav B, Pandey A, Kumar LR, Tyagi RD (2020) Bioconversion of waste (water)/residues to bioplastics—A circular bioeconomy approach. *Bioresour Technol* 298(2019):122584. <https://doi.org/10.1016/j.biortech.2019.122584>

Yan C et al (2016) Cellulose/microalgae composite films prepared in ionic liquids. *Algal Res* 20:135–141. <https://doi.org/10.1016/j.algal.2016.09.024>

Yang J, Ching YC, Chuah CH (2019) Applications of lignocellulosic fibers and lignin in bioplastics: A review. *Polymers (Basel)* 11(5):1–26. <https://doi.org/10.3390/polym11050751>

Zahari MAKM, Ariffin H, Mokhtar MN, Salihon J, Shirai Y, Hassan MA (2015) Case study for a palm biomass biorefinery utilizing renewable non-food sugars from oil palm frond for the production of poly(3-hydroxybutyrate) bioplastic. *J Clean Prod* 87:284–290. <https://doi.org/10.1016/j.jclepro.2014.10.010>

Zeller MA, Hunt R, Jones A, Sharma S (2013) Bioplastics and their thermoplastic blends from *Spirulina* and *Chlorella* microalgae. *J Appl Polym Sci* 130(5):3263–3275. <https://doi.org/10.1002/app.39559>

Zhang C, Wang C, Cao G, Wang D, Ho S-H (2020) A sustainable solution to plastics pollution: an eco-friendly bioplastic film production from high-salt contained *Spirulina* sp. residues. *J Hazard Mater* 388:121773. <https://doi.org/10.1016/j.jhazmat.2019.121773>

Chapter 2: Plasticized PLA films for food applications by “green” solvent casting – method and characterization.

~

Premises to Chapter 2.

The following Chapter, currently under submission, defines all criteria related to the Material Science and Chemical Engineering side of the Product Development path defined in the main Introduction. In particular, at a laboratory scale, optimal solution and casting procedures with all the corresponding process variables are defined, which are currently under patenting procedures, while an in-depth material characterization under mechanical, thermal and interfacial standpoints permitted advanced morphological considerations about the critical effect of the amount of plasticizer added to the material in the casting phase.

~

2.1. - Introduction

Worldwide plastic consumption has increased since its first appearance in the industrial world, so that nowadays its use is essential to all kinds of industries, in particular to the packaging chain, which handles the 40% of the total plastics used in the overall industrial production (Ortega et al., 2021).

The advantages of plastic materials have always been their low cost and weight, and ease of manipulation. Nevertheless, the source and recyclability of most of the used plastics are labeled as unsustainable (Elsawi et al. 2017).

The constant intensification of polymers need is nowadays partially overcome by the production of biocompatible plastics as an alternative to non-renewable materials (Coppola et al., 2021). These plastics often show features that meet market requirements and, at the same time, do not incur accumulation in the environment as they are highly biodegradable, or even compostable (Kale et al., 2007). As per the conventional petrol-based plastics, many of these materials can be recycled so that their life cycle is not reduced to the single use.

In this context poly(lactic acid) (PLA) is one of the most favorable polymers among the renewable/biodegradable class of polymers (Pretula et al., 2016). PLA is a polymer labeled as an aliphatic polyester; it can be derived from highly renewable food waste sources such the ones containing starches (Singhvi et al., 2013). Yet, the

synthesis methods sourcing from biomasses are still under research and optimization, so that PLA cost is yet not so convenient to justify its uses as a general purpose polymer (Spiridon et al., 2015). A way to overcome this disadvantage is to use a blend of PLA and other less expensive polymers/fillers.

The aim of this paper is to give a clear indication of to what extent relatively high plasticizer/PLA ratios have an effect on the thermal and mechanical features of the obtained films. It is important to make clear that the approach of this work is to investigate the feasibility of the use of PLA films especially in food applications, which makes essential to approach the experimentations using food safe solvents: PLA obtained by solvent casting has been widely investigated through the use of solvents with high affinity like chloroform methylene chloride and acetonitrile, which can easily being used at room temperature (Youngjae Byun 2011). As a way to investigate a more food-safe procedure PLA/plasticizer blends were prepared using a green food-safe ester solvent, as a substitute to the more commonly used ones, which are mainly labeled as unsuitable for food uses (Marino, 2005; Duarte et al., 2014).

In this study, solvent casting method was chosen over extrusion film casting to address the intrinsic film denseness and thickness tuning capabilities of the plasticizer itself, as shown in the next sections; as a consequence a dedicated solvent casting technique has been designed. Details are kept confidential and not disclosed in the

following descriptions because the technique itself is currently undergoing patenting procedures.

Speaking of mechanical features, the most common downside of PLA is its intrinsic brittleness, which causes any sort of difficulty when trying to apply this polymer as film for packaging scopes. As polymeric films should exhibit high deformation capability, a wide spectrum of fillers and plasticizers are commonly used as additives to polymer formulations (Petchwattana et al., 2018). Among all plasticizers, the one chosen in this work has a good biocompatibility, a relatively low cost and high availability.

A very critical importance for the final features of the film resides in the casting method: in this study PLA solutions with different fractions of plasticizer (^PG) were prepared and cast using an automatic film casting machine. The solution casting method permits to obtain films with highly controlled thickness, a good ^PG/PLA blending and absence of defects, so to ensure high homogeneity of morphological and mechanical features throughout the whole sample.

2.2 - Materials and Methods

2.2.1 - PLA/^PG solution preparation

All samples are based on PLA (Sigma Aldrich, 3 mm nominal granule size) solutions. On that basis, different ^PG mass fractions were added to generate different composites. As a result, an array of samples with fixed PLA amount and increasing ^PG were prepared.

Each sample has been prepared on a basis of 30 g of solution, to operate the automated casting procedure properly (as described in section 2.2), with enough solution to generate approximately 700 cm² area films per sample.

Right before the solution preparation, the PLA underwent a 24h desiccation procedure at 120°C in a ventilated oven (Binder ED32) to extract any residual water content (Byun et al., 2012). For each sample 30g of solvent were put in a flask, while the ^PG has been added in a precise step of the solution formation for best dispersion. The solution was kept at a optimum temperature for a time that permitted the achievement of the complete solution.

Temperature monitoring was carried out by a thermocouple (TFA Lab Thermometer IP65) in contact with the solution. Once the solution was prepared, it was cooled down to a specific pouring temperature.

2.2.2 - Film casting

Film casting was performed on an automatic casting machine (Porometer Memcast) by pouring the prepared solutions in the reservoir of the casting knife set at a 500 μm gap. With this gap films with a final 34 ± 20 μm thickness were obtained. Each casting was performed with a resulting film area of 700 ± 20 cm^2 . As an indicative value film apparent densities fall in the area of 3000 ± 200 kg/m^3 , thus confronting this data with the PLA density stated on the PLA producer Technical Data Sheet (1.24 g/cm^3) the films exhibit void fraction values of 0.55 ± 0.25 (YousefniaPasha, et al., 2021; Algieri et al., 2021)

Casting plate temperature was kept at a optimum temperature to achieve a defined temperature difference between the casting solution and the plate, thus avoiding excessive temperature differences which could cause excessive diffusive mass fluxes and tensions in the film itself. The casting velocity was set at 1 cm/s , slow enough to let the viscous solution relax inner extrusion stresses accumulated during the casting (Kahrs et al., 2020; Lassenguette et al., 2022).

The casting machine was held at conditions of controlled solvent evaporation rates, which is critical to create the denser possible (non-porous) layer film. After this procedure, the casting was completed submerging the film in distilled water for residual solvent elimination, then dried at ambient temperature air overnight.

Some of the samples obtained are shown in the following Figure 13, in which a decrease in transparency is evident for sample with higher ^pG amount.

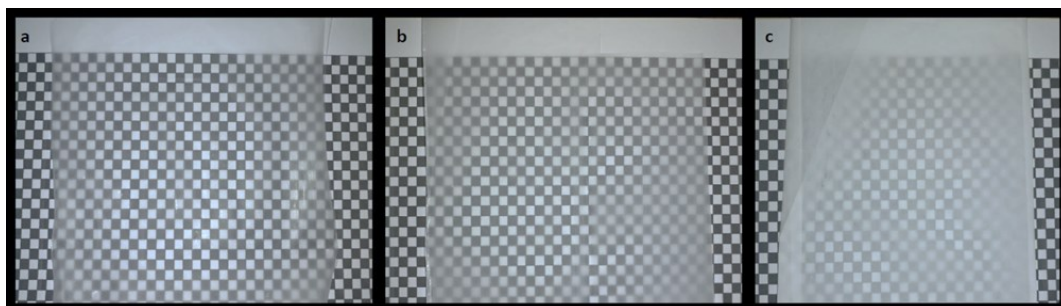


Figure 13: Three of the PLA/^pG films prepared. A gradual decrease in transparency is evident in samples with more plasticizer.

2.2.3 - Film characterization

Functional groups present in the prepared films were evaluated collecting infrared spectra of the film surface in Attenuated Total Reflection Infrared mode by FT-IR ATR Spectrometer (Perkin Elmer, Spectrum One).

Water contact angle (WCA) on the film surfaces was measured by sessile drop method at ambient temperature by using CAM 200 contact angle meter (KSV Instruments LTD, Helsinki, Finland). The sessile drop was formed by depositing a drop of water on the surfaces by using an automatic microsyringe. Results are the mean of six measurements on different parts of the sample surface.

Thermal characterizations of the samples were conducted by thermal gravimetric analysis (TGA) and differential scanning calorimetry (DSC) at ENEA

Trisaia. TGA tests were conducted on a *NETZSCH TG 209F1 Libra*, running 10°C per minute temperature ramps between 20 and 500°C on a constant 250 ml/min flux of nitrogen. DSC tests were performed on a *NETZSCH DSC300* running 10°C per minute temperature ramps between 0 and 200°C on a constant 250 ml/min flux of nitrogen.

Mechanical tests were employed to identify tensile properties and tear resistance. Tensile tests have been carried out at DIMEG (UNICAL) according to ASTM D882-18 (ASTM International). PLA sheets were cut into 9 mm-width strips. Samples dimensions are reported in Figure . Initial thickness of each film was evaluated through scanning electron microscope (SEM) images analysis (Thermo Scientific Phenom Pure). Tests have been conducted using an electromechanical testing machine, MTS Criterion Model 42 (MTS Corporation, USA) with a crosshead displacement rate equal to 12.5 mm/min, as suggested for low-deformable films (i.e., lower than 20%). Initial grip separation has been fixed equal to 10 mm (Figure 4). At least five samples have been tested for each sample condition. Through tensile tests the following mechanical properties have been evaluated: Young's modulus (E), maximum strength (σ_{\max}) and elongation at break (ϵ_{brk}). Strain measurement has been carried out using Digital Image Correlation (DIC) technique. A high-resolution camera (GigE, Prosilica GT), with a 2448x2050 pixel resolution (pixel dimensions 3.45 μm x3.45 μm) was employed for acquiring images of samples during mechanical

tests through an acquisition board (DAQ-STD-8D, National Instrument) with an acquisition speed of 15 fps. The VIC-2D software (correlated Solution) was employed for images analysis.

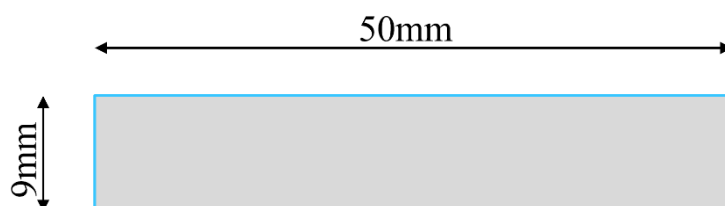
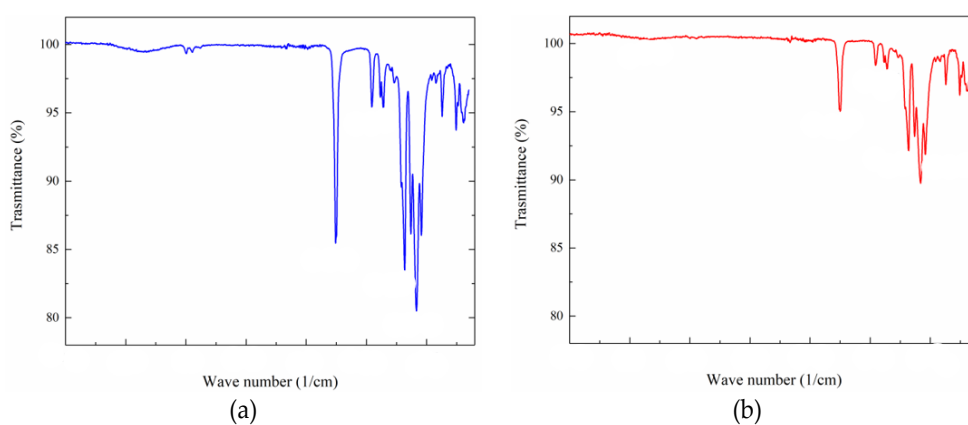


Figure 14: Schematic of samples employed for tensile tests.

2.3 - Results

2.3.1 - FT-IR analysis

FT-IR analyses were performed to confirm the presence of the plasticizer in the plasticized films. In Figure the spectra of different prepared samples are shown (peaks values kept confidential).



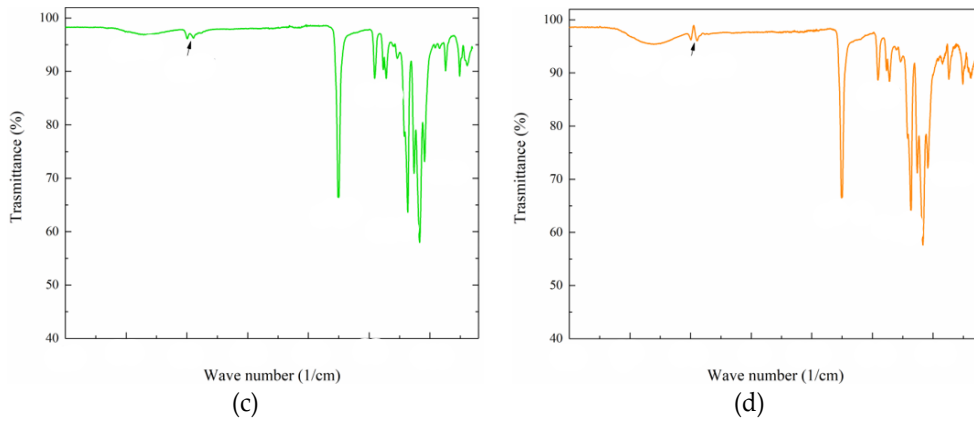


Figure 15: FT-IR spectra of the analyzed samples

2.3.2 - Water contact angle

Water contact angle (WCA) of pure PLA film – which by literature falls within the 75°-85° range - was $87.5^\circ \pm 1.8$ [21,22]. The addition of the plasticizer determined a reduction of the WCA (see Figure 16) due to the presence of the surface hydrophilic groups that improve the interaction of the water with the film surface.

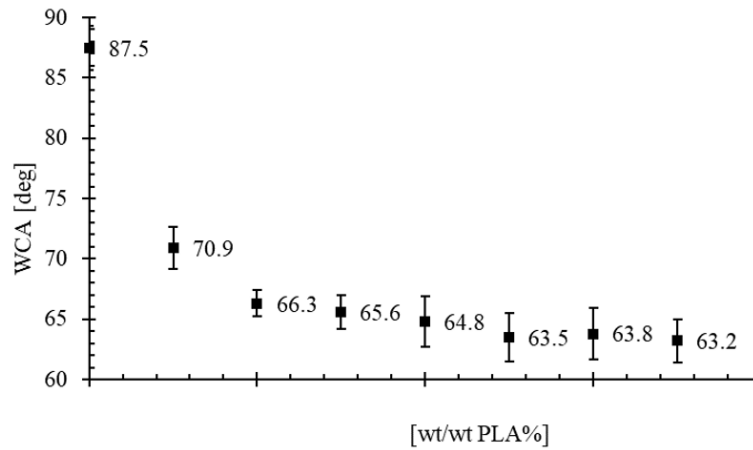


Figure 16: WCA values of the PLA/P/G samples plotted against samples P/G content.

2.3.3 - Scanning electron microscopy

SEM imaging was performed on a ZEISS Cross Beam 350. Cross section images of the samples show how the addition of higher amounts of plasticizer has a huge impact on the morphology of the samples, which tends towards a less dense matrix and higher sample thickness. As discussed in the next sections, this feature critically affects the other characterizations.

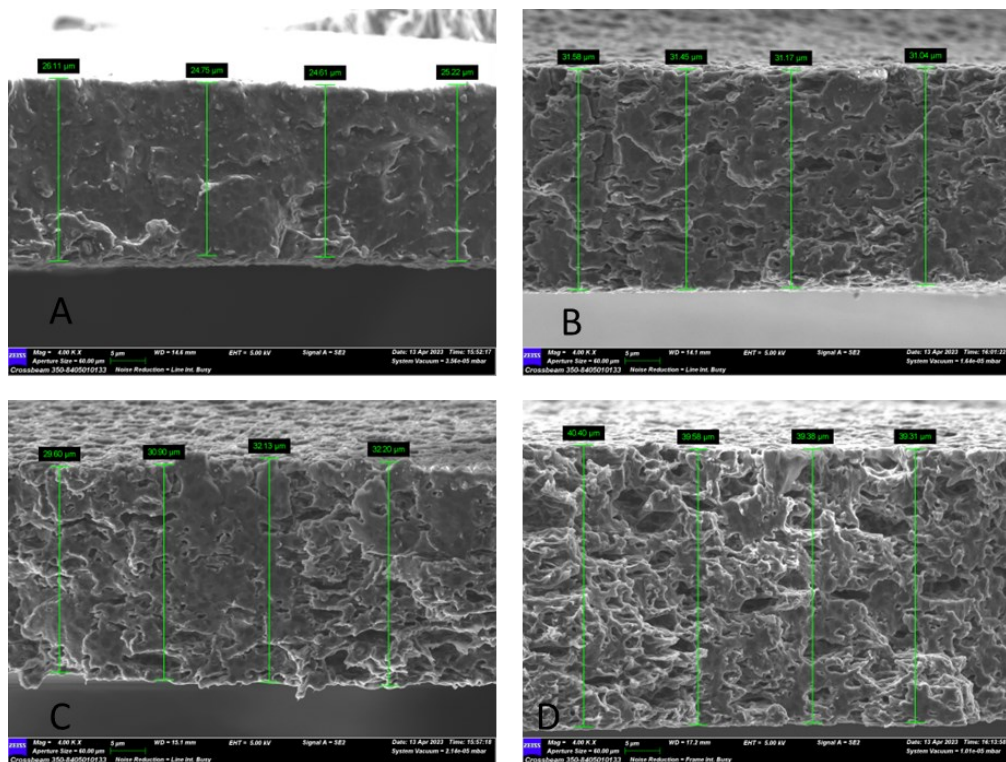


Figure 137: SEM images (cross sections) of samples with thickness quotes at increasing plasticizer content. It is clear how the morphology of the samples changes with the increase of plasticizer content towards a less dense matrix.

2.3.4 - X-Ray diffraction

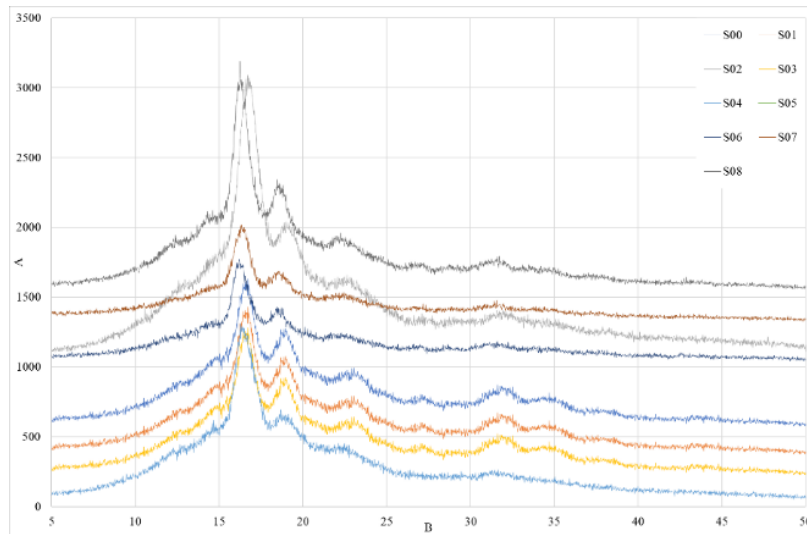


Figure 18: XRD analysis of the samples (vertically shifted for better visualization).

In figure 18 above, the characteristic peaks of PLA are exposed, with the expected peak for each of the samples at $2\theta \approx 17$, representative of the material.

2.3.5 - Thermal stability

Thermal gravimetric analysis (TGA) and differential scanning calorimetry (DSC) were performed to investigate the effect of the plasticizer addition on the crystallinity and on the thermal degradation behavior of the polymer matrix. Results are shown in figures 19 and 20 below and discussed in the next section. As per the whole sample array, TGA and DSC were also performed on pure plasticizer and original PLA material for better comparison and understanding.

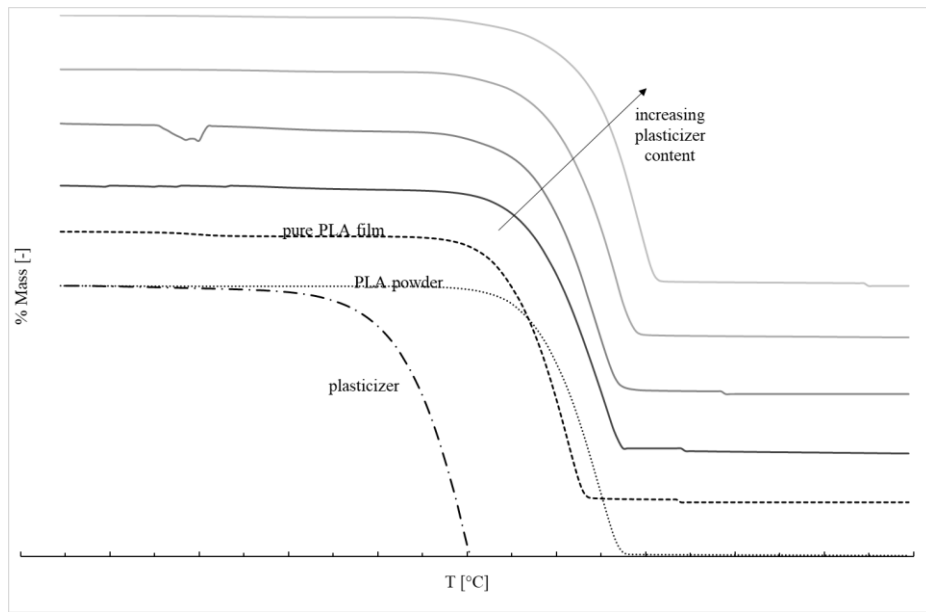


Figure 19: TGA analysis results on PLA/P/G samples (vertically shifted with higher P/G ratios samples above), pure plasticizer and PLA powder.

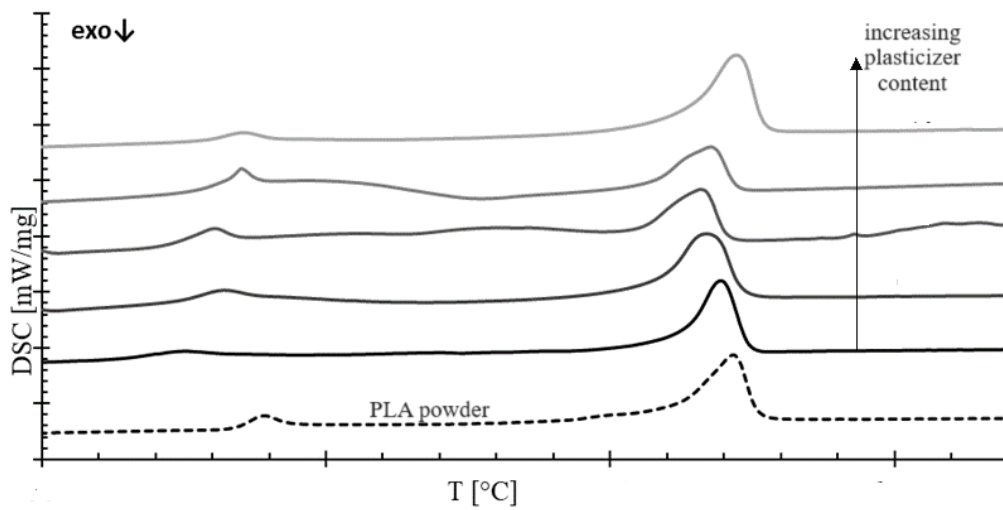


Figure 20: DSC analysis results on PLA/P/G samples (vertically shifted) and PLA powder.

2.3.6. - Mechanical properties

Load-displacement curves obtained for PLA films are reported in Figure . Moreover, the main mechanical properties are reported in Table . Samples fabricated

with neat PLA exhibit fragile behavior, with an abrupt failure and good mechanical properties.

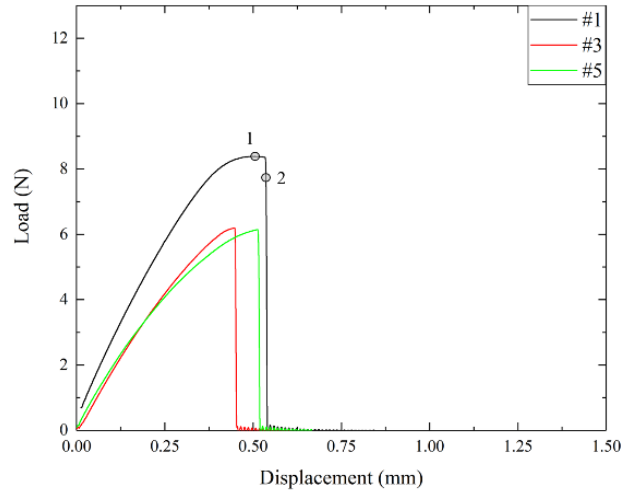


Figure 21: Load displacement curves obtained for PLA samples.

Table 6: Mechanical properties of PLA samples.

Sample	E (GPa)	σ_{\max} (MPa)	ϵ_{brk} (mm/mm)
S00	2.97±0.20	52.48±7.14	0.022±0.005
S01	2.16±0.12	32.82±0.92	0.049±0.008
S02	1.80±0.05	28.32±0.99	0.052±0.011
S03	1.28±0.19	19.78±0.56	0.050±0.008
S04	1.28±0.10	17.57±0.41	0.035±0.013
S05	1.11±0.04	16.22±0.59	0.018±0.005
S06	0.87±0.07	11.34±1.18	0.016±0.007

The influence of plasticizer addition on mechanical properties of PLA samples was investigated. The main mechanical properties are compared in Figure while numerical values are reported in Table above.

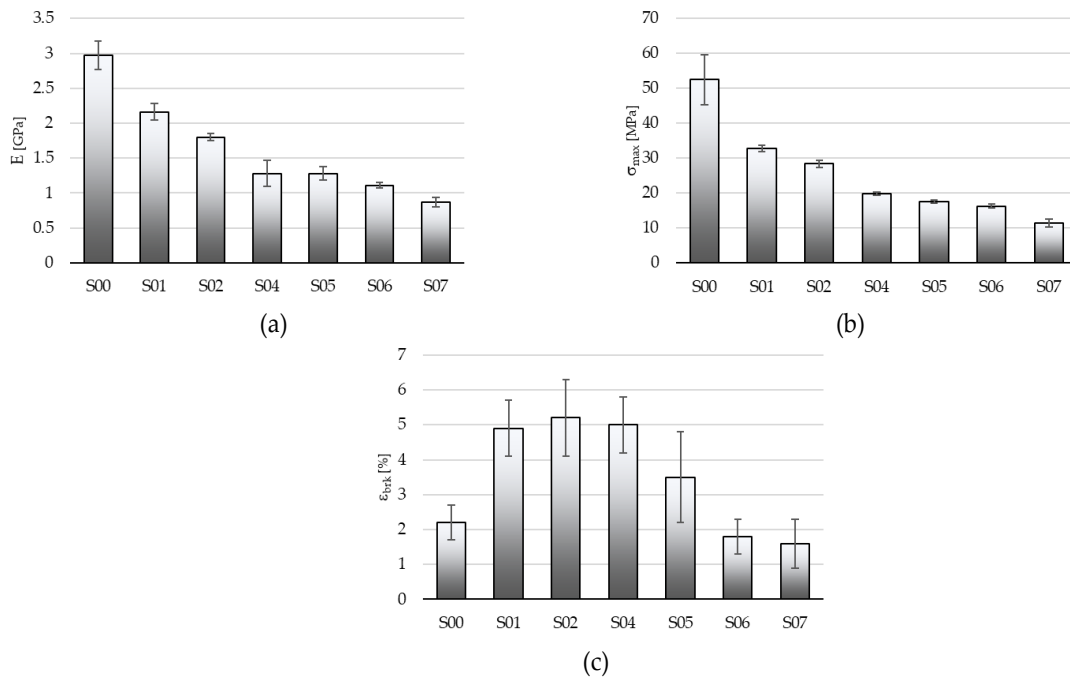


Figure 22: (a) Young modulus (b) maximum strength and (c) elongation at break obtained for PLA samples with different percentages of plasticizer.

2.3.7. - Water vapor transmission rate

Water vapor transmission rate (WVTR) tests were performed to check the effect of an increasing amount of plasticizer in the PLA matrix on water vapor permeation. It is worth mentioning that this variable is crucial when the polymer film is intended to be used in any food packaging application (Turan 2019).

As the WVTR value changes very steeply with the amount of plasticizer and being the usual ratios of plasticizers for the packaging uses in a lower range in respect to the previous used ratios, a new set of samples at lower concentrations has been cast and analyzed (named S01*, S02* and so on).

The test followed a gravimetric procedure: samples were inserted in an aluminum cell of 100ml volume with gasketed top¹. The gasketed top has an open central section with a 10 cm² area. The cell is filled with 80ml of distilled water so to leave proper headspace for the water vapor to be generated, while the sample is placed under the gasketed top (fig. 23). The whole cell is placed at 30°C with controlled external humidity and weighted each 30 minutes for 6 hours. Water mass loss is traced and results in mg/(h*cm²) are presented (fig. 24). (P.Cazón 2022)

The value for the S00 sample, which is the control sample with no plasticizer, seems to fairly reflect the literature data, with a value of 1.73 mg/(h*cm²) compared to the 1.52 mg/(h*cm²) value found in literature. (Shogren 1997)

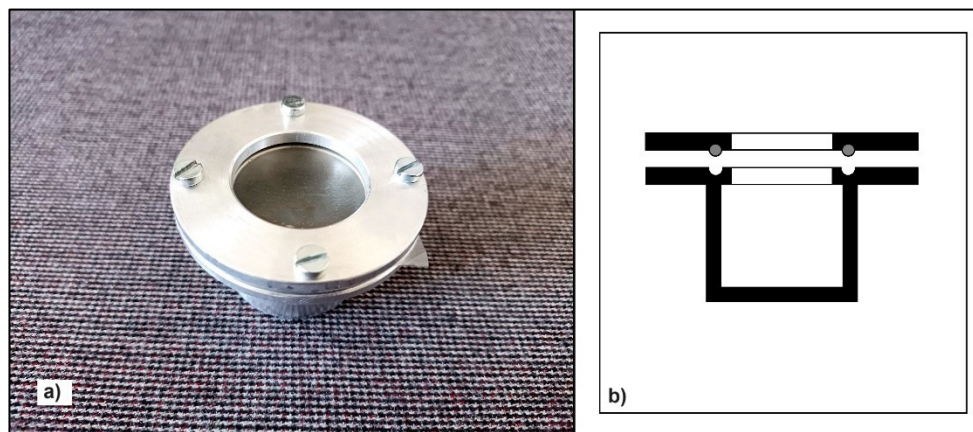


Figure 143: WVTR test cell (a), diametral cutline section of the vessel and the gasketed top.
(b).

¹ Courtesy of ITM-CNR.

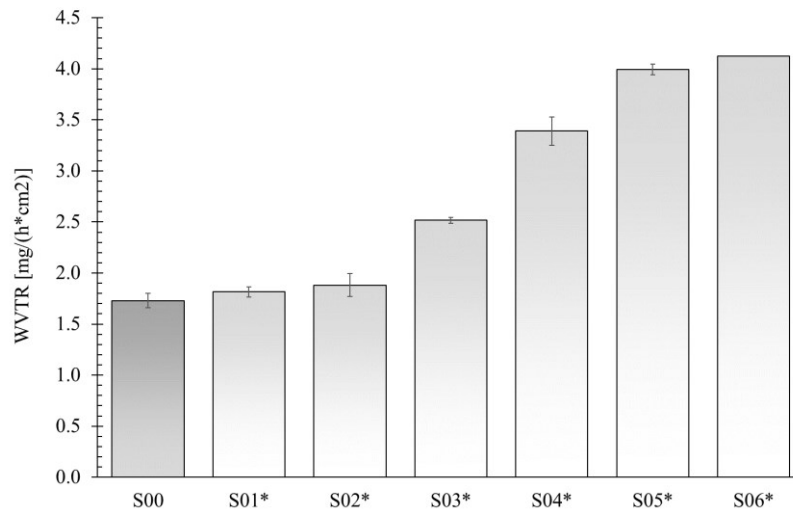


Figure 154: Results for WVTR tests, in $\text{mg}/(\text{h} \cdot \text{cm}^2)$: histograms for control sample (in dark grey colour) and samples with different percentages of P G.

2.4 - Discussion

2.4.1 FT-IR analysis

FT-IR tests show for the pristine PLA film a peak at 1755.57 cm^{-1} due to the stretching vibration of C=O of the ester groups. In addition, the band at 1454.92 cm^{-1} is attributed to the deformation of C-H in the methyl group [20]. The peaks at 1180 cm^{-1} and 1080 cm^{-1} are the C-O-C stretching [11]. These peaks were also evident in the plasticized samples. The presence of the plasticizer is evidenced by the band at around 3500 cm^{-1} caused by stretching of O-H bonds due to inter or intra-molecular hydrogen bonds. In addition, the less pronounced peak around 3000 cm^{-1} is attributable to the -CH groups.

2.4.2 Water contact angle

The plasticizer, as stated before, caused steep WCA value drops because of the considerable -OH groups interaction with water. As shown in Figure 16 this effect is more prominent for lower ratios of plasticizer: WCA values decrease as plasticizer ratios increase with an asymptotic tendency for very high ratios (towards a value of 63°, value exhibited at the highest ratio), thus following a monotone profile resembling a negative logarithmic dependency throughout the whole spectrum (Figure 25).

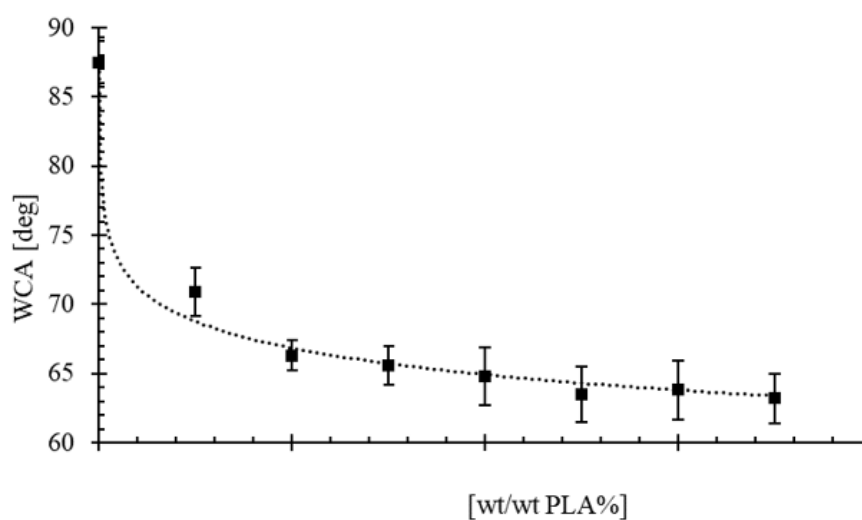


Figure 25: WCA negative logarithmic fitting on total sample array.

2.4.3 - SEM imaging

SEM cross section imaging evidentiates that higher ratios of plasticizer leads to the formation of a less dense polymer matrix with higher thickness: it is evident how higher PG content results in polymer matrix with higher void ratios, especially in

respect to the neat PLA sample, which appears strictly dense. The addition of plasticizer have no effect on the casting procedure in terms of solvent evaporation rates and consequent stratification as no evidence for inner layers formation - with different morphologies and void ratios – is found.

2.4.4 - Thermal stability

Since the TGA analysis show how plasticizer degradation is complete for temperatures lower than 250°C, a crucial consideration can be done considering this particular temperature. In figure 26 the values of TGA percent mass losses at 250°C are reported against the plasticizer ratios used during sample preparation.

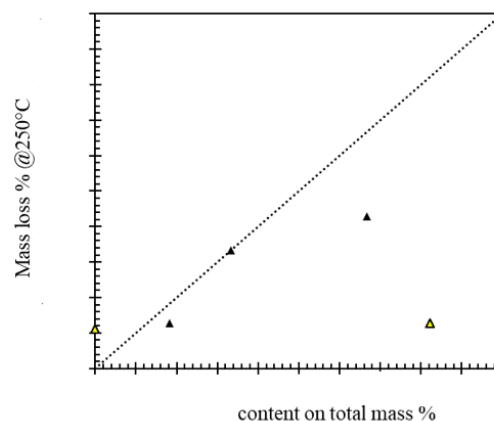


Figure 26: Total mass loss (TGA analysis) at 250°C in comparison to P/G mass percentage used for sample preparation.

In figure 26 above TGA tests mass loss data at 250°C are deduced for different samples so that the mass loss can be directly compared to the plasticizer concentration (in weight fraction percentages) of the relative samples. A comparison with the 1:1

correlation is clear enough to state that, within a considerably little deviation, all the mass loss occurred at temperatures lower than 250°C belong to plasticizer degradation alone, so that the whole plasticizer present in the samples degrades under those circumstances. Another clear effect worth commenting is due to the stripping effect of water on the plasticizer for ratios, which is evident for samples at ratios higher than 50%.

DSC tests show how the presence of plasticizer did not affect the crystallization ratio of the samples, in fact, no significant change among the samples in the subdue area under the main peak at around 150°C is found.

2.4.5 - Mechanical properties

Regarding the neat PLA samples, the mechanical properties identified are in agreement with results obtained in other works (De Silva et al., 2014; Ozkoc et al., 2009; Sharma et al., 2019). In particular, Sharma et al. (Sharma et al., 2019) found the following values for tensile modulus, elongation at break and maximum strength respectively: 2.4 GPa, 5% and 47 MPa, while some slight differences could be attributed to the different raw materials used.

The main failure mechanisms are reported in the snapshots below (Figure). Neat PLA samples are characterized by a fragile failure mode, whit a sudden sample

fracture and an abrupt load drop. The failure mechanism of all samples is unaffected in respect to neat PLA samples.

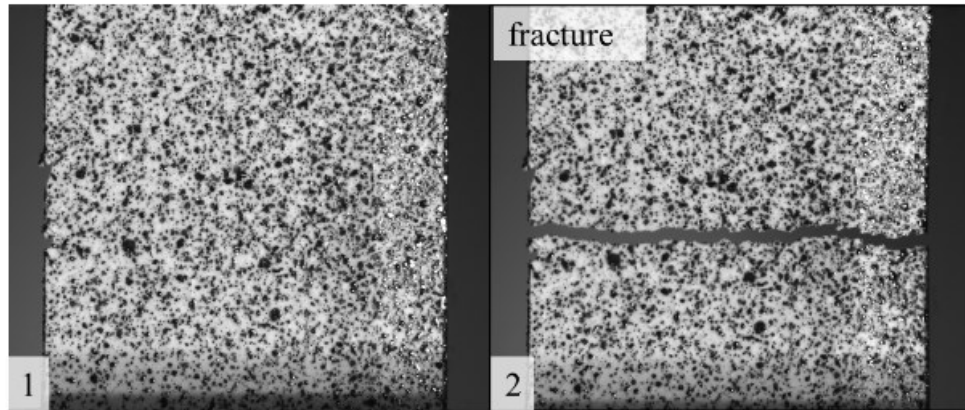


Figure 27: Fracture mechanism of PLA samples.

Plasticizer addition consistently modifies the samples mechanical properties: it reduces the mechanical properties (Young modulus and maximum stress) while the elongation at break is improved. The first effect is strongly related to the channeling and higher porosity exhibited with higher ^PG ratios with resulting overall weaker matrix. Deformation at break is higher in the samples what retain the higher ^PG amounts– with a peak for samples with intermediate ratios (the ones that do not incur in the above-mentioned stripping effect). This result was predictable since the expected plasticizing effect of improved ductility, while at the same time this normally implies a decrease of the other mechanical properties. Overall, the best compromise between ductility and mechanical properties was achieved with low ^PG ratio samples, while, to achieve high deformations, samples with intermediate plasticizer ratios would be considered having the best performance. Changes in the

main mechanical properties are reported in Figure 28 as deviations calculated in respect to value obtained for neat PLA samples.

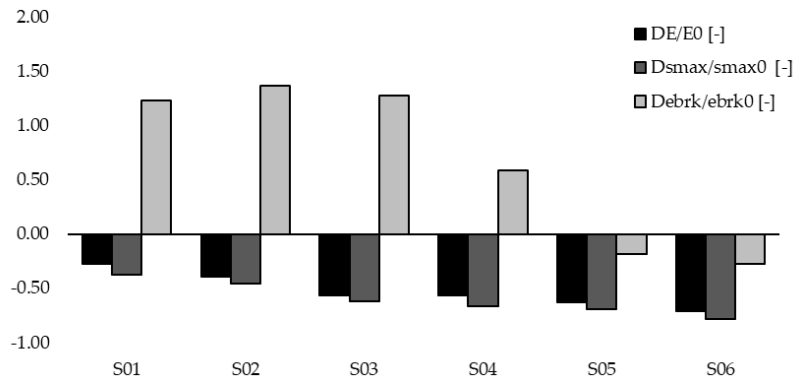


Figure 28: Mechanical property increments of PLA samples: Young modulus (in $\Delta E/E_{S00}$), maximum strength (in $\Delta\sigma/\sigma_{S00}$) and elongation at break (in $\Delta\varepsilon/\varepsilon_{S00}$) exhibited by samples with different percentages of plasticizer as deviation in respect to the control sample (S00).

2.4.6 - WVTR tests

WVTR tests results show how an increase in plasticizer concentration increases the value of vapor transmittance with two evident behaviors: a very steep change at the lower range and a slower increase in the higher range, thus tracing a sigmoid-like non-linear dependency on the whole range of concentrations (Fig. 29). The dependency follows the hints shown in the SEM analysis, where higher P_G ratios translate in higher matrix void ratios with bigger channeling. Bigger channeling represents easier pathways for the water vapor to pass through the film. This whole effect is clearly tunable by the casting methodology and the amount of plasticizer used.

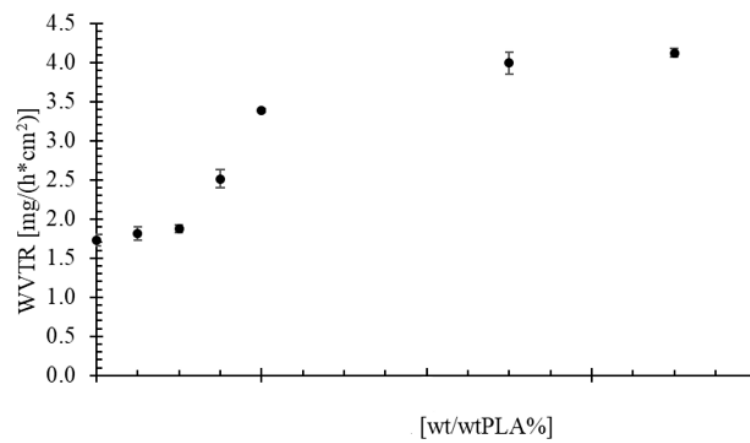


Figure 29: WVTR results (with standard deviations) plotted against plasticizer percentages clearly show a sigmoidal behaviour.

2.5 – Conclusions

PLA is a valuable polymer to be used for food (and nonfood) bio-compatible packaging uses. To meet food-safe requirements, PLA films were cast with a more food-safe green solvent in respect to the standardized PLA solvents, leading to the definition of new casting method procedures². The use of plasticizers is quite mandatory to obtain the desired mechanical features from any type of polymer film; in this study, the chosen plasticizer has proven to be a valid alternative to more commonly used additives, especially for its high compatibility with food uses. A very interesting feature resides in the ^pG-PLA interaction during the casting phase: different fractions of plasticizer lead to a very different results, mainly in terms of film morphology, with highly porous films for high ^pG ratios; thus, critically impacting all mechanical features, with lower yields and higher elongations. In conclusion, this methodology proved to have good perspective of use in the food packaging universe, with high possibilities for product optimization and features tunability.

² *Currently under patenting procedures.*

2.5 – References (Chap. 2)

- Oliver-Ortega, H.; Tresserras, J.; Julian, F.; Alcalá, M.; Bala, A.; Espinach, F.X.; Méndez, J.A. Nanocomposites Materials of PLA Reinforced with Nanoclays Using a Masterbatch Technology: A Study of the Mechanical Performance and Its Sustainability. *Polymers* 2021, 13, 2133, doi:10.3390/polym13132133.
- Elsawy, M.A.; Kim, K.-H.; Park, J.-W.; Deep, A. Hydrolytic Degradation of Poly(lactic Acid) (PLA) and Its Composites. *Renewable and Sustainable Energy Reviews* 2017, 79, 1346–1352, doi:10.1016/j.rser.2017.05.143.
- Coppola, G.; Gaudio, M.T.; Lopresto, C.G.; Calabro, V.; Curcio, S.; Chakraborty, S. Bioplastic from Renewable Biomass: A Facile Solution for a Greener Environment. *Earth Syst Environ* 2021, 5, 231–251, doi:10.1007/s41748-021-00208-7.
- Kale, G.; Kijchavengkul, T.; Auras, R.; Rubino, M.; Selke, S.E.; Singh, S.P. Compostability of Bioplastic Packaging Materials: An Overview. *Macromol. Biosci.* 2007, 7, 255–277, doi:10.1002/mabi.200600168.
- Pretula, J.; Slomkowski, S.; Penczek, S. Poly(lactides)—Methods of Synthesis and Characterization. *Advanced Drug Delivery Reviews* 2016, 107, 3–16, doi:10.1016/j.addr.2016.05.002.
- Singhvi, M.; Gokhale, D. Biomass to Biodegradable Polymer (PLA). *RSC Adv.* 2013, 3, 13558, doi:10.1039/c3ra41592a.
- Spiridon, I.; Leluk, K.; Resmerita, A.M.; Darie, R.N. Evaluation of PLA–Lignin Bioplastics Properties before and after Accelerated Weathering. *Composites Part B: Engineering* 2015, 69, 342–349, doi:10.1016/j.compositesb.2014.10.006.
- Marino, D.J. Ethyl Acetate*. In *Encyclopedia of Toxicology*; Elsevier, 2005; pp. 277–279 ISBN 978-0-12-369400-3.
- K. Duarte, C.I.L. Justino, A.M. Gomes, Teresa Rocha-Santos, Armando C. Duarte, Chapter 4 - Green Analytical Methodologies for Preparation of Extracts and Analysis of Bioactive Compounds, *Comprehensive Analytical Chemistry* (2014), Elsevier, Volume 65, Pages 59-78,
- Petchwattana, N.; Sanetuntikul, J.; Narupai, B. Plasticization of Biodegradable Poly(Lactic Acid) by Different Triglyceride Molecular Sizes: A Comparative Study with Glycerol. *J Polym Environ* 2018, 26, 1160–1168, doi:10.1007/s10924-017-1012-7.
- Iulianelli, A.; Algieri, C.; Donato, L.; Garofalo, A.; Galiano, F.; Bagnato, G.; Basile, A.; Figoli, A. New PEEK-WC and PLA Membranes for H₂ Separation. *International Journal of Hydrogen Energy* 2017, 42, 22138–22148, doi:10.1016/j.ijhydene.2017.04.060.
- Othman, S.H.; Hassan, N.; Talib, R.A.; Kadir Basha, R.; Risyon, N.P. Mechanical and Thermal Properties of PLA/Halloysite Bio-Nanocomposite Films: Effect of Halloysite Nanoclay Concentration and Addition of Glycerol. *Journal of Polymer Engineering* 2017, 37, 381–389, doi:10.1515/polyeng-2016-0062.
- Byun, Y.; Whiteside, S.; Thomas, R.; Dharman, M.; Hughes, J.; Kim, Y.T. The Effect of Solvent Mixture on the Properties of Solvent Cast Poly(lactic Acid) (PLA) Film. *J. Appl. Polym. Sci.* 2012, 124, 3577–3582, doi:10.1002/app.34071.
- Pandele, A.M.; Constantinescu, A.; Radu, I.C.; Miculescu, F.; Ioan Voicu, S.; Ciocan, L.T. Synthesis and Characterization of PLA-Micro-Structured Hydroxyapatite Composite Films. *Materials* 2020, 13, 274, doi:10.3390/ma13020274.
- YousefniaPasha, H.; Mohtasebi, S.S.; Tabatabaekolooor, R.; Taherimehr, M.; Javadi, A.; Soltani Firouz, M. Preparation and Characterization of the Plasticized Poly(lactic Acid) Films Produced by the Solvent-casting Method for Food Packaging Applications. *J. Food Process. Preserv.* 2021, 45, doi:10.1111/jfpp.16089.
- Algieri, C.; Chakraborty, S.; Pal, U. Efficacy of Phase Inversion Technique for Polymeric

Membrane Fabrication. *Journal of Phase Change Material* 2021, 1,
doi:<https://doi.org/10.58256/jpcm.v1i1.10>.

Kahrs, C.; Gühlstorf, T.; Schwellenbach, J. Influences of Different Preparation Variables on Polymeric Membrane Formation via Nonsolvent Induced Phase Separation. *J Appl Polym Sci* 2020, 137, 48852, doi:[10.1002/app.48852](https://doi.org/10.1002/app.48852).

Lasseguette, E.; Fielder-Dunton, L.; Jian, Q.; Ferrari, M.-C. The Effect of Solution Casting Temperature and Ultrasound Treatment on PEBAX MH-1657/ZIF-8 Mixed Matrix Membranes Morphology and Performance. *Membranes* 2022, 12, 584, doi:[10.3390/membranes12060584](https://doi.org/10.3390/membranes12060584).

ASTM ASTM D882 Test Method for Tensile Properties of Thin Plastic Sheeting; ASTM International;

Wang, W.; Gong, Y.; Sun, Q.; Li, L.; Xu, A.; Liu, R. High Performance Polyvinyl Alcohol/Poly(lactic Acid) Materials: Facile Preparation and Improved Properties. *J of Applied Polymer Sci* 2022, 139, doi:[10.1002/app.52470](https://doi.org/10.1002/app.52470).

Ratner, B.D. Surface Modification of Polymers: Chemical, Biological and Surface Analytical Challenges. *Biosensors and Bioelectronics* 1995, 10, 797–804, doi:[10.1016/0956-5663\(95\)99218-A](https://doi.org/10.1016/0956-5663(95)99218-A).

Burg, K.J.L.; Holder, W.D.; Culberson, C.R.; Beiler, R.J.; Greene, K.G.; Loeb sack, A.B.; Roland, W.D.; Mooney, D.J.; Halberstadt, C.R. Parameters Affecting Cellular Adhesion to Polylactide Films. *Journal of Biomaterials Science, Polymer Edition* 1999, 10, 147–161, doi:[10.1163/156856299X00108](https://doi.org/10.1163/156856299X00108).

De Silva, R.; Pasbakhsh, P.; Goh, K.; Chai, S.-P.; Chen, J. Synthesis and Characterisation of Poly(Lactic Acid)/Halloysite Bionanocomposite Films. *Journal of Composite Materials* 2014, 48, 3705–3717, doi:[10.1177/0021998313513046](https://doi.org/10.1177/0021998313513046).

Ozkoc, G.; Kemaloglu, S. Morphology, Biodegradability, Mechanical, and Thermal Properties of Nanocomposite Films Based on PLA and Plasticized PLA. *J. Appl. Polym. Sci.* 2009, 114, 2481–2487, doi:[10.1002/app.30772](https://doi.org/10.1002/app.30772).

Sharma, S.; Singh, A.A.; Majumdar, A.; Butola, B.S. Tailoring the Mechanical and Thermal Properties of Poly(lactic Acid)-Based Bionanocomposite Films Using Halloysite Nanotubes and Poly(ethylene Glycol) by Solvent Casting Process. *J Mater Sci* 2019, 54, 8971–8983, doi:[10.1007/s10853-019-03521-9](https://doi.org/10.1007/s10853-019-03521-9).

P.Cazón, E.Morales-Sanchez, G.Velazquez, M.Vázquez. 2022. «Measurement of the Water Vapor Permeability of Chitosan Films: A Laboratory Experiment on Food Packaging Materials.» This: *J. Chem. Educ.* 99: 2403–2408.

Shogren, R. 1997. «Water vapor permeability of biodegradable polymers.» *J Environ Polym Degr* 5: 91-95.

Turan, D. 2019. «Water Vapor Transport Properties of Polyurethane Films for Packaging of Respiring Foods.» *Food Eng. Rew.* 13: 54–65. doi:[10.1007/s12393-019-09205-z](https://doi.org/10.1007/s12393-019-09205-z).

Youngjae Byun, Scott Whiteside, Ron Thomas, Mahalaxmi Dharman, Jeremy Hughes, Young Teck Kim. 2011. «The effect of solvent mixture on the properties of solvent cast poly(lactic acid) (PLA) film.» *Applied Polymer Science* 3577-3582.

Chapter 3: Modeling of specific migration from food contact materials.

~

Premises to Chapter 3.

The following article, published on Journal of Food Engineering (Elsevier Ltd., 2023) is the first of the two chapters where the ICT field, by means of Finite Elements Modeling, is applied on the Product Development route. In this case, the method is aimed at precisely evaluating the release rates of compounds (additives, metals, etc.) from packaging materials to foodstuff and from production plant components to food streams as a reliable method for compliance testing. Two examples are shown: the migration of Octadecyl-3-(3,5-di-tert-butyl-4-hydroxyphenyl) from a plastic wrap to a ready-made sandwich, and the migration of metals from a 316-iron production line component to a liquid-like food stream, in compliance with the testing standards given by the European legislation. The method then is proposed with a user-friendly dedicated GUI, by which any packaging or component producer should be able to test their materials by uploading a CAD file of the component and inserting the component's features and process conditions.

~

Modeling of specific migration from food contact materials.

Francesco Petrosino¹ · Gerardo Coppola¹ · Sudip Chakraborty¹ Stefano Curcio¹

¹University of Calabria, Department of DIMES, via Pietro Bucci, Cubo 42A,
87036 Rende, Cosenza, Italy

PUBLISHED ON: *Journal of Food Engineering* – Elsevier Ltd.
Volume 357, November 2023, 111652
© The Author(s) 2021

<https://doi.org/10.1007/s41748-021-00208-7>

3.0 - Abstract

The estimation by either reliable experimental techniques or accurate computational models aimed at calculating the release of components/additives from packaging materials and process lines towards food matrices represent one of the most exciting research topics in food science and technology. In recent years, the migrants release from food contact materials has been regulated by various standards that often refer to purely experimental methods so to determine and quantify the components which are transported to the food. This work aimed to propose an innovative modeling approach for the simulation of the release of some migrants from both packaging and process materials. Specifically, the release of Octadecyl-3-(3,5-di-tert-butyl-4- hydroxyphenyl), an additive used during polyethylene films

production, to a food matrix consisting of a sandwich was modeled. In addition, the release of Chromium, Manganese and Nickel from AISI 316L steel components in contact with acid solutions was analyzed to simulate some typical conditions occurring in the food industry when aggressive fluids come in contact with steel parts. A very good agreement between the experimental data and the model prediction was also obtained.

Keywords: *Food modeling - Diffusion - Transport phenomena - Computational-fluid-dynamic*

3.1 - Introduction

European regulations impose strict restrictions on the specific migration of additives contained in food contact materials (Barnes et al., 2006; Coppola et al., 2021). To certify the actual compliance with these regulations, specific migration tests are performed exploiting definite experimental standards to determine the amount of additives released in food matrixes and any possible overcoming of the limits imposed by the law (Piotrowska, 2004; Lestido-Cardama et al., 2022).

However, such experimental tests need sophisticated instruments to be completed and, in most cases, are focused on the determination of a single substance; therefore, to get a broader and more complete insight into the additives released in

the food, it is often necessary to repeat the experimental tests with a significant consumption of economic resources. Furthermore, it is worthwhile remarking that many food-grade packaging materials typically comprehend the so-called non-intentionally added substances (NIAS). The toxicity of which can be assessed only by sophisticated methods based on the precise identification of all the substances and on the actual availability of the pure chemical standard, which is necessary to perform accurate analyses (Groh and Muncke, 2017; cabdirect, 2022; Hoppe et al., 2016). Due to these objective difficulties, experimental tests are often carried out by simplified methods that can only partially reproduce the processes to be simulated (Molina-Besch and Pålsson, 2020).

Several studies dealing with determining the release of components from food contact materials are available in the literature. These papers have explored many different aspects of specific migration from food contact materials and, in particular, have presented detailed studies about the degradation of antioxidants in polypropylene packaging during microwave heating (Piotrowska, 2004), the migration occurring from multi-layer barriers (Úbeda et al., 2017), the release of additives from PVC films (Petersen et al., 1995; Fenyvesi et al., 2007; Bouma and Schakel, 2010), the experimental evaluation of migrants transport by innovative FPSE (fabric phase sorptive extraction) techniques (Kabir et al. 2017; Zilfidou et al., 2018; Aznar et al., 2016), the estimation of titanium dioxide migration from laminate

packaging (Chen et al., 2019; Forooghi et al., 2022), the migration of endocrine disrupting chemical substances (Muncke, 2011; Muncke, 2009; Ong et al., 2022), the migration occurring from active packaging (Tovar et al., 2005; Wyrwa and Barska, 2017; Silva and Jafari, 2022; López-Cervantes et al., 2010).

Any system in which food is in contact with polymeric or metallic materials is characterized by a significant degree of variability and uncertainty due to food composition and pH, packaging heterogeneity, temperature shifts occurring during storage, and different retention times (Poças et al., 2008; Chung et al., 2002).

One possible strategy to overcome some of the previous problems is represented by mathematical modeling aimed at the formulation of robust and predictive tools allowing estimating the transport of migrants towards foods in a vast variety of processes and operating conditions and taking into account the main characteristics of both food and packaging. Such models can be either deterministic, empirical, stochastic, or probabilistic (Poças et al., 2008; Chung et al., 2010). However, it is worthwhile noting that, among the papers published in the field, only a limited number of them regard the exploitation of modeling approaches to estimate the specific migration in food. A purely computational approach may exhibit significant advantages since, thanks to reliable numerical methods, a variety of models can be implemented and solved, thus attaining a detailed simulation and a prediction of specific migration processes and of the influence of some of the most critical

parameters on system behavior (Erdogdu et al., 2022, Olivier, 2020; Benbettaïeb et al., 2020). A trustworthy modeling approach responds to an emerging need in food science and technology, namely the precise characterization of the actual interactions between the materials and the food matrices in contact with them. The exploitation of modeling can significantly innovate the current standardized methodologies since properly validated computational methods are characterized by greater flexibility, lower costs, shorter execution time and the broader possibility of analyzing complex systems, thus becoming a valid and convenient tool for those companies who are called to characterize existing materials or to develop new products. In this context, analytical mathematical models are mentioned in some European directives as a possible alternative to traditional experimental methods (Direttiva 2002/72/CE, 2022). In particular, the results obtained from computer simulations, followed by appropriate data reprocessing, allow determining some critical representative parameters and drawing a quick comparison with the imposed regulatory limits.

If such simulations are properly designed, based on them, realistic applications can be implemented with a simple interface that shows the end user a very intuitive GUI (Graphical User Interface). Thanks to the user-friendly interface, different critical parameters can be chosen: the geometry of the system, the physical properties of the migrants and materials involved, and all the operational parameters such as

temperature, time or a set of times at which the solutions are calculated, the domain discretization and much more, depending on the type of application implemented.

Moreover, multiscale approaches must be mentioned because of their importance in this area (Curcio et al., 2018; De Luca et al., 2021; Petrosino et al., 2019). A multiscale model can retrace different detail scales by investigating the problem at sub-nanosopic, nano, micro and macroscopic scales to derive some parameters with rigorous approaches without resorting to empirical or experimental methods (Petrosino et al., 2020; Petrosino et al., 2022).

Such methods are entirely flexible and show a high potential for solving many problems that appear too complex to be experimentally analyzed. This brings a not-inconsiderable level of innovation to the operating methods of the client company, which can carry out tests simply and economically before the realization of packaging rather than the application of a new line for the treatment of food in contact with certain materials along the production process. The applications in food processing can be the most varied and utterly adaptable to any industrial context.

Based on the considerable relevance of the modeling methods in the area of specific migration in food systems and given the shortage of similar approaches in the literature, the present paper is aimed to propose an innovative modeling approach for the simulation of the release of some migrants from both packaging and process materials. As specified hereafter, both the release of an additive used during

polyethylene films production to a food matrix and of main stainless-steel components was analyzed to simulate some typical conditions occurring in the food industry. Experimental tests of the metal release were accurately replicated in the laboratory for model validation.

3.2 - Specific migration models

The presented research work has implemented models of specific migration from materials or objects to foods they are in contact with. The first part shows a model acting to simulate the release of Octadecyl-3-(3,5-di-tert-butyl-4-hydroxyphenyl), contained in a polyethylene film, towards a wrapped sandwich. Next, the release phenomena were analyzed on a metal-food interface that simulates the contact between metal components, widely found in all production equipment, and a simulant solution replicating food physio-chemical features. Specifically, the release of chromium, manganese and nickel into an aqueous solution simulant has been analyzed. Experimental tests of the metal release were accurately replicated in the laboratory for model validation. Finally, a user-friendly standalone application regarding the simulation of the release throughout the previously defined metal-food interface, has been implemented. This enables the use of the modeling tools mentioned above by a less experienced user so that a consistent check for compliance

with the migration limits imposed by regulations can be brought out internally and easily within the industry.

3.2.1 - Specific migration in a food matrix

In the first part of the research, an ad-hoc model has been implemented in the MATLAB programming environment to illustrate the computational calculation and the related simulation of the specific migration of some constituents. The simulated compounds are present in low-density polyethylene (LDPE) film used for sandwich storage (wrapping).

The polyethylene film has a thickness of 100 μm , and the migrating substance is Octadecyl-3-(3,5-di-tert-butyl-4-hydroxyphenyl). The programming starts with constructing the model data set with geometry and polymer characteristics, as reported in appendix A section.

The 3D Fick diffusion model has been defined, and the diffusion coefficient of the migrant through the sandwich has been calculated, which in this case can be likened to a medium of fatty substances (Caro and Ruthven, 2006; Sanches Silva et al., 2009). The diffusion coefficient has been calculated using the relationship presented in the 2002/72/EC regulations as reported in appendix B section. (Commission Directive 2002/72/EC, 2022; Simoneau et al., 2017) The used relationship also includes the temperature dependence of the diffusion coefficient

(Weissberg, 2004). Once the sandwich is packed for storage, its temperature is altered in an unsteady manner. However, the unsteady state characteristic time is orders of magnitude smaller than food storage time (different days), and to analyze the release during the storage period of the sandwich, the model refers to an average temperature equal to that of the refrigerator (5 °C).

The presence of further intermediate fluid/gas phases interfaces between the polymer film and the food matrix was rightly neglected. However, this choice leads to conservative results that can be refined by inserting an additional diffusion layer into the model.

The third step is represented by the definition of the geometry of the model; in this case, it is representable, with good approximation, by one-eighth of a parallelepiped; this is due to the symmetry considerations that can be made regarding the expected results: migrant penetration profiles from the sandwich faces inward are expected to be symmetrical concerning the x-y, x-z, and y-z faces so that the model resolution can be implemented for a domain restricted to one-eighth of the entire sandwich so that the computational efforts are significantly reduced (Fig. 30).

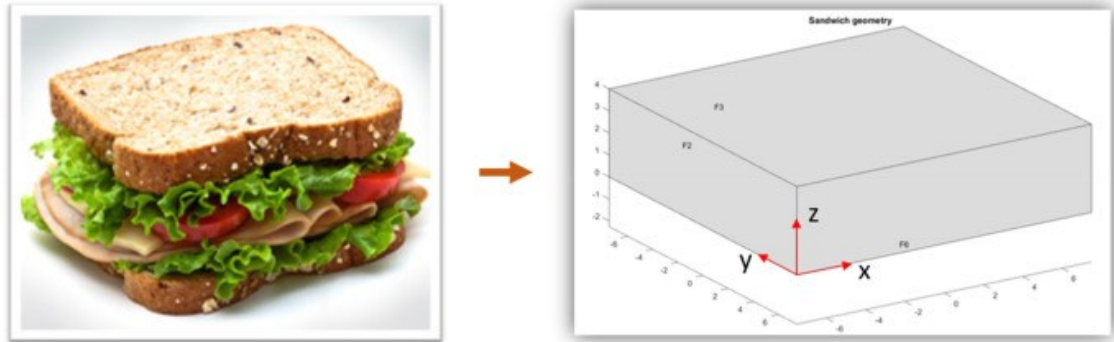


Figure 30: Geometry design.

The computational mesh for the numerical resolution of the model was so generated (Fig. 31). An optimization process performed on the generated mesh led to a mesh with tetrahedral elements. (Ladeveze et al., 1991). The main features of the applied mesh are reported in Table 7.

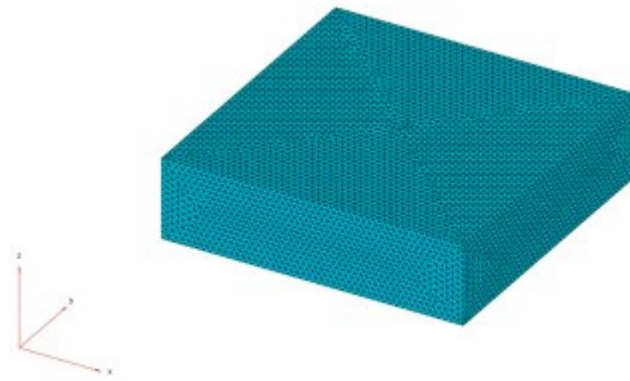


Figure 31: Mesh of the simulated sandwich model.

Table 7: Main features of the optimized mesh used for the computation.

<i>Number of nodes</i>	3*385,663
<i>Number of elements</i>	10*275,756
<i>Maximum element size [mm]</i>	0.3000
<i>Minimum element size [mm]</i>	0.1500

Finally, the boundary conditions (BCs) of the system were defined. A symmetry condition on the faces generated by the simplifying cuts in the domain has been applied, so BCs of Neumann type were imposed. On the remaining outer faces of the domain Dirichlet-type BCs are implemented (appendix C). A partition coefficient of the migrant at the polymer-food interface was defined equal to 1 in agreement to the EU directive 2002/72/EC as a conservative value to define the wall concentration of the model (Commission Directive 2002/72/EC, 2022; Simoneau et al., 2017). In Fig. 32, a quick and comprehensive representation of the model is reported.

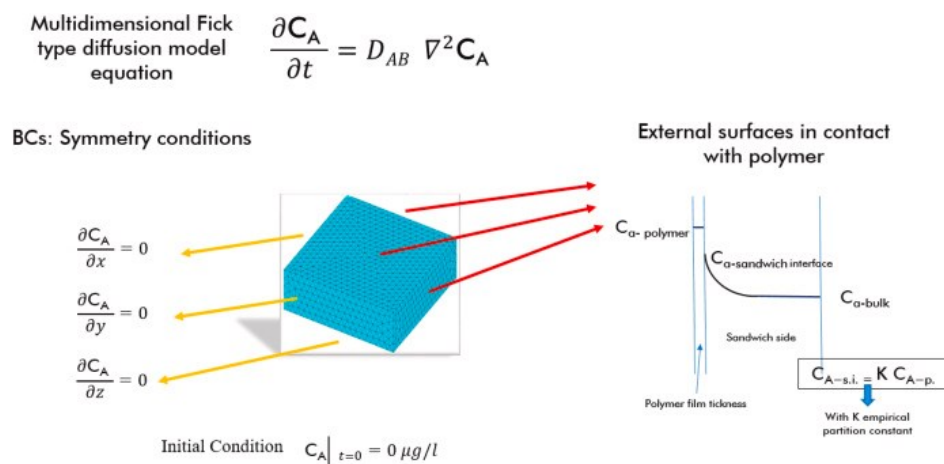


Figure 33: Model representation.

The model was then computed by “solvePDE” Matlab tool as reported in appendix D section.

Once the simulation has been run, the migrant time-dependent concentration profiles in the sandwich at different times are obtained as reported in Section 3.1. From these concentration profiles, by appropriately processing the data, it is possible

to determine any information regarding the analyzed phenomena. For example, in the context of specific migration in food, it is of interest to have an estimation of the amount of migrants per unit volume present in the sampled food over time. In this regard, concentration profiles can be integrated to calculate the desired information.

3.2.2 - Nickel, manganese and chromium release from AISI 316L stainless steel.

In the second part of this work, a model was developed to estimate the release of certain components present in AISI 316L steel, intended for food use, into acidic solutions. This model aims to replicate and study the potential release that could occur from piping and other parts to various process fluids used in the food industry or from various kitchenware. According to the regulations and the papers currently available, the acid solution used as food simulant consisted of glacial acetic acid at 3% at temperatures between 50 and 100 °C (Casaroli et al., 2022; Institute for Health and Consumer Protection, 2009).

The software Comsol Multiphysics was used to implement the model in this case. The analyzed case is a steel piece immersed in an acid solution for 30 min. In this way, it was possible to understand whether the material used complied with the release limits imposed by the regulations (Kamerud et al., 2013).

Initially, a set of parameters were defined to saturate the initial state of the simulation and to time-dependent model equation sets, including the initial interface concentrations of the migrants and their diffusion coefficients in an aqueous environment. As shown in Fig. 34, the geometry of an AISI 316L fitting previously drawn in a CAD environment was imported. The geometry was then used to draw its complementary part to realize a surrounding liquid domain. Then the 3D model mesh was made after considering a cutaway of the whole domain for symmetry.

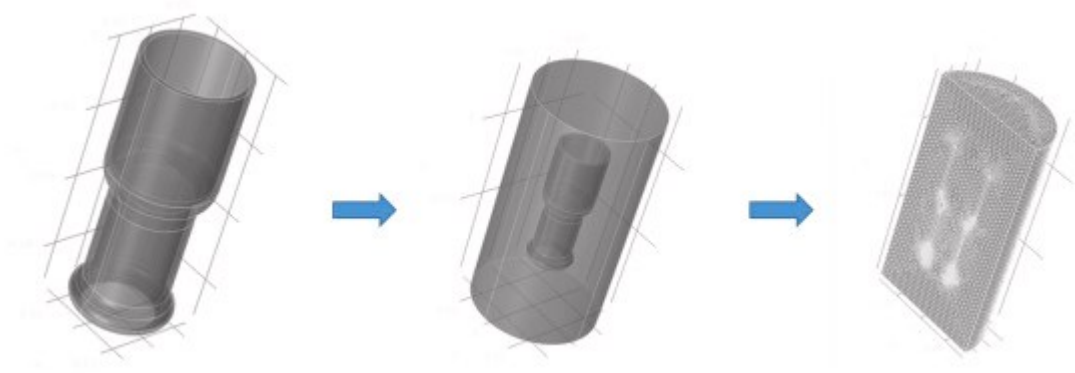


Figure 34: CAD geometry of the stainless-steel part (left), complementary fluid domain (center), model mesh (right).

Having defined the geometry, the transport of diluted species problem was characterized from the steel-liquid interface to the bulk of the solution (see Fig. 35). Transport was again modeled by the Fick's diffusion law. Liquid-side interface concentrations were estimated and set equal to equilibrium concentrations following some well-assessed literature studies (Sato et al., 2012). The nickel, manganese and chromium migrants are present in their ionic state into the liquid-side of the interface

and their diffusion coefficients were estimated from literature with a temperature-dependent formulation (Sato et al., 2012; Kariuki and Dewald, 1996).

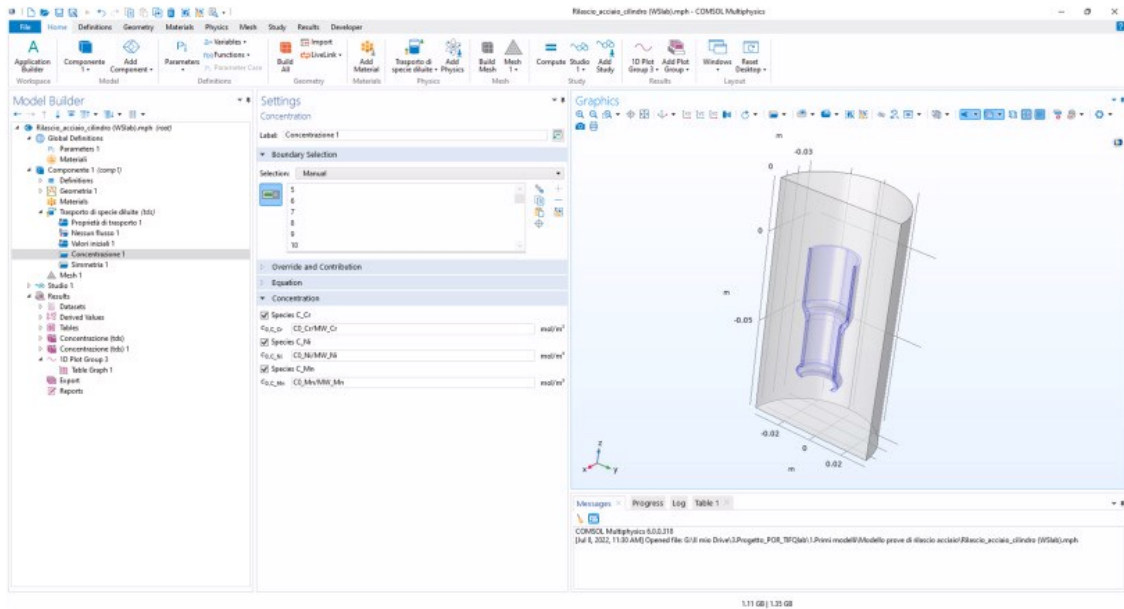


Figure 35: Comsol Multiphysics interface. The previously defined interface concentrations were used to define the model boundary conditions.

Once the model was implemented, a transient study of component release was carried out. This study gave results spanning 30 min as imposed by regulations (Mauricio-Iglesias, 2016). The solution-side concentration profiles and the average concentration in the liquid over time were so collected. The results obtained are reported in section 3.2.

3.2.3 - Standalone application of stainless steel components release in acid solutions

Based on the presented model in the previous section, a standalone application was implemented to simulate the same metal-solution interface with a simplified geometry of the cylindrical type; this complies with the experimental setups imposed by the European Directive 2002/72/EC (Commission Directive 2002/72/EC, 2022). The user will be able to change the geometry dimensions of both the part and the surrounding liquid container, the viscosity, density and molecular weight of the solvent, the density of the steel and its percentages of chromium, manganese and nickel, as well as the simulation temperature and simulation time. The simulation can be run on consequent multiple passes to simulate a renewal of the solvent after a specific time of simulation (a testing procedure considered by the EU regulations) and the restoration of the initial driving force of the phenomena (null concentration of migrants in the solvent domain) multiple times. This was brought “tricking” the simulation: a laminar flow physical module was added in the fluid domain so that, in between the simulation runs, the simulant is set to flow and leave the domain of the model (this takes few seconds of simulation) to be replaced by a volume of “fresh” solution. In this way, new initial conditions will be set by which the releasing solid part retains the concentrations calculated at the last iteration from the previous run and the solvent is again at null concentration.

The data input interface is presented in Fig. 36 and is very user-friendly. Once the data is entered, one can click on the interactive buttons on the left to generate the new geometry, mesh and start model computation, respectively.

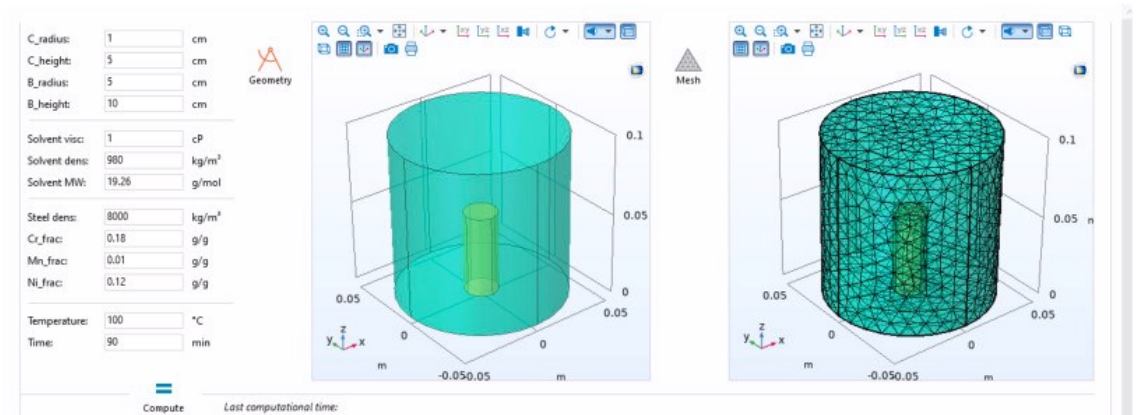


Figure 36: Data input interface of the application for the simulation of the stainless steel component release.

Once the simulation is carried out, three graphs will be returned showing the average concentrations of Chromium, Manganese and Nickel in the solvent side over time. Also, the exact final concentration value for each component is shown aside. Simulation results examples are reported in Section 4.3.

3.3 - Experimental

The stainless-steel industrial piece release test was replicated in the laboratory for an appropriate experimental validation of the implemented model. Release tests were performed by putting the stainless-steel sample in a simulating solution of acetic acid 3%. The reference temperature of 60 °C was regulated by a thermostatic bath

and a K-type thermocouple was used to monitor the temperature. A laboratory beaker with 1 L capacity was used as a container; it was equipped with a cap to prevent solution evaporation. Sample was inserted into the simulating bath when it reached the desired temperature. Different solution samples were taken every 5 min until 30 min in very small amounts so that the final concentration was not affected by the withdrawal. The experimental test was performed at least in triplicate. Following the appropriate methods as reported in the literature (Okano et al. 2015; Wu et al., 2021), the ions complexation with sodium diethyldithiocarbamate solution (1.17×10^{-2} mol/L) was firstly performed. The metal complexes solution was concentrated using a compact evaporator in a water bath (40 °C). After pre-concentration it was possible to determine Ni, Mn and Cr amount in the solution using Jasco ultra-HPLC measurement (L-column 2 ODS; mobile-phase acetonitrile: water 65:35 v/v; flow rate, 1.0 mL/min; column temperature, 40 °C) by setting detection wavelengths equal to 590 nm for Ni, 530 nm for Mn and 370 nm for Cr and injection volume to 10 μ L.

3.4 - Results and discussions

Based on the presented models, the obtained results are reported and discussed in the following sections.

3.4.1 - Concentration profiles of polymeric additives in a food matrix

The first simulation represented the following situation: an LPDE film with a thickness of 100 μm is used to wrap a sandwich; the food is stored in a refrigerator at 5 °C, and the release of Octadecyl-3-(3,5-di-tert-butyl-4-hydroxyphenyl) from the polymer to the food was simulated over time. The density of the polymer is found to be 0.945 g/cm³, while the migrant - with reference number PM-Ref No = 68,320 - has a specific migration limit (SML) of 6 mg/kg after 7 days, a molecular weight (MW) of 531 g/mol and an initial concentration (C₀) of 3000 mg/kg. As suggested by the directive 2002/72/EC (Simoneau et al., 2017), in absence of specific data, in order to model worst case scenarios, the partition coefficient, *k*, of the migrant at the interface between the polymer and the food was taken equal to 1. Downstream of the previous information, migration of the component into the analyzed food matrix was simulated using the previously implemented and illustrated model. The following 3D profiles (Fig. 37) were obtained within the sandwich domain.

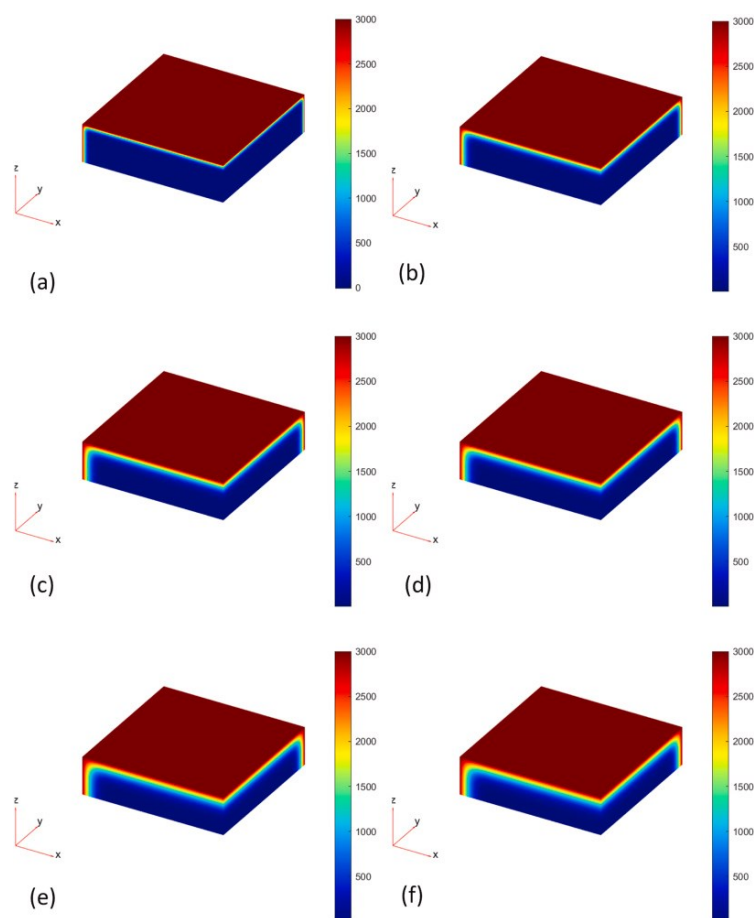


Figure 37: Octadecyl-3-(3,5-di-tert-butyl-4-hydroxyphenyl) concentration profiles in the sandwich during time. (a) 5 days, (b) 10 days, (c) 20 days, (d) 30 days, (e) 40 days, (f) 50 days.

From the obtained concentration profiles, it was possible to calculate the amount of additive present in the food matrix at the reported time shown in Table 8.

Table 8: Migrant concentration present in the food matrix at different exposure times.

t [days]	5	10	20	30	40	50
C [mg/kg]	3.2	5.9	9.8	14.3	18.1	23.1

These results show that the maximum storage time of the food in the simulated conditions may be a little more than 10 days, after this time span the food acquires a migrant concentration above the limit imposed by the regulations. The obtained

results are in good agreement with both the shelf life of refrigerator-stored sandwiches and the values reported by European regulations (Simoneau et al., 2017) as a confirmation of the reliability of the implemented approach.

3.4.2 - Concentration profiles of nickel, manganese and chromium from a stainless-steel piping part

The following concentration profiles represent the major migrant components present in 316 steel due to the simulation study described in Section 2.2. Chromium, Manganese and Nickel are present in the steel with compositions of 0.18, 0.01 and 0.12 g/g (Kamerud et al., 2013). The simulation temperature is set equal to 60 °C. Fig. 38 shows the concentration profile of a model section at different release times 0, 10 and 30 min.

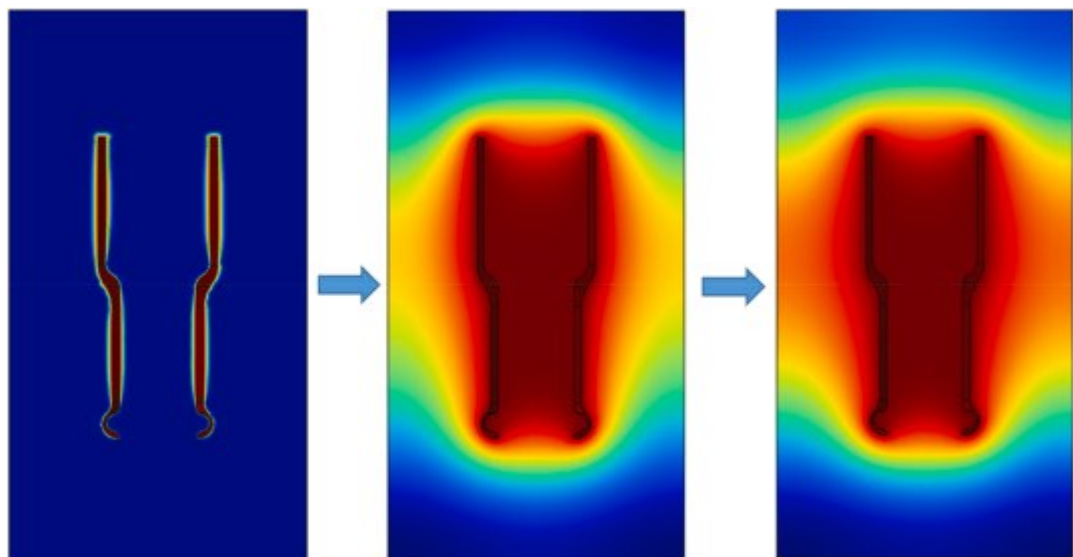


Figure 38: Concentration profiles of Chrome migrant at 0, 10 and 30 min (from left to right).

From the post-processing of the performed studies, the mean concentration curves of the solution over time were derived and shown in Fig. 39. In the same figure the experimental results were reported as well and a very good agreement with the modeling data was observed, The used experimental setup was also shown in Fig. 40.

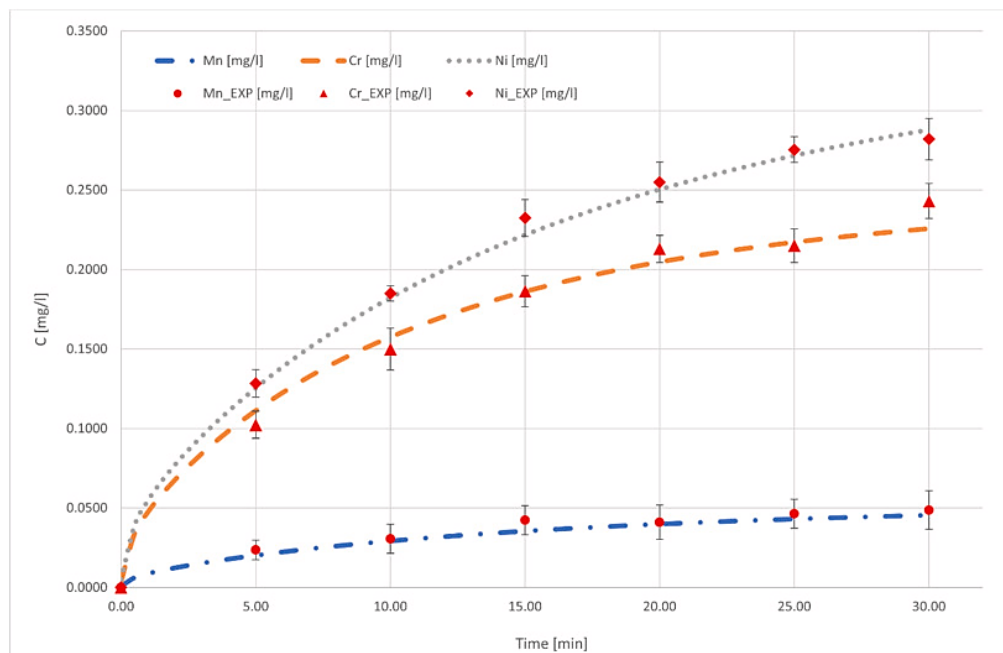


Figure 39: Average concentration profiles of Chrome, Nickel and Manganese [mg/l] over time [min]. Modeling and experimental.



Figure 40: Experimental setup for the metal release test.

From these results, it can be deduced that Nickel, which is the most released component, after 30 min, is present with a concentration of 0.290 mg/L. At the same time, Manganese and Chromium are present with concentrations of 0.046 and 0.226, respectively.

3.4.3 - Standalone application uses.

A simulation was carried out for a geometry with an outer cylinder representing the solvent (simulant) domain with a radius of 5 cm and a height of 20 cm and an inner cylinder representing a 316-steel part with 1 cm radius and 5 cm height releasing Cr, Mn and Ni. The solvent was characterized using a viscosity of 1 cP, a density of 980 kg/m³ and a MW of 19.26 g/mol. At the same time, the steel was set with a density of 8000 kg/m³ and initial Cr, Mn and Ni concentrations of 0.18, 0.01 and 0.12

g/g, respectively. The simulation temperature was set to be 100 °C, and a contact time of 90 min was considered.

Fig. 41, Fig. 42, Fig. 43 show the concentration profiles, in mg/L, for the three migrant components.

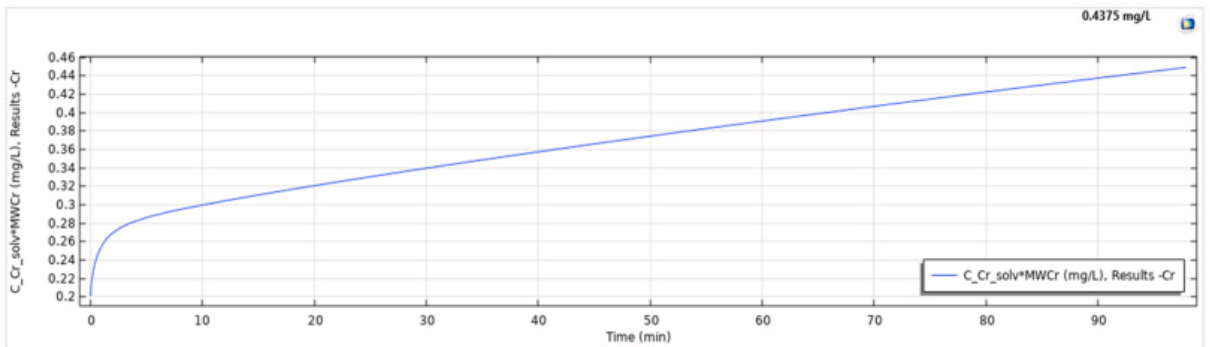


Figure 41: Chromium concentration profile [mg/L] in 90 min of release at 100 °C.

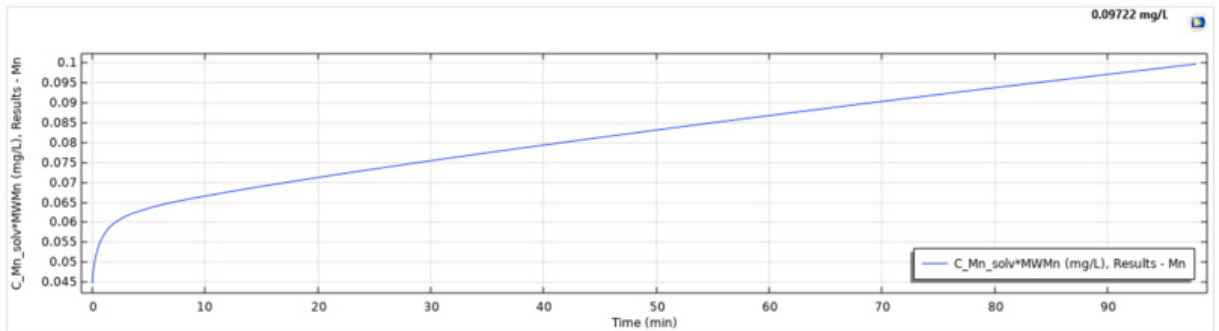


Figure 42: Manganese concentration profile [mg/L] in 90 min of release at 100 °C.

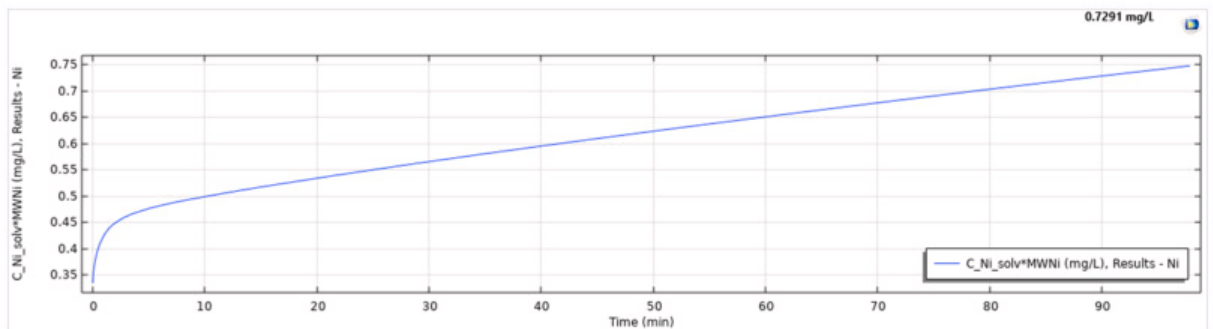


Figure 43: Nickel concentration profile [mg/L] in 90 min of release at 100 °C.

With the implemented application, it was possible to quickly estimate the amount of components released into the solution after 90 min of contact at 100 °C. They were found to be 0.438, 0.097 and 0.729 mg/L for Cr, Mn and Ni, respectively. It is worth noting how, by increasing the temperature from 60 to 100 °C, the concentrations at 30 min increased significantly, as expected.

3.5 - Conclusions

In the presented paper, different innovative modeling approaches were developed to simulate the release of some migrant substances from food industry packaging and process materials. The amount of Octadecyl-3-(3,5-di-tert-butyl-4-hydroxyphenyl) contained in a polyethylene film wrapping a refrigerated countertop food sandwich was initially estimated and found to be 5.9 mg/kg at day 10, which is within regulatory limits (6 mg/kg) and by which the valuable shelf life of the food can be estimated.

In addition, a migration model of Chromium, Manganese and Nickel from a steel part to a surrounding aqueous environment was developed. After 30 min of exposure, at a temperature of 60 °C the surrounding acid solution contained the three components with concentrations of 0.226 mg/L, 0.046 mg/L and 0.290 mg/L for Chromium, Manganese and Nickel, respectively. A computational application was implemented for the same release interface, and a migration simulation was

performed at 100 °C for 90 min. The concentrations obtained are significantly higher than the previous ones due to the longer exposure time and the higher temperature. Comparing the concentrations at 30 min for both the simulations it is possible to note a significantly higher concentration of migrants in solution at 100 °C, as expected. A very good agreement with the metal release experimental tests was also obtained.

The implemented modeling approach responds to the emerging need in the food industry due to the strict regulations that impose a very low limit value of migrant concentration into the food matrix diffused during processing and storage. The use of the presented modeling approaches can significantly innovate the specific migration field avoiding the exploitation of long, laborious, and very approximative experimental methodologies and replacing them with flexible, lower cost, and faster modeling-based tools. The significant innovation determined by the proposed modeling approach is also confirmed by some European directives that admit mathematical modeling as a reliable tool to calculate the specific migration limit in food substances.

CRedit author statement.

F. Petrosino: Conceptualization, Software, Validation, Formal analysis, Investigation, Data Curation, Writing - Original Draft, Visualization.

G. Coppola: Conceptualization, Software, Methodology, Investigation, Writing - Review & Editing.

S. Chakraborty: Conceptualization, Methodology, Validation, Writing - Review & Editing, Supervision.

S. Curcio: Conceptualization, Methodology, Resources, Writing - Review & Editing, Supervision, Project administration, Funding acquisition.

Declaration of competing interest

The authors declare that they have no known competing financial interests or personal relationships that could have appeared to influence the work reported in this paper.

3.6 - Appendix

A. Model data set

```
%sandwich geometry

l_xy=15; % [=]cm

l_z=4; % [=]cm

%polymer LPDE

p_thick=0.01; %polymer thickness [=]cm

p_dens=0.945; %polymer density [=]g/cm3

Ap_os=11.5; %upper bound polymer specific diffusion parameter [=]-

tao=0; %polymer specific activation energy parameter [=]K

R=8.3145; %gas constant [=]J/mol*K

%migrant Octadecyl-3-(3,5-di-tert-butyl-4-hydroxyphenyl) propionate

SML=6; %specific migration limit [=]mg/Kg

Mr=531; %relative molecular mass of migrant [=]-

Cp0=3000; %initial concentration of migrant in polymer [=] mg/Kg

%Cp0=Cp0*0.945/1e3; % " [=]mg/cm3

%migration contact condition

Kpf=1; %partition coefficient of the migrant between P and F [=]-

T=5; %temperature [=]°C

t=20*1e4; %time [=]days

t=t*24*3600; % " [=] seconds
```

B. Diffusion coefficient

```
%diffusion coefficient calculation

Ap_s=Ap_os-tao/T;

exp_term=Ap_s-0.1351*Mr^(2/3)+0.003*Mr-R*10454/(R*(T+273.15));

Dp_s=10^4*exp(exp_term); %upperbound diffusion coefficient [=]cm2/s
```

C. Boundary conditions

```
%BCs

applyBoundaryCondition(model,'face',[3,4,5],'u',Cp0); %dirichlet

applyBoundaryCondition(model,'face',[1,2,6],'g',0); %neumann

%coefficients

specifyCoefficients(model,'m',0,'d',1,'c',Dp_s,'a',0,'f',0);
```

D. PDE solve

```
%transient solution

ng=10; %number of grafics solution

tlist = 0:t/ng:t; %solution savings times

setInitialConditions(model, 0);

R = solvepde(model,tlist);

u = R.NodalSolution;

for i=1:ng

    figure(i+2)

    pdeplot3D(model,'ColorMapData',u(:,i));

    %title(['Concentration profile at t=' num2str((i-1)*t/(5*24*3600),'%03i')
'days'])

end
```

References (Chap.3)

- Aznar, M., Alfaro, P., Nerin, C., Kabir, A., Furton, K.G., 2016. Fabric phase sorptive extraction: an innovative sample preparation approach applied to the analysis of specific migration from food packaging. *Anal. Chim. Acta* 936, 97–107. <https://doi.org/10.1016/J.ACA.2016.06.049>.
- Barnes, K., Sinclair, R., Watson, D., 2006. Chemical migration and food contact materials. *Chem. Migrat. Food Contact Mater.* 1–464. <https://doi.org/10.1533/9781845692094>.
- Benbettaieb, N., Mahfoudh, R., Moundanga, S., Brachais, C.H., Chambin, O., Debeaufort, F., 2020. Modeling of the release kinetics of phenolic acids embedded in gelatin/chitosan bioactive-packaging films: influence of both water activity and viscosity of the food simulant on the film structure and antioxidant activity. *Int. J. Biol. Macromol.* 160, 780–794. <https://doi.org/10.1016/J.IJBIOMAC.2020.05.199>.
- Bouma, K., Schakel, D.J., 2010. Migration of phthalates from PVC toys into saliva simulant by dynamic extraction. *Food Addit. Contam.* 19 (6), 602–610. <https://doi.org/10.1080/02652030210125137>.
- cabdirect, 2022. Guidance on best practices on the risk assessment of non intentionally added substances (NIAS) in food contact materials and articles. <https://www.cabdirect.org/cabdirect/abstract/20163135771> (accessed June 28, 2022).
- Caro, J., Ruthven, D., 2006. Diffusion fundamentals I 22–24 September, 2005, Leipzig, Germany. *Catal. Commun.* 7, 920. <https://doi.org/10.1016/j.catcom.2005.11.001>.
- Casaroli, A., et al., 2022. Metals release from stainless steel knives in simulated food contact. *Food Addit. Contam. Part B Surveill.* 15 (3), 203–211. <https://doi.org/10.1080/19393210.2022.2075473>.
- Chen, J., Dong, X., Zhang, Q., Ding, S., 2019. Migration of titanium dioxide from PET/TiO₂ composite film for polymer-laminated steel. *Food Addit. Contam.: Part A* 36(3), 483–491. <https://doi.org/10.1080/19440049.2019.1577992>.
- Chung, D., Papadakis, S.E., Yam, K.L., 2002. Simple models for assessing migration from food-packaging films. *Food Addit. Contam.* 19 (6) <https://doi.org/10.1080/02652030210126389>.
- Chung, D., Papadakis, S.E., Yam, K.L., 2010. Simple models for assessing migration from food-packaging films. *Trends Food Sci. Technol.* 19 (6), 611–617. <https://doi.org/10.1080/02652030210126389>.
- Commission Directive 2002/72/EC, 2022. Commission Directive 2002/72/EC relating to plastic materials and articles intended to come into contact with foodstuffs. | UNEP Law and Environment Assistance Platform. <https://leap.unep.org/countries/eu/national-legislation/commission-directive-200272ec-relating-plastic-materials-and> (accessed July 06, 2022).
- Coppola, G., et al., 2021. Bioplastic from Renewable Biomass: A Facile Solution for a Greener Environment. *Earth Syst. Environ.* 5, 231–251. <https://doi.org/10.1007/s41748-021-00208-7>.
- Curcio, S., Petrosino, F., Morrone, M., De Luca, G., 2018. Interactions between proteins and the membrane surface in multiscale modeling of organic fouling. *J. Chem. Inf. Model.* 58 (9), 1815–1827. <https://doi.org/10.1021/acs.jcim.8b00298>.
- De Luca, G., Petrosino, F., Di Salvo, J.L., Chakraborty, S., Curcio, S., 2021. Advanced descriptors for long-range noncovalent interactions between SARS-CoV-2 spikes and F. Petrosino et al. *Journal of Food Engineering* 357 (2023) 11165213 polymer surfaces. *Sep. Purif. Technol.* 282 <https://doi.org/10.1016/J.SEPPUR.2021.120125>.
- Direttiva 2002/72/CE, 2022. Direttiva 2002/72/CE - Certifico Srl. <https://certifico.com/chemicals/legislazione-chemicals/264-legislazione-chemicals-food/7135-direttiva-2002-72-ce> (accessed June 20, 2022).

- Erdogdu, F., et al., 2022. Mathematical modeling—computer-aided food engineering. *Food Eng. Innov. Across Food Supply Chain* 277–290. <https://doi.org/10.1016/B978-0-12-821292-9.00007-8>.
- Fenyvesi, E., et al., 2007. Permeability and release properties of cyclodextrin-containing poly(vinyl chloride) and polyethylene films. *J. Inclusion Phenom. Macrocycl. Chem.* 57 (1–4), 371–374. <https://doi.org/10.1007/S10847-006-9256-1/TABLES/2>.
- Forooghi, E., Ahmadi, S., Farhoodi, M., Mortazavian, A.M., 2022. Migration of Irganox 1010, Irganox 1076, and Titanium dioxide into Doogh and corresponding food simulant from laminated packaging. *J. Environ. Health Sci. Eng.* 20 (1), 363–373. <https://doi.org/10.1007/S40201-021-00782-Y/FIGURES/5>.
- Groh, K.J., Muncke, J., 2017. In Vitro toxicity testing of food contact materials: state-of-the-art and future challenges. *Compr. Rev. Food Sci. Food Saf.* 16 (5), 1123–1150. <https://doi.org/10.1111/1541-4337.12280>.
- Hoppe, M., de Voogt, P., Franz, R., 2016. Identification and quantification of oligomers as potential migrants in plastics food contact materials with a focus in polycondensates – a review. *Trends Food Sci. Technol.* 50, 118–130. <https://doi.org/10.1016/J.TIFS.2016.01.018>.
- Institute for Health and Consumer Protection, 2009. Guidelines on Testing Conditions for Articles in Contact with Foodstuffs (With A Focus on Kitchenware) - A CRL-NRL-FCM Publication, first ed. 2009. OPOCE. Accessed: Jun. 09, 2023. [Online]. Available: <https://publications.jrc.ec.europa.eu/repository/handle/JRC51601>.
- Kabir, A., Mesa, R., Jurmain, J., Furton, K.G., 2017. Fabric phase sorptive extraction explained. *Separations* 4 (2), 21. <https://doi.org/10.3390/SEPARATIONS4020021>.
- Kamerud, K.L., Hobbie, K.A., Anderson, K.A., 2013. Stainless steel leaches nickel and chromium into foods during cooking. *J. Agric. Food Chem.* 61 (39), 9495. <https://doi.org/10.1021/JF402400V>.
- Kariuki, S., Dewald, H.D., 1996. Evaluation of diffusion coefficients of metallic ions in aqueous solutions. *Electroanalysis* 8 (4), 307–313. <https://doi.org/10.1002/ELAN.1140080402>.
- Ladeveze, P., Pelle, J.P., Rougeot, P., 1991. Error estimation and mesh optimization for classical finite elements. *Eng. Comput. (Swansea)* 8 (1), 69–80. <https://doi.org/10.1108/EB023827/FULL/XML>.
- Lestido-Cardama, A., et al., 2022. Characterization of polyester coatings intended for food contact by different analytical techniques and migration testing by LC-MSn. *Polymers* 14 (3), 487. <https://doi.org/10.3390/POLYM14030487>.
- Lopez-Cervantes, L., Sanchez-Machado, D.I., Pastorelli, S., Rijk, R., Paseiro-Losada, P., 2010. Evaluating the migration of ingredients from active packaging and development of dedicated methods: a study of two iron-based oxygen absorbers. *Food Addit. Contam.* 20 (3), 291–299. <https://doi.org/10.1080/0265203021000060878>.
- Mauricio-Iglesias, M., 2016. Optimal experimental design in the evaluation of food packaging compliance with safety regulations. *IFAC-PapersOnLine* 49 (7), 1133–1138. <https://doi.org/10.1016/J.IFACOL.2016.07.355>.
- Molina-Besch, K., Pålsson, H., 2020. A simplified environmental evaluation tool for food packaging to support decision-making in packaging development. *Packag. Technol. Sci.* 33 (4–5), 141–157. <https://doi.org/10.1002/PTS.2484>.
- Muncke, J., 2009. Exposure to endocrine disrupting compounds via the food chain: is packaging a relevant source? *Sci. Total Environ.* 407 (16), 4549–4559. <https://doi.org/10.1016/J.SCITOTENV.2009.05.006>.
- Muncke, J., 2011. Endocrine disrupting chemicals and other substances of concern in food contact materials: an updated review of exposure, effect and risk assessment. *J. Steroid Biochem. Mol. Biol.* 127 (1–2), 118–127. <https://doi.org/10.1016/J.JSBMB.2010.10.004>.

- Okano, G., et al., 2015. HPLC-spectrophotometric detection of trace heavy metals via 'cascade' separation and concentration. *Int. J. Environ. Anal. Chem.* 95 (2), 135–144. <https://doi.org/10.1080/03067319.2014.994619>.
- Olivier, Vitrac., 2020, Mar. PITTCON Conference & Expo. Ong, H.T., Samsudin, H., Soto-Valdez, H., 2022. Migration of endocrine-disruptin chemicals into food from plastic packaging materials: an overview of chemical risk assessment, techniques to monitor migration, and international regulations. *Crit. Rev. Food Sci. Nutr.* 62 (4), 957–979. <https://doi.org/10.1080/10408398.2020.1830747>.
- Petersen, J.H., Nielsen, P.A., Naamansen, E.T., 1995. PVC cling film in contact with cheese: health aspects related to global migration and specific migration of DEHA. *Food Addit. Contam.* 12 (2), 245–253. <https://doi.org/10.1080/02652039509374299>.
- Petrosino, F., De Luca, G., Curcio, S., Wickramasinghe, S.R., Chakraborty, S., 2022. Micro-CFD modelling of ultrafiltration bio-fouling. *Sep. Sci. Technol.* 1–10. <https://doi.org/10.1080/01496395.2022.2075759>.
- Petrosino, F., Curcio, S., Chakraborty, S., De Luca, G., 2019. Enzyme immobilization on polymer membranes: a quantum and molecular mechanics study. *Computation* 7 (4), 56. <https://doi.org/10.3390/computation7040056>.
- Petrosino, F., Hallez, Y., De Luca, G., Curcio, S., 2020. Osmotic pressure and transport coefficient in ultrafiltration: a Monte Carlo study using quantum surface charges. *Chem. Eng. Sci.* 224, 115762. <https://doi.org/10.1016/j.ces.2020.115762>.
- Piotrowska, B., 2004. Toxic components of food packaging materials. *Toxins in Food* 313–333, 10.1201/9780203502358-18/TOXIC-COMPONENTS-FOOD-PACKAGINGMATERIALS-BARBARA-PIOTROWSKA.
- Poças, M.F., Oliveira, J.C., Oliveira, F.A.R., Hogg, T., 2008. A Critical Survey of Predictive Mathematical Models for Migration from Packaging. *Crit. Rev. Food Sci. Nutr.* 48 (10), 913–928. <https://doi.org/10.1080/10408390701761944>.
- Sanches Silva, A., Cruz Freire, J.M., Sendon, R., Franz, R., Losada, P.P., 2009. Migration and diffusion of diphenylbutadiene from packages into foods. *J. Agric. Food Chem.* 57 (21), 10225–10230. https://doi.org/10.1021/JF901666H/ASSET/IMAGES/JF2009-01666H_M005.GIF.
- Sato, H., Yui, M., Yoshikawa, H., 2012. Ionic diffusion coefficients of Cs⁺, Pb²⁺, Sm³⁺, Ni²⁺, SeO₂-4 and TcO₄- in Free Water Determined from Conductivity Measurements. *J. Nucl. Sci. Technol.* 33 (12), 950–955. <https://doi.org/10.1080/18811248.1996.9732037>.
- Silva, A.S., Jafari, S.M., 2022. The Evolution of Food Packaging, the Active Food Packaging Concept and Its Current and Future Trends, pp. 3–12. https://doi.org/10.1007/978-3-030-90299-5_1.
- Simoneau, C., et al., 2017. Practical Guidelines on the Application of Migration Modelling for the Estimation of Specific Migration. Publications Office. <https://doi.org/10.2788/04517>.
- Tovar, L., Salafranca, J., Sanchez, C., Nerin, C., 2005. Migration studies to assess the safety in use of a new antioxidant active packaging. *J. Agric. Food Chem.* 53 (13), 5270–5275, 10.1021/JF050076K/ASSET/IMAGES/LARGE/JF050076KF00003.JPEG.
- Úbeda, S., et al., 2017. Overall and specific migration from multilayer high barrier food contact materials - kinetic study of cyclic polyester oligomers migration. *Food Addit. Contam. Part A Chem. Anal. Control Expo Risk Assess* 34 (10), 1784–1794. <https://doi.org/10.1080/19440049.2017.1346390>.
- Weissberg, H.L., 2004. Effective diffusion coefficient in porous media. *J. Appl. Phys.* 34 (9), 2636. <https://doi.org/10.1063/1.1729783>.
- Wu, X., Keegan, J., Behan, P., 2021. Migration analysis of Cr, Ni, Al, Fe, Mn, Cu, Zn, and Mo in internet-bought food serving stainless-steel utensils by ICP-MS and XRF. *Food Addit. Contam. Part B Surveill.* 14 (4), 256–263. <https://doi.org/10.1080/19393210.2021.1946168>.
- Wyrwa, J., Barska, A., 2017. Innovations in the food packaging market: active packaging. *Eur. Food Res. Technol.* 243 (10), 1681–1692.

<https://doi.org/10.1007/S00217-017-2878-2/TABLES/2>.

Zilfidou, E., Kabir, A., Furton, K.G., Samanidou, V., 2018. Fabric phase sorptive extraction: current state of the art and future perspectives. *Separations* 5 (3), 40. <https://doi.org/10.3390/SEPARATIONS5030040>.

Chapter 4: Modeling HVED functional compounds

extraction.

~

Premises to Chapter 4

The following Chapter describes the work done in collaboration with Prof. Anet Režek Jambrak³ where, through Finite Elements Modeling application, the extraction kinetics of a high added value compound is modeled. The novelty of the whole aim of the study targets two topics: the first resides in the extraction of high added value compounds, from vegetal matters, which can effectively be used as active compound in bio-packaging formulations; while the second lies in the process itself: a High Electric Voltage Discharge method has been used and modeled as a convenient and efficient extraction method. All the above translates very well in terms of the overall Product Development field: the choice of components to be used to confer the “active” features to the packaging are surely sorted by effectiveness and availability and economicity, so the use of waste vegetal masses and economically convenient methods to retrieve high added values compounds allows the choice to

³ Faculty of Food Technology and Biotechnology, University of Zagreb.

steer towards new solutions, while finely Modeling these procedures can easily bring to an optimum of the extraction method itself.

~

4.1 – Introduction

Hydroxytyrosol (HTyr) is a biophenol mostly present in olive oils and oil by-products, with strong antioxidant activity. This compound has already been used as functionalizing agent in poly(vinyl alcohol) (PVA) active films (through solvent casting method). The effect of HTyr were found to affect water absorption behavior, migration rates of food stimulants, water vapor permeabilities and antioxidant features in the film samples. Moreover, HTyr visibly produced an enhancement of the crystallinity degree of the films.

With these assumptions, the development of a novel, sustainable and safe active food packaging as alternative to the petroleum-based ones represents a basis for product improvements and process intensifications. (Fortunati et al., 2017).

Given that olive oil by-products and other forms of food waste can be a great and cheap source for high value bioactive compounds such as HTyr, conventional procedures such as soaking solvent extractions, aside being economically favorable and uncomplicated, they typically require long times, high temperature and a very bulky solvent need (Contreras et al., 2019). Novel extraction procedures as high voltage electrical discharge (HVED) extraction have and still are being developed and optimized to overcome the well-known drawbacks of conventional solvent

extractions (Chemat et al., 2017; Li, Ma, Li, Zhang, & Dai, 2017; Li et al., 2017; Rocha et al., 2018).

HVED extraction is a has gained significant notoriety in food applications (Boussetta & Vorobiev, 2014; Puértolas & Barba, 2016). Being it a non-thermal technique, the mechanism is mostly based on the electrical breakdown of vegetal substrates. Through applying high voltage discharges – by electrodes directly submerged in the aqueous solvent- very abrupt phenomena like shock waves, liquid turbulences, UV radiations, cavitation and concentrated free radicals formation result in the collapse of the vegetal matrices and cellular structures, with a consistent increase of the mass transfer of the active components towards the solvent phase with the consequent increase of extraction efficiencies (Boussetta et al., 2009).

Through the definition of all transport phenomena involved during the HVED, a very precise modeling of the process can bring out high optimization capability, including scaleup and process design possibilities towards a proper industrial application which could optimize the added values of the food by-products and wastes generated by the food chain.

The following describes a first attempt of modeling based on the HVED extraction data provided by Prof. Anet Režek Jambrak and of the related simulation runs on COMSOL Multiphysics 6.5.

4.2 - Experimental data fitting

The first scope of the modeling was the extrapolation of extraction kinetics from the given extraction data (Chan et al., 2014). The compound on which the modeling has been built is Hydroxytyrosol, which has been proved to have antimicrobial effects in active food packagings (Fortunati et al., 2017). The data were given at 3 different time values: 3, 6, 9 min, three Ethanol/Water fractions: 0, 25, 50% and at 3 different applied voltage amplitudes: 15, 20, 25 kV. Mass concentrations were given in ng/ml (Table 9).

Table 9: Data of the extraction runs array given by UniZa.

<i>Run</i>	<i>Treatment time [min]</i>	<i>Voltage [kV]</i>	<i>Ethanol content [%]</i>	<i>Hydroxytyrosol [ng/ml]</i>
<i>ON1</i>	3	20	50	163
<i>ON2</i>	9	20	0	201
<i>ON3</i>	3	20	0	3
<i>ON4</i>	3	25	0	5
<i>ON5</i>	9	25	25	226
<i>ON6</i>	9	20	25	177
<i>ON7</i>	9	20	50	124
<i>ON8</i>	9	25	50	126
<i>ON9</i>	3	25	25	144
<i>ON10</i>	9	25	0	4
<i>ON11</i>	3	25	50	127
<i>ON12</i>	3	20	25	147
<i>OA1</i>	3	15	50	137
<i>OA2</i>	9	15	0	15
<i>OA3</i>	3	15	0	73

OA4	3	20	0	356
OA5	9	20	25	166
OA6	9	15	25	157
OA7	9	15	50	120
OA8	9	20	50	161
OA9	3	20	25	157
OA10	9	20	0	1
OA11	3	20	50	123
OA12	3	15	25	137

Some data were given twice for the same set of variable values, so the actual data considered were resulting from a mean of the results of all repeated sets. The sets of data considered in the modeling were the ones with no ethanol involved.

A fitting curve of the mass concentration as a function of time has been obtained for each voltage amplitude, as shown in the Figure 44.

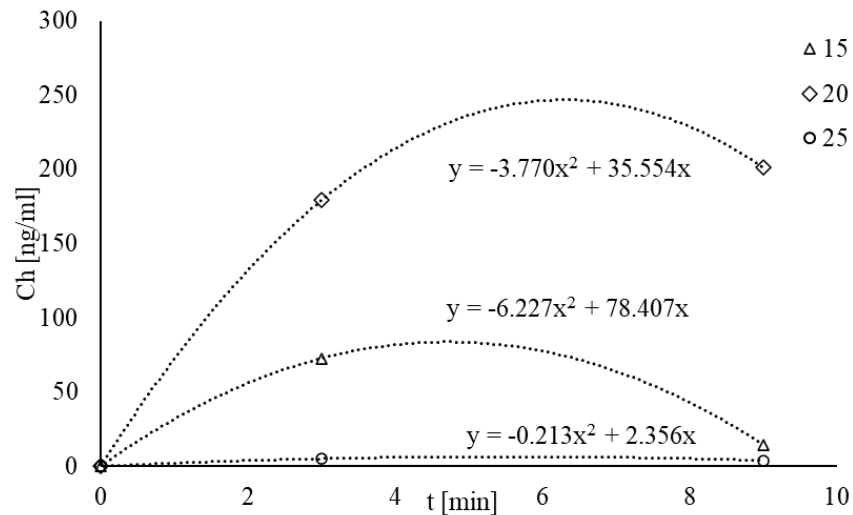


Figure 44: Fitting of mass concentration data as a function of time.

The presence of few time step values per curve resulted in a degree of uncertainty in the fitting itself, considering that for a more efficient fitting more data at different time steps are needed. The fact that curves are not positive monotones indicates that a process of decomposition of the targeted compound takes place after a certain extraction time, this probably due to the electrical discharge strength.

The three mass concentration fittings are reported as second order polynomials:

$$Ch_{15kV} = -3.770t^2 + 35.554t \quad \text{Eq.1}$$

$$Ch_{20kV} = -6.227t^2 + 78.407t \quad \text{Eq.2}$$

$$Ch_{25kV} = -0.213t^2 + 2.356t \quad \text{Eq.3}$$

Where values of Ch are in *ng/ml*, t in *min*.

Being Ch(t) in the form of $Ch(t)=A*t^2+B*t$, both **A** and **B** terms have been parametrized as a function of the applied voltage to obtain a single function system dependent from time and voltage amplitude.

Fitting curves for the **A** and **B** parameters as a function of the applied voltage (in *kV*) are shown in the graph below.

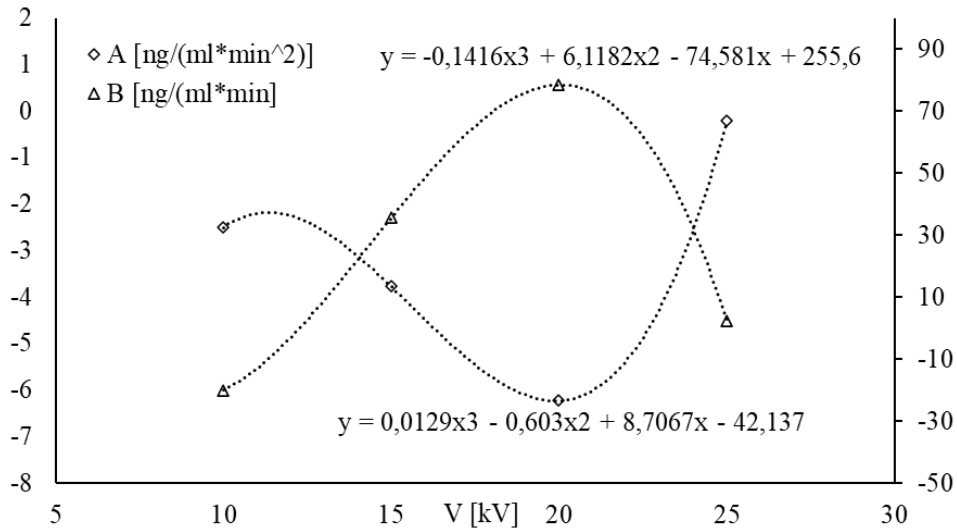


Figure 45: Fitting of the *A* and *B* parameters as a function of the applied voltage.

The resulting fitting equations, taken as simple polynomials, are shown below as a system defining the involved extraction kinetics:

$$\begin{cases} \mathbf{Ch}_{(t,V)} = A_{(V)}t^2 + B_{(V)}t \\ A_{(V)} = 0.0129V^3 - 0.603V^2 + 8.7067V - 42.137 \\ B_{(V)} = -0.1416V^3 + 6.1182V^2 - 74.581V + 255.6 \end{cases} \quad \text{Eqs.4,5,6.}$$

4.3 - Comsol 5.6 implementation

All simulation parameters and defined functions in Comsol Multiphysics physics tree are reported below.

4.3.1 – Parameters

All the parameters defined in the simulation are listed in the following Table 10, being them: geometrical reactor variables, solvent and solute physical variables,

applied voltage amplitude and step frequency, Stokes-Einstein correlation parameters for the calculation of the diffusion coefficient, kinetics fitting parameters (A_{Vfix} , B_{Vfix}), and the two extraction kinetics equations defined in the previous section.

Table 10: Description of the parameters declared in the simulations.

Name	Expression	Value	Description
d_r	10[cm]	0.1 m	Reactor diameter
h_r	15[cm]	0.15 m	Reactor height
Vfix	20	20	Applied voltage
MWh	154[g/mol]	0.154 kg/mol	Hydroxytyrosol mol. w.
B	$1.38E-23[m^2*kg/(K*s^2)]$	1.38E-23 J/K	Boltzmann constant
T	25[degC]	298.15 K	Temperature
Visc	1E-3[Pa*s]	0.001 Pa·s	Solvent viscosity
R	0.7[nm]	7E-10 m	Average particle size
Dw	$B*T/(6*pi*Visc*R)$	3.1183E-10 m ² /s	Diffusion coefficient (Stokes-Einstein)
Tkv	$1.5E-5[m^2/s]$	$1.5E-5 m^2/s$	Turbulent kinetic viscosity
dt	0.01[min]	0.6 s	time delta
Freq	1[Hz]	1 Hz	frequency
A_Vfix	$0.0129*(Vfix)^3 - 0.603*(Vfix)^2 + 8.7067*(Vfix) - 42.137$	-6.003	A(V) fitting curve
B_Vfix	$-0.1416*Vfix^3 + 6.1182*Vfix^2 - 74.581*Vfix + 255.6$	78.46	B(V) fitting curve

4.3.2 - Definitions

4.3.2.1 - Functions

One peculiar model condition is defined as function, in fact the applied voltage is defined as a square wave function, to recall and tune all the variables that can be imposed with proper laboratory extraction runs (Table 11).

Table 11: Definition of the functions used for the time-dependent applied voltage.

Function name	wv1	Vsteps	C_h
Function type	Waveform	Analytic	Analytic
Description	Value	Value	Value
Type	Square	$0.5 + wv1(t*Freq)$	$A_Vfix*t^2 + B_Vfix*t$
Size of transition zone	0.05	t	t
Duty cycle	0.2	Value	Value
Angular frequency	$2*pi$	s	min
Amplitude	0.5	-	ng/ml

In figure 46 below, a representation of the functions describing (a) the time-dependent applied voltage and (b) the resulting voltage profile in the reactor when $V \neq 0$.

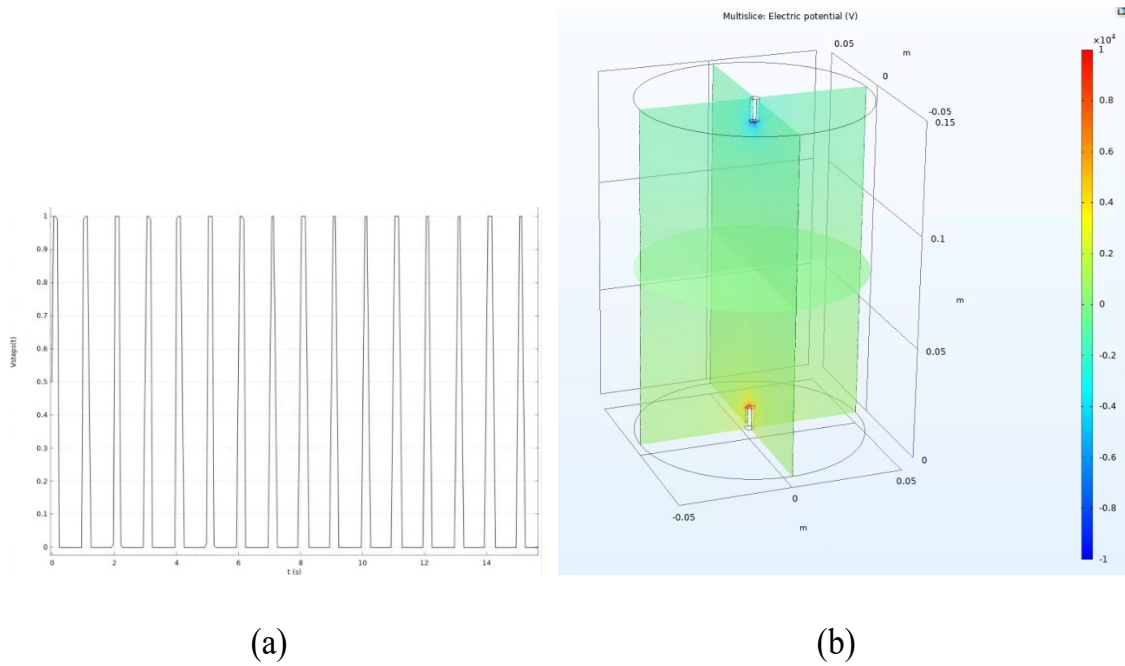


Figure 46: graphical representations of the (a) applied voltage and (b) resulting voltage amplitude profile (when $V \neq 0$).

4.3.2.2 - Probes

The concentration profiles have been followed by the definition of two concentration probes used to store the concentration values in each domain node over time: $AvMC_{solv}$ in the solvent domain and $AvMC_{porous}$ in the porous media domain.

Table 12: Probes definition features.

	$AvMC_{solv}$	$AvMC_{porous}$
Probe type	Domain probe	Domain probe
Geometric entity level	Domain	Domain
Selection	Geometry geom1: Dimension 3: Domain 2	Geometry geom1: Dimension 3: Domain 1
Description	Value	Value
Expression	ch*MWh	ch*MWh

Unit	ng/ml	ng/ml
Description	ch*MWh	ch*MWh

4.3.2.3 - Materials

The defined materials in the two domains are water (taken from the COMSOL library) and a new material defined as vegetal matter (*Leaves*). All the physical variables used in the model are listed in Tables 13 and 14.

Table 13: Water physical properties.

Water, liquid		
Coefficient of thermal expansion	alpha_p(T)	<i>analytic</i>
Bulk viscosity	muB(T)	<i>analytic</i>
Dynamic viscosity	eta(T)	<i>piecewise</i>
Ratio of specific heats	gamma_w(T)	<i>analytic</i>
Electrical conductivity	5.5e-6 [S/m]	
Heat capacity at constant pressure	Cp(T)	<i>piecewise</i>
Density	rho(T)	<i>piecewise</i>
Thermal conductivity	k(T)	<i>piecewise</i>
Speed of sound	cs(T)	<i>interpolation</i>
Relative permittivity	80	

Table 14: Vegetal matter (leaves) physical properties.

Leaves	
Porosity	0.4
Relative permittivity	1
Electrical conductivity	0.0002 [S/m]

4.3.3 - Transport of Diluted Species in Porous Media

The mass transfer differential equations run by the physical model are reported below:

$$\frac{\partial(\epsilon_p c_i)}{\partial t} + \frac{\partial(\rho c_{p,i})}{\partial t} + \nabla \cdot \mathbf{J}_i + \mathbf{u} \cdot \nabla c_i = R_i + S_i \quad Eq.7$$

$$\mathbf{J}_i = -(D_{Dj} + D_{ej})\nabla c_i - z_i \mu_{me,j} F C_i \nabla V \quad Eq.8$$

The transport mechanisms undertake calculations considering effects due to convection, migration in the electric field and mass transfer in a porous media.

The porous domain (vegetal matter domain) is defined by a bed density of 600 kg/m³ and a pellet density of 800 kg/m³.

The extraction kinetics has been set as the first derivative over time of the previously defined **Ch(t)** function, and the solvent domain (water domain) is defined by applying the previously defined diffusion coefficient, as described in the following Table 15.

Table 15: Domains definitions.

	Description	Value
Leaves	Total rate expression	(1/MWh)*d(C_h(t), t)
	Reacting volume	Pore volume
Water	Source	Material
	Material	Water, liquid (mat1)
	Diffusion coefficient	User defined
	Diffusion coefficient	Dw

The Migration in Electric Field calculations are defined by defining the electric potential as the above-mentioned square wave function multiplied by the voltage amplitude value $V_{fix} * V_{steps(t)}$ and by setting the mobility parameter as following the Nerst-Einstein relation.

4.3.4 - Mesh

The calculation mesh, which comprises both the porous (vegetal matter) domain and the liquid (solvent) domain was set such that any further mesh refinement would not affect modeling results. Table 16 below collects all the features, while a graphical representation of the mesh and statistics of its main quality parameters is proposed in Figure 46.

Table 16: Mesh features.

Description	Value
Minimum element quality	0.2004
Average element quality	0.6693
Tetrahedron	282120
Triangle	17146
Edge element	1156
Vertex element	32
Maximum element size	0.00525
Minimum element size	2.25E-4
Curvature factor	0.3
Resolution of narrow regions	0.85
Maximum element growth rate	1.35
Predefined size	Extra fine

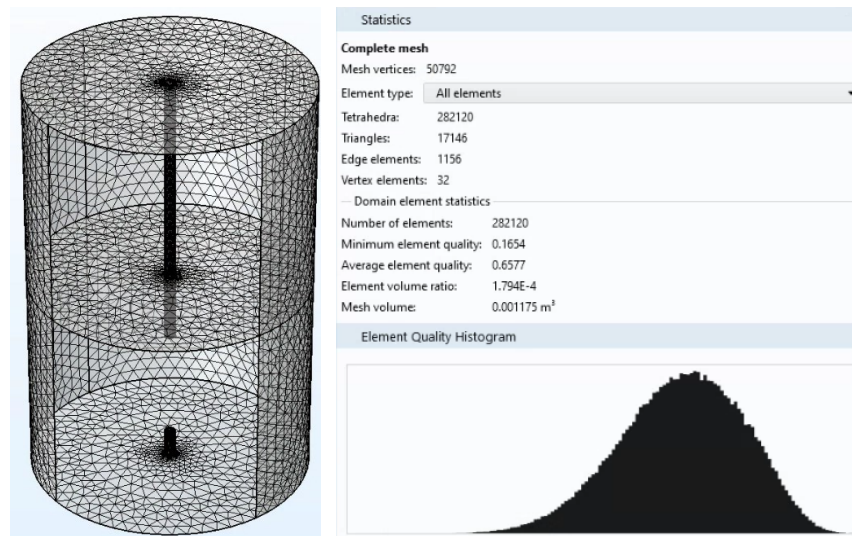


Figure 46: Graphical representation and quality parameters of the chosen calculation mesh.

4.4 - Time Dependent Study - results.

The results were obtained by running a time-dependent problem of the PDE system collecting the whole transport phenomena addressed in the study. The computation of the whole extraction time (10 minutes) lasted 30 minutes.

Results of the simulation are shown in the following Table 17 and Figures 47 and 48.

Table 16: Computation results in both solvent and porous domain over simulation time.

Time (min)	Ch [ng/ml] Solvent domain	Ch [ng/ml] Porous domain
0.0000	1.4303E-6	0.0014772
0.010000	0.0014711	0.77828
0.020000	0.0035189	1.5523
0.040000	0.0089205	3.0923

0.08000	0.022160	6.1487
0.16000	0.046866	12.180
0.32000	0.093832	23.960
0.64000	0.18409	46.258
1.2800	0.34729	86.039
2.2800	0.54561	136.46
3.2800	0.67968	175.12
4.2800	0.75195	202.03
5.2800	0.79894	220.91
6.2800	0.82626	229.23
7.2800	0.83982	226.03
8.2800	0.84646	210.99
9.2800	0.85555	183.98
10.280	0.85610	145.01

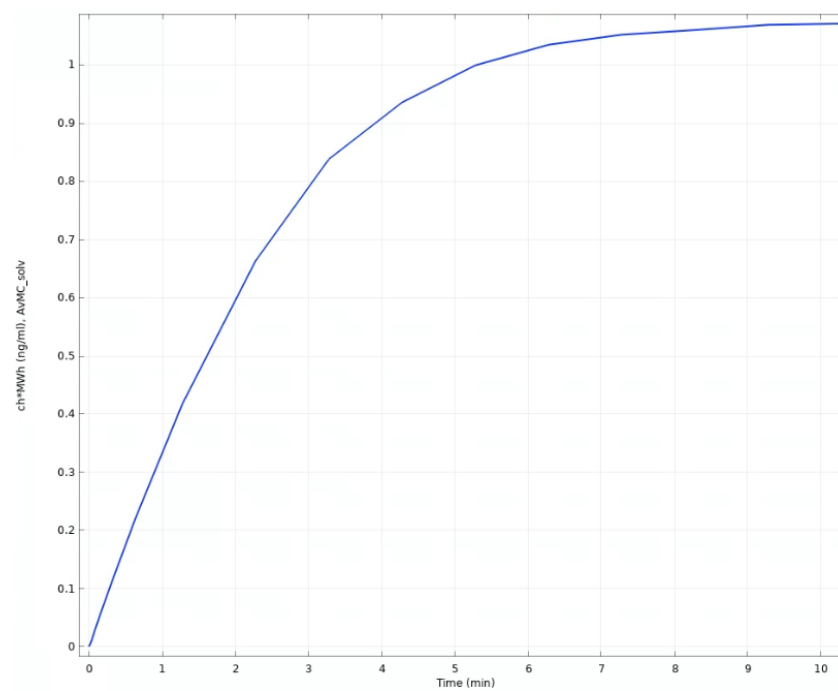


Figure 167: Solute concentration profile in the solvent domain.

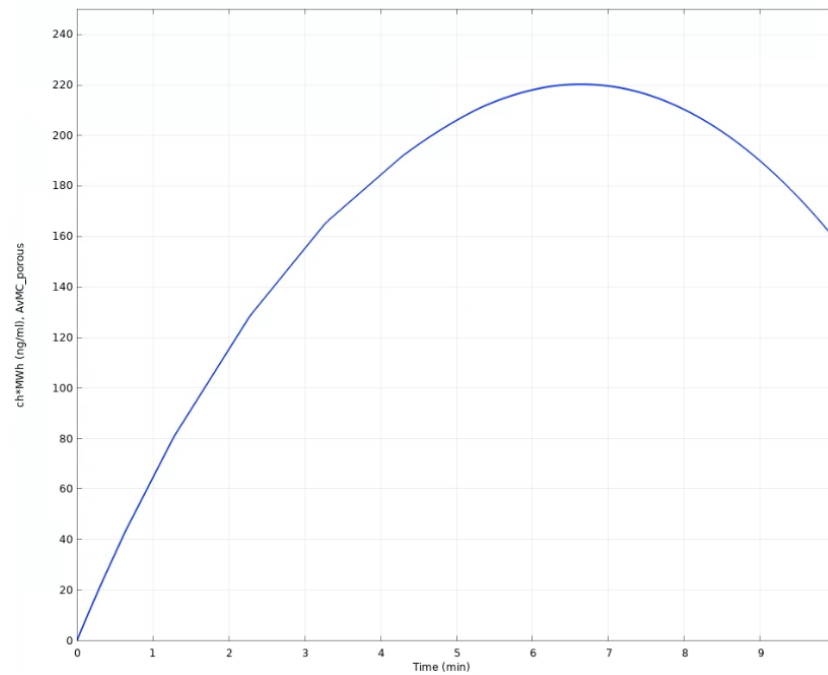


Figure 48: Solute concentration profile in the porous domain.

In the following Figure 49, results at different times are shown through the whole calculation domain, where a high concentration gradient is clear at the interface between the two domains (solvent and porous).

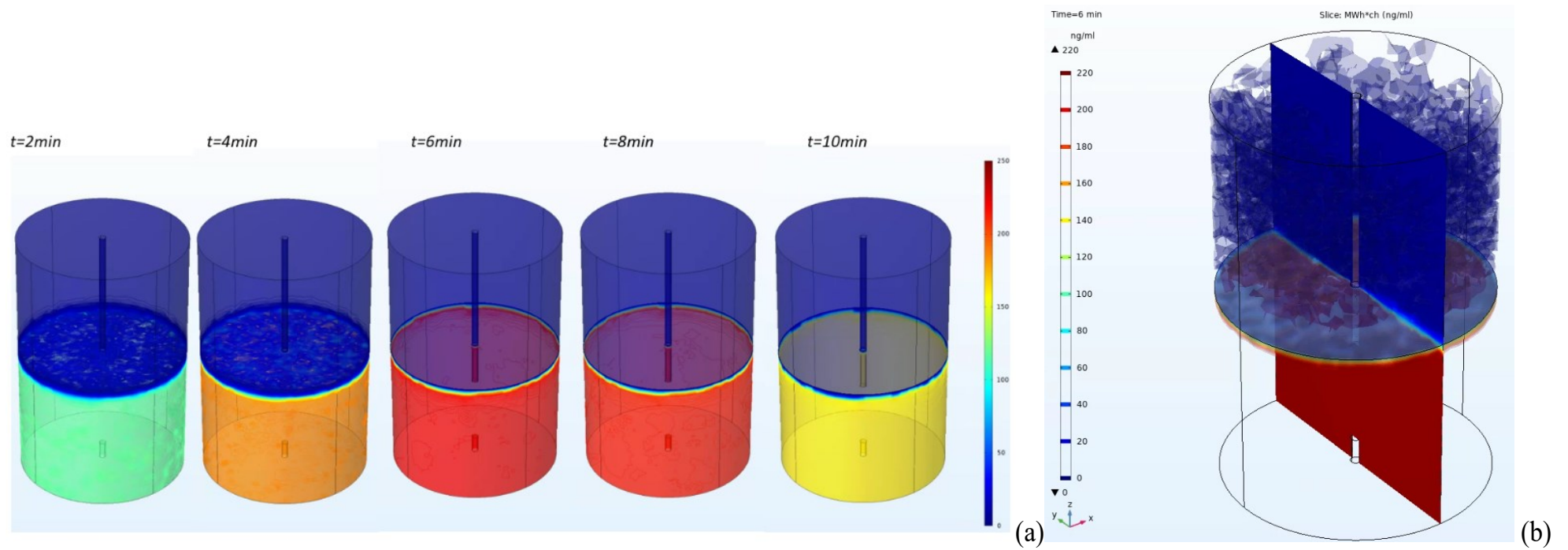


Figure 49: Concentration profiles in the caculations domain (a) at intermediate simulation times and (b) at 6 minutes, concentration gradients at the interface between the domains are evident.

As expected, the bulk of the transport phenomena is retraceable at the interface between the two domains, where the discontinuity of the transport rates (and transport coefficient) resides.

4.5 – Conclusions.

A first model of the HVED extraction reactor has been built to trace a first attempt for a precise extraction simulation. The definition of the transport variables, the characterization of the two phases, of which the solid one defined as a porous domain where the solvent is able to create its channeling and its contact interfaces with the solute, represent a solid foundation for a model reflecting real operative conditions. The electric discharge has been modeled as a periodic condition to retain the ability to tune the main operative parameters (voltage amplitude and frequency). As a consequence, the model is a valid representation of the extraction kinetics as experienced in the Uniza laboratories. As main further enhancement of the modeling capabilities, a deeper understanding of each of the effects - like shock waves, liquid turbulences, UV radiations, cavitation and concentrated free radicals formation – and a consequent approach towards the modeling of each of those (possibly with the use of a multiscale modeling approach) as a contribution to the overall extraction effect will give very broad simulation and process optimization capabilities.

References (Chap.4)

- Fortunati, E., Luzi, F., Fanali, C., Dugo, L., Belluomo, M. G. et al. (2017). Hydroxytyrosol as Active Ingredient in Poly(vinyl alcohol) Films for Food Packaging Applications. *Journal of Renewable Materials*, 5(2), 81–95.
- S.Y. Lee, S.J. Lee, D.S. Choi, and S.J. Hur, Current topics in active and intelligent food packaging for preservation of fresh foods. *J. Sci. Food Agric.* 95, 2799–2810 (2015).
- J. Gomez Estaca, C. Lopez de Dicastillo, P. Hernandez Munoz, R. Catala, and R. Gavara, Advances in antioxidant active food packaging. *Trends Food Sci. Technol.* 35, 42–51 (2014)
- Chung-Hung Chan, Rozita Yusoff, Gek-Cheng Ngoh, Modeling and kinetics study of conventional and assisted batch solvent extraction (2014), *Chemical Engineering Research and Design*, Volume 92, Issue 6, Pages 1169-1118
- Tânia B. Ribeiro, Teresa Bonifácio-Lopes, Pilar Morais, Arménio Miranda, João Nunes, António A. Vicente, Manuela Pintado, Incorporation of olive pomace ingredients into yoghurts as a source of fibre and hydroxytyrosol: Antioxidant activity and stability throughout gastrointestinal digestion (2021) *Journal of Food Engineering*, Volume 297
- Pérez-Barrón, G., Montes, S., Aguirre-Vidal, Y. et al. Antioxidant Effect of Hydroxytyrosol, Hydroxytyrosol Acetate and Nitrohydroxytyrosol in a Rat MPP+ Model of Parkinson's Disease (2021). *Neurochem Res* 46, 2923–2935.
- Youseef Ahmed Wani, F.A. Masoodi, Rehana Akhter, Towseef Akram, Adil Gani, Nadeem Shabir, Nanoencapsulation of hydroxytyrosol in chitosan crosslinked with sodium bisulfate tandem ultrasonication: Techno-characterization, release and antiproliferative properties (2022), *Ultrasonics Sonochemistry*, Volume 82
- Mahmoudi, A., Hadrach, F., Bouallagui, Z. et al. Comparative study of the effect of oleuropein and hydroxytyrosol rich extracts on the reproductive toxicity induced by bisphenol A in male rats: biochemical, histopathological, and molecular analyses (2023). *Environ Sci Pollut Res* 30, 78735–78749
- Belén Caballero-Guerrero, Antonio Garrido-Fernández, Fernando G. Feroso, María África Fernández-Prior, Juan Cubero-Cardoso, Claudio Reinhard, Laura Nyström, Antonio Benítez-Cabello, Elio López-García, Francisco Noé Arroyo-López. Modeling the antimicrobial effects of olive mill waste extract, rich in hydroxytyrosol, on the growth of lactic acid bacteria using response surface methodology (2023) *Food Science*, Volume 88, Issue 10, Pages 4059-4067
- Ana Ballesteros-Gómez, Antonio Serrano-Crespín, Soledad Rubio. Supramolecular-solvent based extraction of hydroxytyrosol from brines of the processing of table olives, (2023) *Separation and Purification Technology*, Volume 322
- Arantzazu Valdés García, Nerea Juárez Serrano, Ana Beltrán Sanahuja and María Carmen Garrigós (2020), Novel Antioxidant Packaging Films Based on Poly(ϵ -Caprolactone) and Almond Skin Extract: Development and Effect on the Oxidative Stability of Fried Almond

Chapter 5: ANNs as a valid tool for active food bio packaging optimization.

~

Premises to Chapter 5

In the following Chapter, currently in “under submission” phase, artificial neural networks (ANNs) are utilized as an advanced tool for product development. This Chapter delivers a convenient ANN-driven optimization methodology to correlate the amount of multiple functional compounds used in the packaging samples to their effect on the water vapor transmission rates (WVTR), one of the main features of the final packaging itself. The study investigates the combined effect of 6 different functional compounds in the main PLA polymer matrix: a Design of Experiment is generated, so that a minimal array of samples is produced to retrieve precise dependencies between the amounts of functional compounds and the WVTR values. The samples in the array were cast and WVTR test were performed. The results were then fed to the dedicated ANN by which the complex relationships between compounds amounts and WVTR values can be explicated giving full access to feature optimization. The functionalized samples, along with the film casting

methodology described in Chapter 2, is under patenting phase, therefore some of the data of the research are here omitted.

~

5.1 - Introduction

Artificial neural networks (ANNs) utilize jointed calculus nodes – the so-called neurons - to create a network capable of modeling intricate functional dependencies. ANNs usage specifically suits such problems that involve multiple parameters with the use of non-linear interpolations, therefore not easily embraceable by conventional mathematical methodologies. Hence, ANNs have seen increasing use for the determination of mechanical and physical materials properties, particularly for complex composite materials.

Throughout the years, a series of material science-related studies has been published about the use of ANNs, for example as an attempt to predict tensile strength and density predictions, bending strength and hardness estimations of reinforced composites, and prediction of void fractions in Al₂O₃/SiC cakes (N. Altinkok et al., 2004 – 2005 - 2006). The neural network approach of all these studies is very alike except for the inputs and the targets, being them relatively the type and properties of materials. (Wei et al., 2019)

To obtain ANNs with effective performances, a satisfactory amount of experimental data should be available (Feng et al., 2019). Throughout the training and testing procedures, either ANN structure, learning algorithm and tuning parameters should be optimized based on the peculiar problem addressed each time

(Abiodun et al., 2018). When the ANN results are optimized and well-trained on the available data, it is possible to retrieve adequate results when working on any new array of input data other than the ones experienced during training and testing phases. (Venkatasubramanian, 2018)

ANNs are compiled by a number of neurons set to operate in parallel. The simplest neuron type is defined by a series of simple operations. The input of the neuron is defined as follows: a weighted input $i \cdot w$, which is a scalar multiplication of a input i and a weight w , both scalar variables, is summed to a scalar called bias b . The resulting neuron input $n = i \cdot w + b$ is fed as input for a transfer function F , which produces a scalar o as output. (Curcio et al., 2006)

Both weight and bias can be modified during the training step to shape the neural network towards a requested behavior. ANNs can modeled on a single layer, in which weights and biases values are constantly adjusted to generate a correct targets vector in respect to a specific input vector (da Silva et al., 2016). Multilayer networks can be modeled too, these being supervised networks with a minimum of 3 layers: the input layer, at least one hidden layer and the output layer (Yan and Wang, 2022). The output layer generates the network output, which is confronted to a target vector, generally constituted by a fraction of the experimental data set (inputs). The delta between network outputs and the target is employed to update weights and biases values in the training phase through a learning algorithm capable of

minimizing the delta itself (Freeman et al., 1991). Therefore, ANNs architecture is defined by the number of layers and neurons involved, by the transfer function chosen for each layer, by the connections between the layers and between the neurons of the single layers, and by the inputs utilized. ANNs architectures are critical to obtain a reliable prediction and to define the computational workforce required; the higher the number of neurons composing the hidden layers the more the network can result powerful, but with higher computational efforts (Curcio et al., 2005).

In this study, the capabilities of ANNs are employed in the characterization of an important feature of functionalized PLA films. The aim is to define a correlation between the amounts of plasticizer, types and amounts NPs dispersed in the film and the water vapor transmission rate (WVTR). This feature is crucial to define the usability of polymer films in food packaging and the prediction on the actual shelf life of the products themselves (Sängerlaub et al., 2018). WVTR of polymer films is often accounted in quality controls and to test packaging suitability for food uses. (Bleisch et al., 2014; Langowski, 2008).

5.2 - Materials and methods – samples and testing.

Samples were prepared with similar methods described in Chapter 2, with the exception of the use of NPs, which were dispersed in the PLA solutions. Five NP types were chosen among the ones could improve mostly the WVTR values and other

mechanical features of the film while being economically accessible, food-safe and unharmed for the environment; here referred as ^{NP}A, ^{NP}B, ^{NP}C, ^{NP}D, ^{NP}F, along with the same plasticizer (^PG) utilized in Chapter 2. WVTR tests were performed with the methods presented in Chapter 2 on an array of 66 samples defined by a design of experiment (DOE) – mixture type. The DOE defined the minimal set of samples needed to define a correlation between the input – three different mass fractions of ^PG and NPs in each sample – and the target – the corresponding WVTR values – by the use of ANNs. (Davidov-Pardo et al., 2023)

In Table 18 below, the list of samples generated by the DOE is presented with the three amounts L, M, H defined for each functional compound.

Table 18: Samples array generated by the “mixture” type DOE (continued).

<i>Sample</i>	<i>^PG</i>	<i>^{NP}A</i>	<i>^{NP}B</i>	<i>^{NP}C</i>	<i>^{NP}D</i>	<i>^{NP}E</i>
<i>S_001</i>	H	0	0	0	0	0
<i>S_002</i>	M	L	0	0	0	0
<i>S_003</i>	M	0	L	0	0	0
<i>S_004</i>	M	0	0	L	0	0
<i>S_005</i>	M	0	0	0	L	0
<i>S_006</i>	M	0	0	0	0	L
<i>S_007</i>	L	M	0	0	0	0
<i>S_008</i>	L	L	L	0	0	0
<i>S_009</i>	L	L	0	L	0	0
<i>S_010</i>	L	L	0	0	L	0
<i>S_011</i>	L	L	0	0	0	L
<i>S_012</i>	L	0	M	0	0	0
<i>S_013</i>	L	0	L	L	0	0
<i>S_014</i>	L	0	L	0	L	0
<i>S_015</i>	L	0	L	0	0	L
<i>S_016</i>	L	0	0	M	0	0
<i>S_017</i>	L	0	0	L	L	0
<i>S_018</i>	L	0	0	L	0	L

<i>S_019</i>	L	0	0	0	M	0
<i>S_020</i>	L	0	0	0	L	L
<i>S_021</i>	L	0	0	0	0	M
<i>S_022</i>	0	H	0	0	0	0
<i>S_023</i>	0	M	L	0	0	0
<i>S_024</i>	0	M	0	L	0	0
<i>S_025</i>	0	M	0	0	L	0
<i>S_026</i>	0	M	0	0	0	L
<i>S_027</i>	0	L	M	0	0	0
<i>S_028</i>	0	L	L	L	0	0
<i>S_029</i>	0	L	L	0	L	0
<i>S_030</i>	0	L	L	0	0	L
<i>S_031</i>	0	L	0	M	0	0
<i>S_032</i>	0	L	0	L	L	0
<i>S_033</i>	0	L	0	L	0	L
<i>S_034</i>	0	L	0	0	M	0
<i>S_035</i>	0	L	0	0	L	L
<i>S_036</i>	0	L	0	0	0	M
<i>S_037</i>	0	0	H	0	0	0
<i>S_038</i>	0	0	M	L	0	0
<i>S_039</i>	0	0	M	0	L	0
<i>S_040</i>	0	0	M	0	0	L
<i>S_041</i>	0	0	L	M	0	0
<i>S_042</i>	0	0	L	L	L	0
<i>S_043</i>	0	0	L	L	0	L
<i>S_044</i>	0	0	L	0	M	0
<i>S_045</i>	0	0	L	0	L	L
<i>S_046</i>	0	0	L	0	0	M
<i>S_047</i>	0	0	0	H	0	0
<i>S_048</i>	0	0	0	M	L	0
<i>S_049</i>	0	0	0	M	0	L
<i>S_050</i>	0	0	0	L	M	0
<i>S_051</i>	0	0	0	L	L	L
<i>S_052</i>	0	0	0	L	0	M
<i>S_053</i>	0	0	0	0	H	0
<i>S_054</i>	0	0	0	0	M	L
<i>S_055</i>	0	0	0	0	L	M
<i>S_056</i>	0	0	0	0	0	H

Once the samples were prepared, the WVTR testing took place - as per in Chapter 2 – giving back the results shown by the histogram reported in Figure 50 below.

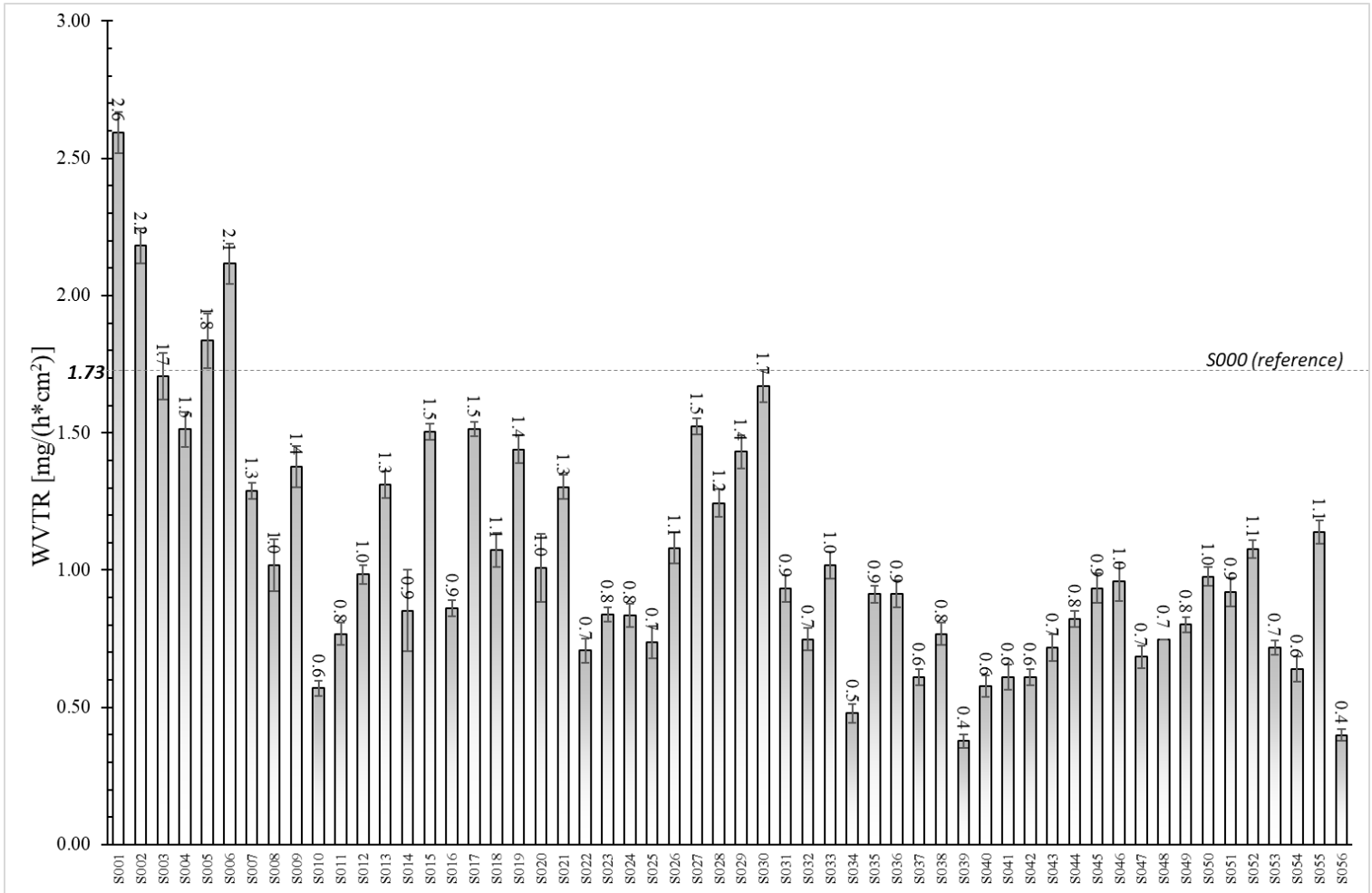


Figure 50: Results of WVTR tests on the sample array generated by the DOE.

5.3 – ANN architecture.

The generated data were fed into MATLAB r2022b and stored as follows: a 6*66 matrix (**In**) with the samples NPs mass fractions defines the Inputs matrix, while a vector – of length 66 - with the WVTR test results, has been stored as **Tar** vector (Table 19).

Table 19: MATLAB data inputs (continued).

	H	0	0	0	0	0	1.73
	M	L	0	0	0	0	2.59
	M	0	L	0	0	0	2.18
	M	0	0	L	0	0	1.71
	M	0	0	0	L	0	1.51
	M	0	0	0	0	L	1.84
	L	M	0	0	0	0	2.12
	L	L	L	0	0	0	1.29
	L	L	0	L	0	0	1.02
	L	L	0	0	L	0	1.38
	L	L	0	0	0	L	0.57
	L	0	M	0	0	0	0.77
	L	0	L	L	0	0	0.98
	L	0	L	0	L	0	1.31
	L	0	0	M	0	0	0.85
	L	0	0	L	L	0	1.5
	L	0	0	L	0	L	0.86
In =	L	0	0	0	M	0	1.51
	L	0	0	0	L	L	1.07
	L	0	0	0	0	M	1.44
	0	H	0	0	0	0	1.01
	0	M	L	0	0	0	1.3
	0	M	0	L	0	0	0.71
	0	M	0	0	L	0	0.84
	0	M	0	0	0	L	0.84
	0	L	M	0	0	0	0.74
	0	L	L	L	0	0	1.08
	0	L	L	0	L	0	1.52
	0	L	L	0	0	L	1.24
	0	L	0	M	0	0	1.43
	0	L	0	L	L	0	1.67
	0	L	0	L	0	L	0.93
	0	L	0	0	M	0	0.75
	0	L	0	0	L	L	1.02
	0	L	0	0	0	M	0.48
	0	L	0	0	0	M	0.91
							Tar =

0	0	H	0	0	0	0.91
0	0	M	L	0	0	0.61
0	0	M	0	L	0	0.77
0	0	M	0	0	L	0.38
0	0	L	M	0	0	0.58
0	0	L	L	L	0	0.61
0	0	L	L	0	L	0.61
0	0	L	0	M	0	0.72
0	0	L	0	L	L	0.82
0	0	L	0	0	M	0.93
0	0	0	H	0	0	0.96
0	0	0	M	L	0	0.68
0	0	0	M	0	L	0.75
0	0	0	L	M	0	0.8
0	0	0	L	L	L	0.98
0	0	0	L	0	M	0.92
0	0	0	0	H	0	1.08
0	0	0	0	M	L	0.72
0	0	0	0	L	M	0.64
0	0	0	0	0	H	1.14
H	0	0	0	0	0	0.4
M	L	0	0	0	0	1.815
M	0	L	0	0	0	1.881
M	0	0	L	0	0	2.516
M	0	0	0	L	0	3.389
M	0	0	0	0	L	0.478
L	M	0	0	0	0	0.562
L	L	L	0	0	0	0.562
L	L	0	L	0	0	0.822
L	L	0	0	L	0	0.832

To approach the neural network computation, one preliminary mathematical rearrangement of the data is needed to scale all values in a restrained range. To achieve this scaling, the MATLAB command **mapminmax** has been applied on both **In** and **Tar**. The **mapminmax** function processes a $n*m$ matrix returning a scaled matrix – within the chosen range - of same size and a process settings array **PS** for consistent processing of values.

The original inputs and targets are normalized in the matrices **In_n** and **Tar_n**, which are then fed in the ANN architecture, having all values normalized in the $[-1,1]$ interval.

The ANN has been set by the MATLAB tool **nftool**, which generates and trains a two-layer feed-forward network able to solve data fitting problems. The network which gave best performances was defined by finding the optimal combination of: training algorithm, layer size (neurons amount) and data division ratios.

The matrices **In_n** and **Tar_n** are calculated in the main MATLAB workspace, then imported in the tool. The input data are randomly divided into training, validation, and test sets with a 0.70/0.15/0.15 ratio. The number of neurons for each layer is set and the network, composed of a hidden layer of 8 neurons, is trained with one of the available algorithms, which are shown in Table 20 below.

Table 20: MATLAB available training algorithms.

Training Algorithm	DESCRIPTION
Levenberg-Marquardt	Usually the fastest training algorithm, while it requires more computing memory than other methods.
Bayesian regularization	Updates weights and biases values by Levenberg-Marquardt optimization, then minimizes a combination of squared errors and weights, defining the combination that produces a network with good generalization. Typically works fine with noisy or modest data sets.
Scaled conjugate gradient backpropagation	Updates weight and bias values by the scaled conjugate gradient method. It is recommended for large problems as it uses gradient calculations, which are more memory efficient than the Jacobian calculations used by the other two methods listed.

In this case, the best performances were found running the Levenberg-Marquardt training algorithm, while overall the ANN gives back a more than acceptable fitting, as shown in the next section.

Along the training stage, validation and test stages are computed, ANN performances are evaluated using the mean squared error and regression assessment.

Below, the neural network MATLAB script generated within the `nftool` is presented.

```
% Solve an Input-Output Fitting problem
with a Neural Network
% Script generated by Neural Fitting app
% Created 17-Nov-2023 10:05:50
%
% This script assumes these variables are
defined:
%
% In_n - input data.
% Tar_n - target data.

x = In_n;
t = Tar_n;

% Choose a Training Function
% For a list of all training functions
type: help nntrain
% 'trainlm' is usually fastest.
% 'trainbr' takes longer but may be
better for challenging problems.
% 'trainscg' uses less memory. Suitable
in low memory situations.
trainFcn = ['trainlm']; % Levenberg-
Marquardt backpropagation.

% Create a Fitting Network
hiddenLayerSize = [8];
net = fitnet(hiddenLayerSize,trainFcn);

% Choose Input and Output Pre/Post-
Processing Functions
% For a list of all processing functions
type: help nnprocess
%net.input.processFcns =
{'removeconstantrows','mapminmax'};
%net.output.processFcns =
{'removeconstantrows','mapminmax'};

% Setup Division of Data for Training,
Validation, Testing
% For a list of all data division
functions type: help nndivision
net.divideFcn = 'dividerand'; % Divide
data randomly
net.divideMode = 'sample'; % Divide up
every sample
net.divideParam.trainRatio = 70/100;
net.divideParam.valRatio = 15/100;
net.divideParam.testRatio = 15/100;

% Choose a Performance Function
% For a list of all performance functions
type: help nnperformance
net.performFcn = 'mse'; % Mean Squared
Error

% Choose Plot Functions
% For a list of all plot functions type:
help nnplot
net.plotFcns =
{'plotperform','plottrainstate','ploterrh
ist', ...
'plotregression','plotfit'};

% Train the Network
[net,tr] = train(net,x,t);

% Test the Network
y = net(x);
e = gsubtract(t,y);
performance = perform(net,t,y)

% Recalculate Training, Validation and
Test Performance
```

```

trainTargets = t .* tr.trainMask{1};
valTargets = t .* tr.valMask{1};
testTargets = t .* tr.testMask{1};
trainPerformance =
perform(net,trainTargets,y)
valPerformance =
perform(net,valTargets,y)
testPerformance =
perform(net,testTargets,y)

% View the Network
%view(net)

% Plots
% Uncomment these lines to enable various
plots.
%figure, plotperform(tr)
%figure, plottrainstate(tr)
%figure, ploterrhist(e)
%figure, plotregression(t,y)
%figure, plotfit(net,x,t)

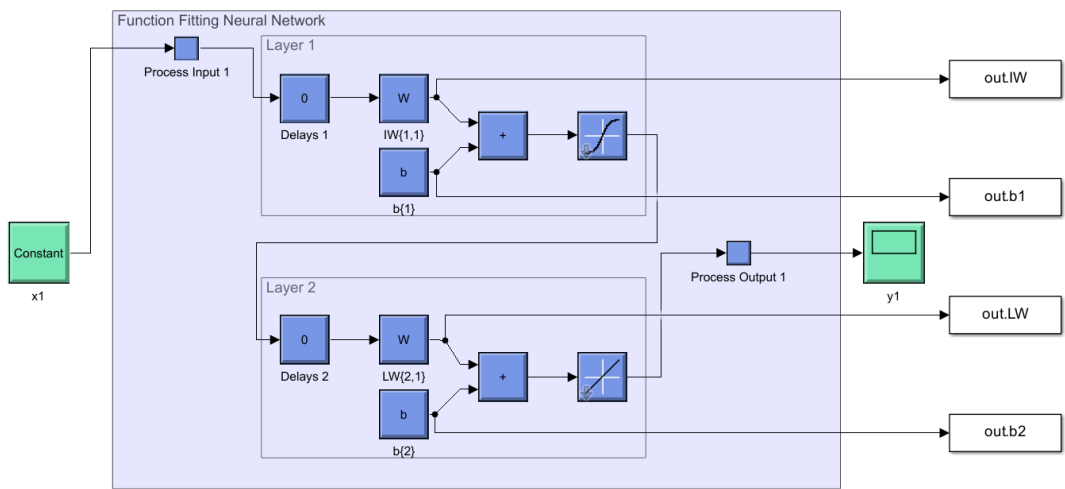
% Deployment
% Change the (false) values to (true) to
enable the following code blocks.
% See the help for each generation
function for more information.
if (false)
    % Generate MATLAB function for neural
network for application
    % deployment in MATLAB scripts or
with MATLAB Compiler and Builder
    % tools, or simply to examine the
calculations your trained neural
    % network performs.

genFunction(net,'myNeuralNetworkFunction'
);
    y = myNeuralNetworkFunction(x);
end
if (false)
    % Generate a matrix-only MATLAB
function for neural network code
    % generation with MATLAB Coder tools.

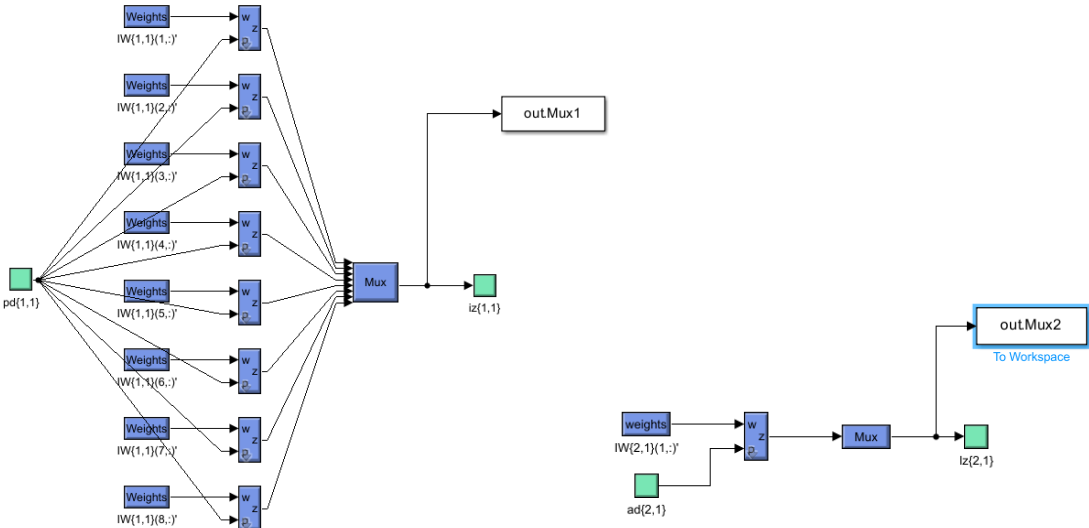
genFunction(net,'myNeuralNetworkFunction'
,'MatrixOnly','yes');
    y = myNeuralNetworkFunction(x);
end
if (false)
    % Generate a Simulink diagram for
simulation or deployment with.
    % Simulink Coder tools.
gensim(net);
end

```

The neural network architecture has been exported into SimuLink to easily retrieve intermediate and final outputs. A graphical representation of the whole ANN and of its inner layers is presented in Figure 51 below, along with the OUT blocks to retrieve the intermediate net data.



a)



b)

Figure 51: SimuLink representation of the fitting neural network used in the study, (a) overview, (b) layers architecture (layer 1 on the left, layer 2 on the right).

5.4 – ANN results and performances.

ANN performances are shown in the following plots in the form of regression fit and error histograms, defined for each of the three phases (Figures 52-53).

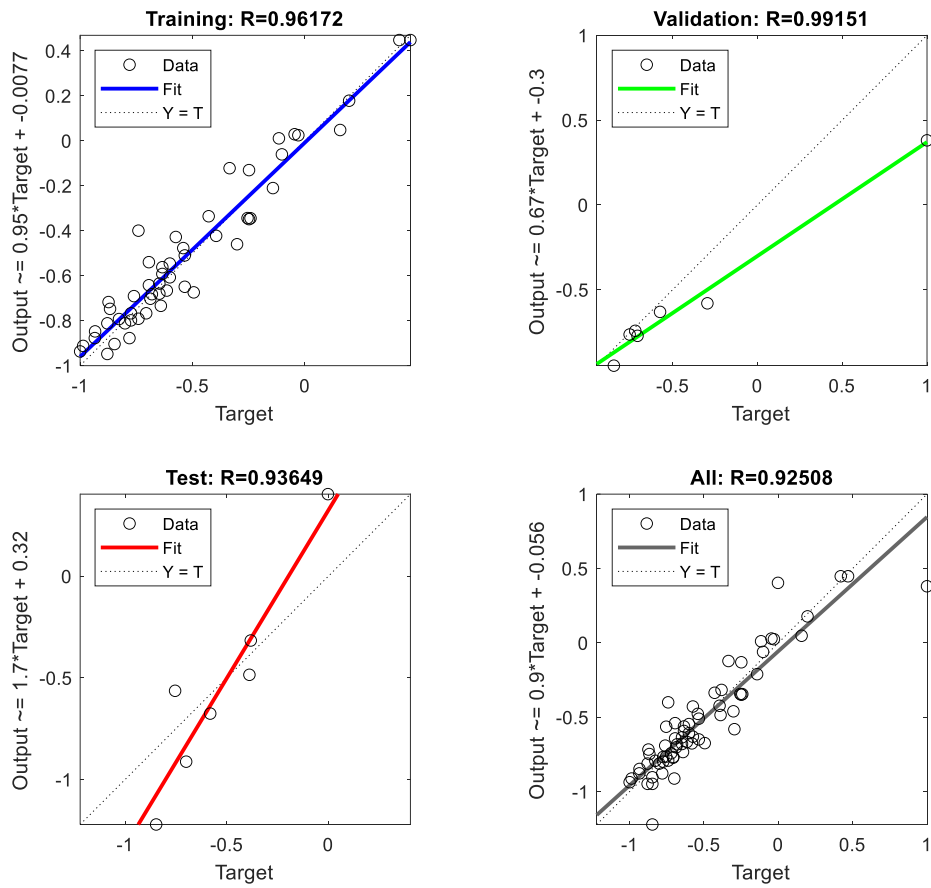


Figure 52: Fitting curves, observation distributions and performances for each ANN run phase.

The values of mean square error and determination coefficient for each phase are reported in Table 21 below for clarity.

Table 21: MSE and R relative to each network run phase.

Phase	Observations	MSE	R
Training	46	0.0096	0.96
Validation	10	0.0690	0.99
Testing	10	0.0583	0.94

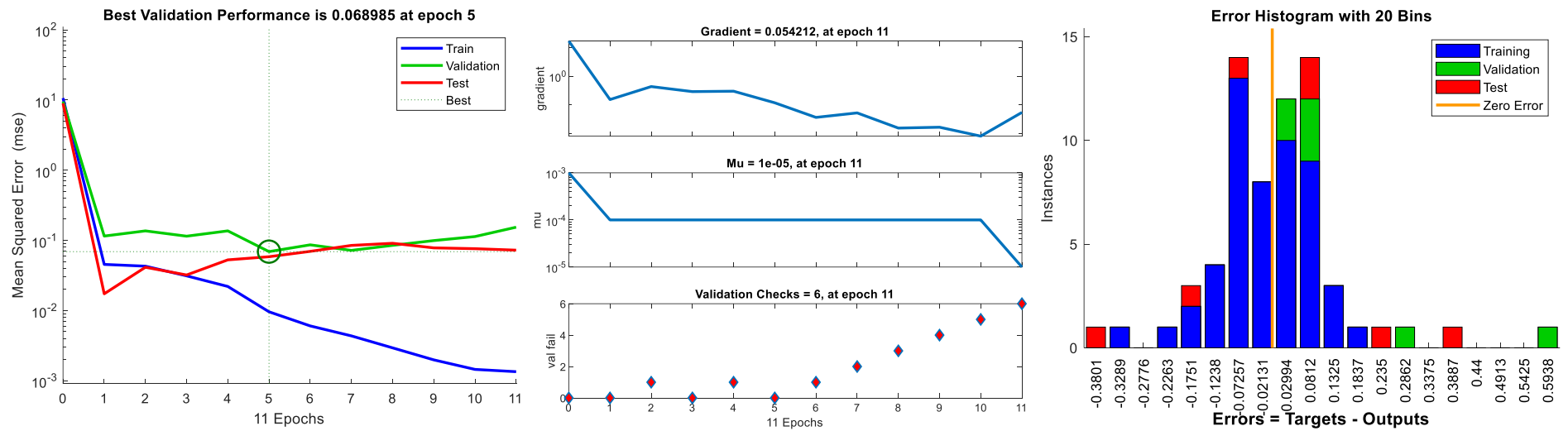


Figure 53: Performance plots for each phase vs calculation epochs, validation checks and errors histogram.

5.5 - Conclusions

By this study, a valid tool to easily and accurately model functionalized polymeric films WVTR was found as a function of the weight fraction of 6 types of NPs. The generated ANN could easily find well fitted correlations between the WVTR values and the amounts of 6 types of functional compounds. A mixture type DOE of 66 samples was constructed as a basis for the sample array casting, acting as a very good feed for the neural network. This study represents a foundation for a fast and precise product optimization in the food packaging field, especially for the development of bio-based and bio-compatible materials. The same fitting procedure could be replicated for different target variables (mechanical features, biodegradability and so on...) towards a comprehensive material characterization and facile and valuable product development: once the correlations are found, a target-based request can be made by the packaging production companies – this meaning asking for a product with precise values of different features -finding the optimum answer with very limited efforts.

References (*Chap 5*)

- Oludare Isaac Abiodun, Aman Jantan, Abiodun Esther Omolara, Kemi Victoria Dada, Nachaat AbdElatif Mohamed, Humaira Arshad. State-of-the-art in artificial neural network applications: A survey. (2018) Helyon Elsevier
- N. Altinkok, R. Koker Modelling of the prediction of tensile and density properties in particle reinforced metal matrix composites by using neural networks. (2006), *Mater Des*, 27 (8)
- N. Altinkok, R. Koker. Mixture and pore volume fraction estimation in Al₂O₃/SiC ceramic cake using artificial neural networks. (2005) *Mater Des*, 26 (4), pp. 305-311
- N. Altinkok, R. Koker. Neural network approach to prediction of bending strength and hardening behaviour of particulate reinforced (Al–Si–Mg) aluminium matrix composites. (2004), *Mater Des*, 25 (7) pp. 595-602
- G. Bleisch, H.-C. Langowski, J.-P. Majschak *Lexikon Verpackungstechnik Behr.*, Hamburg (2014)
- Ivan Nunes da Silva, Danilo Hernane Spatti, Rogerio Andrade Flauzino, Luisa Helena Bartocci Liboni & Silas Franco dos Reis Alves. Artificial Neural Network Architectures and Training Processes (2016) *Artificial Neural Networks* pp 21–28.
- Stefano Curcio, Germana Scilingo, Vincenza Calabrò, Gabriele Iorio. Ultrafiltration of BSA in pulsating conditions: an artificial neural networks approach. (2005) *Journal of Membrane Science*, Volume 246, Issue 2, Pages 235-247
- Stefano Curcio, Vincenza Calabrò, Gabriele Iorio. Reduction and control of flux decline in cross-flow membrane processes modeled by artificial neural networks (2006) *Journal of Membrane Science* Volume 286, Issues 1–2, 15, Pages 125-132
- Shuo Feng , Huiyu Zhou , Hongbiao Dong. Using deep neural network with small dataset to predict material defects. (2019) *Materials & Design* Volume 162, Pages 300-310.
- J.A. Freeman, D.M. Skapura. *Neural networks Algorithms, Applications, and Programming Techniques*. (1991) Addison-Wesley, New York
- H.-C. Langowski. Permeation of gases and condensable substances through monolayer and multilayer structures, (2008), *Plastic packaging*, Wiley-VCH Verlag GmbH & Co, KGaA pp. 297-347
- Davidov-Pardo, G., Arozarena, I. & Marín-Arroyo, M.R. Optimization of a Wall Material Formulation to Microencapsulate a Grape Seed Extract Using a Mixture Design of Experiments. (2013) *Food Bioprocess Technol* 6, 941–951
- Sven Sänglerlaub, Markus Schmid, Kajetan Müller. Comparison of water vapour transmission rates of monolayer films determined by water vapour sorption and permeation experiments. (2018) *Food Packaging and Shelf Life* Volume 17, Pages 80-84
- W. Sha , K.L. Edwards; The use of artificial neural networks in materials science based research (2007) *Materials & Design* Volume 28, Issue 6, Pages 1747-1752
- V. Venkatasubramanian, *The Promise of Artificial Intelligence in Chemical Engineering: Is It Here, Finally?* (2018) *AIChE Perspective*, Wiley
- Jing Wei, Xuan Chu, Xiang-Yu Sun, Kun Xu, Hui-Xiong Deng, Jigen Chen, Zhongming Wei, Ming Lei. Machine learning in materials science. (2019) *Info Mat*. Volume1, Issue3, Pages 338-358
- Jun Yan, Xiangfeng Wang. Unsupervised and semi-supervised learning: the next frontier in machine learning for plant systems biology (2022). *The Plant Journal*, Volume111, Issue6, Pages 1527-1538

Conclusions

All the activities described in this work successfully led to the production of a novel and valid bio-based active packaging film which can easily be addressed to the food chain. The merging between Material Science, Chemical Engineering and Information and Communication Technologies (ICT) allowed a broad view on the topic and a multifaced research which was able to overcome the main issues faced during the development of a reasonable product.

The main outcome of the study is a new array of functionalized PLA-based food-grade packaging films produced at a laboratory scale, while a product development process - with the profitable integration of ICT methodologies - has been hypothesized towards a fast and reliable product design.

The new packaging film obtained can be considered appealing for the market for three main reasons:

- it responds to the need for an active material able to improve the shelf life of the products, thus reducing food wastes at the storage and transportation stages,
- it responds to the need for valid bio-compatible material, following the more and more stringent legislations about packaging and the crescent sensitivity of the end consumer about environmental issues,

- it responds, by the integration of ICT methodologies, to the need for high versatility, so that features of the material can precisely respond to specific market requests.

PLA is, up to date, not really considered as multi-purpose as other synthetic polymers – mostly due to its high brittleness and its quite low thermal resistance – so its use is still restricted to low-stress applications that do not need high thermal resistance and plasticity. Nonetheless, in contrast with the current knowledge about PLA, by an in-depth characterization of the array of functionalized samples produced, some critical changes in mechanical and morphological features emerged: the study was able to validate the assumption that, by the choice of the right types and amounts of functional compounds, the optimization of NPs dispersion, and the optimization of the film casting techniques, many features (mechanical, interfacial, thermal and transpirational) can be finely tuned by a fairly considerable amount to meet the food-chain requests and be fully considered as one of the valid alternatives to the widely used standard synthetic polymers.

In particular, the effect of the functional compounds on WVTR has successfully been taken as subject by ICT optimization techniques. WVTR tests data were fed to a specifically designed ANN to retrieve a precise relationship between the amounts of NPs used and the WVTR values. This revealed a second important consideration: ICT can be a powerful tool in product design; the use of a minimum array of samples

generated by a DOE and a dedicated ANN enables the disclosure of a whole spectrum of possible material features. This directly translates to the fact that, once a complete characterization of the material is done, a specific feature request by the packaging companies can be easily and precisely addressed by the results of an ICT integrated product design procedure.

This said, further studies should be focused on finding the features tunability limits of the material and on how to overcome them, to set the highest bar on material and functional compounds performances.

While screening possible future perspectives of this research, it is clear that modeling and more generally ICT approaches should be favored and further explored for a broader, more precise and straight-forward material and process optimization.

In this context, a full understanding of the material behavior at smaller scales could be critical. As an example, an “ab initio” material modeling approach could give straight-forward access to all material features. This approach is powerful because relies on the basic laws of nature – like quantum mechanics - at molecular scales, without the dependency on dedicated models, giving full access to any material feature and to its interaction with other materials under any physical condition. By this way the need for time-consuming (and sometimes not error-free) laboratory testing would be reduced to a modeling validation experiment campaign.

Moreover, to set the environmentally friendly bar higher, one of the natural evolutions of the work should be the study of efficient ways to exploit enzymatic conversion of vegetal wastes to bio-based polymers. By this way a full closed cycle could be drawn around the food chain and the tightly related packaging industry.

In this context, one critical aspect resides in the fact that these biochemical processes are governed by very complex kinetics, so a complete comprehension of those phenomena would be very difficult and time-consuming if done only relying on standard laboratory procedures. Again, to overcome this critical aspect, a very large importance should be given to the modeling of the bio-chemical processes involved, in order to get on the fastest route to a full characterization of the phenomena.

By the other hand, the ability of the bio-based packaging to help the sustainability of the whole food-chain and logistics chain should be provided by a massive ICT intervention on the packaging design itself, by integrating “intelligent” features (features sensing and control, blockchain reporting) that can vastly improve the benefits of the new developed materials.

Here, a critical aspect resides in the fact that very often “intelligent” or “sensing” solutions - while providing high-end features - are still poorly economically favorable, sometimes even playing against the easiness of recyclability of the packaging itself. This said, strong research efforts on the ICT integration in the

packaging field, with an open eye on their recyclability and on devices designed around bio-compatible sourced materials, would surely help the overall evolution of the packaging market towards at the same time more efficient and bio-compatible solutions.

List of Publications

Below, the list of the 11 articles plus one conference proceedings published during the three-year PhD course, listed from the latest on.

1. *Sanguedolce M., Latino M., Coppola G., Chakraborty S., Filice L.*

On the Polymeric Coating Deposition Techniques to Increase Body Acceptance and Allow Drug Delivery in Smart Bio-devices.

Procedia Computer Science, 2023, Proceedings of the 5th International Conference on Industry 4.0 and Smart Manufacturing

2. *Petrosino, F., Coppola, G., Chakraborty, S., Curcio, S.*

Modeling of specific migration from food contact materials.

Journal of Food Engineering, 2023, 357, art. no. 111652.

3. *Candamano, S., Coppola, G., Mazza, A., Caicho Caranqui, J.I., Bhattacharyya, S., Chakraborty, S., Alexis, F., Algieri, C.*

Batch and fixed bed adsorption of methylene blue onto foamed metakaolin-based geopolymer: A preliminary investigation.

Chemical Engineering Research and Design, 2023, 197, pp. 761-773.

4. *Coppola, G., Gaudio, M.T., Lopresto, C.G., Calabro, V., Curcio, S., Chakraborty, S.*

Correction to: Bioplastic from Renewable Biomass: A Facile Solution for a Greener Environment

Earth Systems and Environment, 2023, 7 (2), p. 581.

5. *Coppola, G., Bhattacharyya, S., Pugliese, V., Algieri, C., Petrosino, F., Siciliano, S., Calabro, V.*

Metal–organic framework application in wastewater treatment: a review Terms and conditions.

Euro-Mediterranean Journal for Environmental Integration, 2023

6. *Algieri, C., Pugliese, V., Coppola, G., Curcio, S., Calabro, V., Chakraborty, S.*

Arsenic removal from groundwater by membrane technology: Advantages, disadvantages, and effect on human health.

Groundwater for Sustainable Development, 2022, 19, art. no. 100815.

7. *Shammas, M.I., Algieri, C., Coppola, G., Chakraborty, S.*

Integrating the Use of Biopolymers in the Facemask Technology Towards Plastic Waste Reduction.

Ethiopian Journal of Health Development, 2022, 36 (1).

8. *Shammas, M.I., Algieri, C., Coppola, G., Chakraborty, S.*

Impact of the COVID-19 face mask disposal on environment and perception of people of the Sultanate of Oman (2022)

Ethiopian Journal of Health Development, 2022, 36 (2), pp. 1-10.

9. *Petrosino, F., Mukherjee, D., Coppola, G., Gaudio, M.T., Curcio, S., Calabro, V., Marra, F., Bhattacharya, P., Pal, U., Khélifi, N., Chakraborty, S.*

Transmission of SARS-Cov-2 and other enveloped viruses to the environment through protective gear: a brief review.

Euro-Mediterranean Journal for Environmental Integration, 2021, 6 (2), art.no. 48.

10. *Algieri, C., Coppola, G., Mukherjee, D., Shamma, M.I., Calabro, V., Curcio, S., Chakraborty, S.*

Catalytic membrane reactors: The industrial applications perspective

Catalysts, 2021, 11 (6), art. no. 691.

11. *Gaudio, M.T., Coppola, G., Zangari, L., Curcio, S., Greco, S., Chakraborty, S.*

Artificial Intelligence-Based Optimization of Industrial Membrane Processes

Earth Systems and Environment, 2021, 5 (2), pp. 385-398.

12. *Coppola, G., Gaudio, M.T., Lopresto, C.G., Calabro, V., Curcio, S., Chakraborty, S.*

Bioplastic from Renewable Biomass: A Facile Solution for a Greener Environment

Earth Systems and Environment, 2021, 5 (2), pp. 231-251.

List of Courses

Below, the list of DIMES courses followed during the PhD period.

_____ (I° year) _____

Prof. Yaroslav D. Sergeyev: “Lipschitz Global Optimization”.

Dr. Gianvincenzo Alfano: “Argumentation in Artificial Intelligence”.

Dr. Raffaele Gravina: “From Modeling to Implementation of Wearable Computing Systems based on Body Sensor Networks”.

_____ (II° year) _____

Eng. Loris Belcastro, Eng. Fabrizio Marozzo: “Functional Programming for Big Data Processing”.

Prof. Adam Teman: “Hardware for Deep Learning”.

Prof. P. Laghi: “Digital technologies and artificial intelligence law”.

_____ (III° year) _____

Prof. Marco Ricci, Dr. Stefano Laureti: “Statistical data analysis and signal processing techniques for imaging and non-destructive testing”.

Conferences

Below, the list of international conferences participations during the PhD period, from the latest on.

Accepted abstract at next WasteEng2024

Waste to wealth: new perspective for process intensification strategy.

Chakraborty S., Coppola G., Gaudio MT., Petrosino F., Pugliese V., Curcio S.

ISM 2023

On the Polymeric Coating Deposition Techniques to Increase Body Acceptance and Allow Drug Delivery in Smart Bio-devices.

Sanguedolce M., Latino M., Coppola G., Chakraborty S., Filice L.

Session Chair and Scientific Committee member at the Euro-Mediterranean Conference for Environmental Integration (EMCEI-23), held in Rende (Cosenza), Italy, from 2 to 5 October 2023.

EMCEI 2023

Bioplastics: opportunities and their role in a more environmentally friendly industrial chain.

Coppola G.

GSA CONNECTS 2022

Arsenic removal from Groundwater by membrane technology – challenges for society.

Coppola G.

EMCEI 2022

A new horizon of Plasmonic Nanomaterials for Environmental Integration

Coppola G., Chakraborty S.

ACS SPRING 2021

Nanomaterials applications for environmental improvement.

Coppola G.

EMCEI 2021

Bioplastics: application in cleaner and greener food industry.

Coppola G., Calabrò V., Curcio S., Chakraborty S.

Other activities

Foreign collaboration with the team of Prof. Anet Režek Jambrak (laboratory for sustainable development, University of Zagreb). Collaboration made in remote modality during Cov-19 lockdown in lieu of period of activity in foreign Institutes.

The following is an excerpt of the Declaration of Cooperation letter signed by Prof. Anet Režek Jambrak at the end of the collaboration period:

Zagreb, 16.03.2023

DECLARATION OF COOPERATION

Dear Gerardo Coppola,

On behalf of the Laboratory for Sustainable development, Faculty of Food Technology and Biotechnology, University of Zagreb, I would like to formally declare your contribution by carrying out research activities on FEM modeling of HVED extraction from vegetal wastes with positive outcomes and tangible roots for further collaborations. Those activities have been performed in the period of 1st January 2022 to 1st April 2022.

Participation to TRUST project, funded by the PRIMA foundation: “Management of industrial Treated wastewater ReUse as mitigation measures to water Scarcity in climaTe change context in two Mediterranean regions” in the

following activities: “WP1 - Waste water treatment technologies implementation, validation and scale up”; “WP4 - Participatory integrated planning of water reuse”.

Participation at STARTCUP CALABRIA 2022 within the team GreenP2E, which proposed a concept design of a piezoelectric energy generator made of waste-sourced materials, winner of the 2nd prize.

Participation at STARTCUP CALABRIA 2023 within the team Am@istics, which proposed a closed-cycled integrated technology to be adopted by the food-chain for the in-house production of agro-food waste sourced functionalized bio-packaging, with the integration of ICT-based logistics.

Co-tutoring and laboratory activities supervision for the following thesis works:

1 - Student: Andrea Curulli

Master’s Degree in Mechanical Engineering (DIMEG – UNICAL).

Thesis: “Mechanical characterization of a PLA membrane and of its nanostructured composites”.

Thesis supervisors: Prof. Pagnotta L., Prof. Candamano S.

2 - Student: Marina Latino

Bachelor's degree in Food Engineering (DIMES – UNICAL).

Thesis: "Preparation and characterization of Chitosan coatings on Titanium slabs for biomedical uses".

Thesis supervisors: Prof. Filice L., Prof. Chakraborty S.

3 - Student: Noemi Turano

Bachelor's degree in Food Engineering (DIMES – UNICAL).

Thesis: Membrane processes in the food industry. A case study: casting, characterization and performances analysis of Cellulose Acetate membranes".

Thesis supervisor: Prof. Vincenza Calabrò.

Acknowledgements

I wish to thank Profs. Stefano Curcio and Sudip Chakraborty for giving me this opportunity. Their strong input to all my PhD activities and their support has proven compelling to the whole work and to a whole new world of research opportunities.

Many thanks to Prof. Anet Režek Jambrak for giving me the opportunity of a productive collaboration.

A big appreciation to Prof. Sebastiano Candamano, who helped to plant the seeds of this work and supported it continuously as it grew.

Big appreciations to the incredibly supportive Dott. Catia Algieri (ITM-CNR), Dr. Corradino Sposato (ENEA Trisaia) and Dr. Chiara Morano (DIMEG) who had key roles in this work.

Many thanks to my fellow laboratory colleagues and all the co-authors of the published papers for the marvelous tireless cooperation.

Thanks to PhD coordinator Prof. Giancarlo Fortino and to all DIMES workforce and professors for the active support to all PhD activities.